



The
University
Of
Sheffield.

Photoreceptor regulation of plant responses to light and carbon dioxide

Jordan Catherine Brown

Department of Molecular Biology and Biotechnology

A thesis submitted for the Degree of Doctor of Philosophy

March 2018

In dedication to my family.

Acknowledgements

I would first like to take this opportunity to thank my supervisor, Dr Stuart Casson, who has been a phenomenal mentor and a hugely important figure to me during my time in Sheffield. I am extremely grateful for his continued patience, steadfast belief in my ability and invaluable support both academically and personally during very difficult stages of my PhD.

I would like to thank Dr Nick Zoulias and Dr Jim Rowe who have continually offered unwavering support and a lot of great times. Thank you to Professor Julie Gray and Dr Lynda Partridge for advising me during my PhD and offering support and guidance.

I would also like to thank colleagues and friends within MBB and APS who have provided help with experiment techniques, equipment use, generally imparted knowledge and who were genuinely there to help throughout my time at Sheffield.

This includes; Kirsty Liversidge, Rachel Denley-Bowers, Colette Baxter and Hannah Sewell for moral support as well as scientific/PhD help. To all members of the Casson, Sorefan, Gray, Flemming and Johnson labs who have been integral to my PhD experience, always offering help and support along the way.

In typical researcher fashion, I would like to thank my funding body, Dept. of MBB at the University of Sheffield, without whom I would not have been able to conduct my research and complete my PhD.

I would also like to thank my family who have always believed in me and kept me going during difficult times; Joseph Hatwell, Catherine Brown, Andrew Brown, Aaron Brown, Adam Brown, Margaret Hamilton, Roy Hamilton, Alan Brown, Mildred Brown, Michelle Clarke, Roberta Spence and David Spence. Thank you to Ian Clarke for helping me throughout my time in scientific research (MSc) and who also encouraged me to apply for a PhD.

I would like to especially thank my partner Joe, who has suffered and celebrated my PhD journey nearly as much as I have. Thank you for weathering the sleepless nights, experiment/equipment failures and nuclear level emotional meltdowns. Also for always being there to celebrate the highs like being awarded the title of SEB Young Plant Scientist 2016, finally finishing my stomatal counts and actually submitting my thesis.

Summary

The scarcity of fresh water resources has highlighted concerns about the high percentage used for agricultural purposes. The strain on freshwater could be alleviated by improving crop water use as this is the largest consuming factor. Stomata are microscopic pores on the leaf epidermis which plants use to regulate their gas exchange. Importantly, stomata are required to balance CO₂ uptake with water loss, with, 1-10 mmol CO₂ taken up per mole of water lost. This is achieved through a combination of altering the aperture of the stomatal pores and regulating the number of stomata that develop on the leaf surface. These changes occur in response to environmental cues and hormone signals (Casson and Hetherington, 2010). An overall genetic pathway of light-controlled stomatal development has advanced the understanding of the regulatory light signaling mechanism. However, it remains unknown how light signaling interacts with other environmental signals, such as that of CO₂, to impact intrinsic developmental pathways.

In this thesis I describe experiments that investigate, *in vivo*, the impact of photoreceptor signaling on CO₂ signal response within the context of stomatal development and function. The final results chapter of this thesis discusses that phyB mutants have altered stomatal response to combined changes in light and CO₂ concentrations. I was able to observe increased water use efficiency of phyB via control of stomatal number, size and aperture. Furthermore I was able to observe that phyB is important to sensing elevated CO₂ in terms of stomatal aperture response. These results indicate a key role of phyB in light and CO₂ signal integration to control stomatal development and response.

Contents

List of Figures.....	11
List of Tables.....	15
1.0 Chapter 1: Introduction.....	17
1.0.1 Food Security and Climate Change	18
1.0.2 Green Revolution	18
1.0.3 Water Scarcity.....	19
1.0.4 Plant Water Use.....	20
1.0.5 Measuring Water Use	20
1.0.6 Stomata.....	22
1.0.7 Stomatal Aperture Control	22
1.0.8 Stomatal Development.....	23
1.0.9 Stomatal Lineage Cell Division	24
1.1.0 Stomatal Development Genetic Pathway	27
1.1.1 MAPK Pathway	33
1.1.2 Environmental Signals and Stomata.....	38
1.1.3 Environment Signals: Light	38
1.1.4 Light Signaling Mechanisms	39
1.1.5 Light Control of Guard Cell Aperture.....	42
1.1.6 Light Regulation of Stomatal Development.....	44
1.1.7 Environmental Signals: CO ₂	49
1.1.8 CO ₂ Signaling Mechanisms	49
1.1.9 CO ₂ Regulation of Stomatal Closure.....	49

1.2.0 CO ₂ Regulation of Stomatal Development.....	51
1.2.1 Environmental Signals: Hormones.....	54
1.2.2 Aims	58
2.0 Chapter 2:.....	59
Materials and Methods	59
2.0.1 General Laboratory Chemicals	60
2.0.2 Seed Lines	60
2.0.3 ½ Murashige and Skoog (MS) Media.....	61
2.0.4 Seed Sterilisation	61
2.0.5 Plant Growth Conditions	61
2.0.6 Genomic DNA Extraction	62
2.0.7 Polymerase Chain Reaction (PCR).....	62
2.0.8 Gel Electrophoresis.....	63
2.0.9 RNA Extraction.....	64
2.1.0 cDNA Synthesis	64
2.1.1 qPCR Analysis	66
2.1.2 Stomatal Impressions.....	68
2.1.3 Microscopy	68
2.1.4 Stomatal Counting.....	69
2.1.5 Infra-red Gas Analysis.....	69
2.1.6 Carbon Isotope Discrimination	70
2.1.7 Stomatal Bioassay	71
2.1.8 Chlorophyll Quantification	72

2.1.9 Dry Weight Measurements	73
2.2.0 Data Analysis	73
2.2.1 Primer Sequences	74
3.0 Chapter 3:	76
Investigating the effects of light and [CO ₂] signal integration on stomatal development.....	76
3.1 Introduction	77
3.2 Aims	78
3.3 Results: Light and [CO ₂] concentration effect stomatal development.....	79
3.4 Light regulation of stomatal development	86
3.5 [CO ₂] regulation of stomatal development	91
3.6 Light and CO ₂ interactions during stomatal development.....	95
3.7 The role of phyB in light and [CO ₂] signal integration	97
3.8 Discussion.....	104
3.9 Key findings:	106
4.0 Chapter 4:	107
Photoreceptor regulation of stomatal development in response to [CO ₂]	107
4.1 Introduction	108
4.2 Aims	109
4.3 Results: cry1cry2 regulates the expression levels of CO ₂ -signal response genes at low [CO ₂].	110
4.4 phyB regulates key stomatal development and CO ₂ -signal response gene expression.....	115

4.5 phyB acts additively with epf2 to regulate key stomatal development genes.	119
4.6 Discussion.....	123
4.7 Key findings:.....	126
5.0 Chapter 5:.....	127
Physiological effects of phyB on plant water use efficiency.	127
5.1 Introduction	128
5.2 Aims	129
5.3 Results: phyB improves water use efficiency (WUE_i)	130
5.4 phyB controls aperture response to elevated $[CO_2]$	139
5.5 phyB mediates the level of ABA signaling and ABA biosynthesis genes..	143
5.6 Carbon isotope discrimination.....	146
5.7 Discussion.....	148
5.8 Key findings:.....	152
6.0.1 Introduction	154
6.0.2 Investigating the effects of light and CO_2 signal integration on stomatal development.....	154
6.0.3 Photoreceptor regulation of stomatal development in response to $[CO_2]$	155
6.0.4 Physiological effects of phyB on plant water use efficiency.....	156
6.0.5 Conclusion	158
6.0.6 Application.....	159
6.0.7 Future work	159
7.0 References	162

8.0 Appendix 176

List of Figures

Figure 1.1	23
Stomatal opening and closing in response to environmental and endogenous signals	
Figure 1.2	26
Diagram of stomatal lineage progression in Arabidopsis	
Figure 1.3	29
Stomatal development in Arabidopsis- transcription factor interactions.	
Figure 1.4	37
Stomatal development in Arabidopsis- Signalling cascade.	
Figure 1.5	48
Light-mediated stomatal development in Arabidopsis.	
Figure 1.6	53
CO ₂ -mediated stomatal development in Arabidopsis	
Figure 1.7	57
Hormone-mediated stomatal development in Arabidopsis	
Figure 2.1	72
Measurements used to calculate stomatal area, aperture area and guard cell (GC) area.	
Figure 3	78

A schematic representation of signal regulation of stomatal development, long-term response.

Figure 3.0 80

DNA gel confirming genotypes of phyB double and triple mutants.

Figure 3.1 84

Stomatal densities (SD) of the abaxial surface of mature leaves for the indicated genotypes.

Figure 3.2 85

Stomatal indices (SI) of the abaxial surface of mature leaves for the indicated genotypes

Figure 3.3 89

Stomatal density of individual genotypes under different light and CO₂ conditions

Figure 3.4 90

Stomatal indices of individual genotypes under different light and CO₂ conditions.

Figure 3.5 93

Stomatal density of individual genotypes under different light and CO₂ conditions

Figure 3.6 94

Stomatal indices of individual genotypes under different light and CO₂ conditions

Figure 3.7 100

Interactions between phyB and components of light signalling (Stomatal Density).

Figure 3.8 101

Interactions between phyB and components of light signalling (Stomatal Index).

Figure 3.9 102

Interactions between phyB and components of CO₂ signalling (Stomatal Density).

Figure 4	103
Interactions between <i>phyB</i> and components of CO ₂ signalling (Stomatal Index).	
Figure 4.1	113
Stomatal development gene expression analysis for Col-0 and <i>cry1cry2</i> .	
Figure 4.2	114
Gene expression analysis of CO ₂ signal response genes for Col-0 and <i>cry1cry2</i> .	
Figure 4.3	117
Stomatal development gene expression analysis for Col-0 and <i>phyB</i> .	
Figure 4.4	118
Gene expression analysis of CO ₂ signal response genes for Col-0 and <i>phyB</i> .	
Figure 4.5	121
Stomatal development gene expression analysis for Col-0, <i>phyB</i> , <i>epf2</i> and <i>phyBepf2</i> .	
Figure 4.6	122
Gene expression analysis of CO ₂ signal response genes for Col-0, <i>phyB</i> , <i>epf2</i> and <i>phyBepf2</i>	
Figure 5.0.1	134
Water use efficiency (WUE _{inst}) of mature leaves for Col-0 and <i>phyB</i>	
Figure 5.0.2	135
A/Ci curves showing Assimilation (A) of mature leaves for Col-0 and <i>phyB</i> plotted against intracellular CO ₂ (C _i).	

Figure 5.0.3 136

Transpiration rates (E) of mature leaves for Col-0 and *phyB* plotted against intracellular CO₂ (C_i).

Figure 5.0.4 137

Intracellular CO₂ concentration (C_i/C_a) of mature leaves for Col-0 and *phyB* plotted against extracellular/ambient CO₂ (C_i).

Figure 5.0.5 138

Total chlorophyll concentrations of mature leaves for Col-0 and *phyB*

Figure 5.0.6 141

Stomatal aperture area (μm²) of mature leaves for Col-0, *phyB*, *35sphyB*, *ca1ca4* and *phyB ca1ca4*.

Figure 5.0.7 142

Total cell area (μm²) of mature leaves for Col-0 and *phyB*.

Figure 5.0.8 145

Gene expression analysis of mature leaves for Col-0 and *phyB*.

Figure 5.0.9 147

Carbon isotope analysis (¹²C:¹³C) of mature leaves for Col-0 and *phyB*.

List of Tables

Table 2.1 **60**

Table showing the seed lines used for analysis of stomatal development.

Table 2.2 **63**

Table showing components and volumes based on required for PCR analysis.

Table 2.3 **63**

Table showing the thermal profile, incubation temperature and times, for PCR.

Table 2.4 **65**

Table showing the components and volumes required for cDNA synthesis.

Table 2.5 **66**

Table showing the thermal profile, incubation temperature and times, for cDNA synthesis.

Table 2.6 **66**

Table showing the components and reaction volumes required for qPCR analysis.

Table 2.7 **67**

Table showing the thermal profile, incubation temperature and times, for qPCR analysis.

Table 2.8 **68**

Layout of excel table used to interpret qPCR data to determine the rate of expression of a sample relative to a control.

Table 2.9 **74-75**

List of forward and reverse primers used for PCR and qRT-PCR of transgenes

Table 3 **82-83**

Known mature leaf response of tested seed lines within this study, to various light and CO₂ concentrations.

1.0 Chapter 1: Introduction

1.0.1 Food Security and Climate Change

The International Panel on Climate Change (IPCC 2014) report shows that climate change is set to exacerbate the current issues surrounding population growth, food production and freshwater availability. Rates and magnitudes of temperature change are becoming more extreme as global temperatures rise due to greenhouse gas emissions. Current global CO₂ levels of ~350 ppm and are rapidly increasing, with CO₂ projections to reach 600 ppm by 2050 and 900 ppm by 2100 (Fig.2.8 IPCC 2014 report). Global temperatures have increased by 0.2°C since 1970 with a projected 1.5-2°C increase by 2100 (IPCC 2014). The rise in global temperatures are likely to continue to melt the Arctic region, warm oceans and increase frequency of hot weather extremes for a longer duration than previously estimated. These factors are causing significant concern due to their impacts on delicate biological ecosystems, such as coral systems, which are not able to evolve alongside the rapid changes in climate. Extreme weather events and regional water distribution impacts are also projected to decrease crop yields (IPCC 2014).

1.0.2 Green Revolution

The Green revolution refers to a boom in research and technology initiatives during the 1960s that enabled a dramatic increase in crop production through the use of herbicides, pesticides, nitrogen-based fertilisers and increased mechanisation (Kendall and Pimentel, 1994). The global population trebled between 1960 and 2000 from 2 billion to 6 billion people and as a result of the green revolution, food production was increased by 250% therefore avoiding widespread famine (Kendall and Pimentel, 1994). There were consequences of the intensive agriculture promoted by the Green Revolution such as increased water use (irrigation) and chemical run-offs beyond cultivation sites, which have exacerbated long-term implications on sustainability (Burney *et al.*, 2010). Crops were most successful in

well-irrigated land, which meant farmers substantially increased water consumption and this has therefore subsequently decreased the global water table (Lipton and Longhurst, 1990).

1.0.3 Water Scarcity

Water scarcity is characterised as a combination of hydrological variability (distribution and movement) and high human use. Approximately 2% of the total Earth's water is useable, 1.5% of this is locked up in ice caps leaving less than 0.5% available for consumption (Damkjaer and Taylor, 2013; Gleeson and Wada, 2013). The global population is projected to increase by 33% from 7 billion to 9.3 billion by 2050 with food demand rising 60% within the same period (Alexandratos and Bruinsma, 2012). Further strain on freshwater availability is set to worsen as the number of people who currently have insufficient access to clean water is set to swell from 1 billion to 2.3 billion by 2050 (Vörösmarty *et al.*, 2000). Globally, 70% of available freshwater reserves are currently used for crop irrigation (Morrison *et al.*, 2008). In some areas, water usage for irrigation has been over-exploited to the extent that large rivers, such as the Yellow River (China), have been reduced to zero flow (effectively dried up, with some shallow pools of stagnant water), which continues to have devastating estuarine, societal and agricultural effects (Wang *et al.*, 2012; Morrison *et al.*, 2008). This current freshwater usage to substantiate demand is not sustainable with predictions of a 40% freshwater deficit to occur by 2030 with a business-as-usual scenario (Morrison *et al.*, 2008). Sanctions have been put in place in many countries, including the UK (Water Act 2003), to restrict and regulate the use of water, however, for these to be long-lasting target reductions, current crop levels must still be achieved whilst reducing water consumption (Morrison *et al.*, 2008). Understanding plant water use and performance could help to achieve 'more crop per drop' and substantially reduce the current pressures on the fresh water table to a sustainable level alleviating the

current fresh water crisis (Marris, 2008; Gagoa *et al.*, 2014).

1.0.4 Plant Water Use

The scarcity of fresh water resources has highlighted concerns about the high percentage used for agricultural purposes, the strain on freshwater could be alleviated by improving crop water use as this is the largest consuming factor. In most instances, plants take up water through their root systems, which this is then primarily used to maintain cell turgor as well as for biochemical processes (e.g. water splitting during photosynthesis). However, of the water that is taken up by a plant, over 90% is lost via transpiration through the leaves (Morrison *et al.*, 2008). Water use efficiency (WUE) refers to the balance between gains (kg of biomass produced or moles of CO₂ assimilated) and costs (m³ water used or moles of water transpired) (Medrano *et al.*, 2015). WUE can be measured from a single leaf to the whole plant as well as canopy level (Gagoa *et al.*, 2014). Increasing numbers of studies are focusing on how to improve WUE in crop models by analysing, mostly at leaf level, short-term (instantaneous gas exchange measurements) and long-term (carbon isotope ratio of dry leaf tissue) plant water use (Farquhar and Richards, 1984).

1.0.5 Measuring Water Use

Infrared gas analysis (*IRGA*) can be used to measure gas exchange of single leaves (or areas of a leaf) and allows the quantification of CO₂ assimilation rates (*A*), transpiration (*E*) and stomatal conductance (*g_s*). Infrared (IR) is used because gas molecules (CO₂ and H₂O in this instance) absorb radiation specifically within this spectrum. The rate of CO₂ fixed by the leaf is determined by measuring the reduction in infrared (IR) wavebands as different CO₂ concentrations [CO₂] are flowed across a chamber. The difference in the amount of ambient CO₂ (*C_a*), flowing from a source to a detector within the chamber, is a function of the amount of CO₂

within the leaf known as intracellular CO₂ (C_i). Instantaneous WUE (WUE_{inst}) refers to the ratio of CO₂ assimilation (A) to transpiration (E), (A/E). Intrinsic WUE (WUE_i) refers to the ratio of CO₂ assimilation (A) to stomatal conductance (g_s), (A/g_s). WUE_i does not take in to consideration cuticular conductance and thus considers stomatal-specific conductances levels (Bierhuizen and Slatyer, 1965).

IRGA provides a transient insight into how plants use water. A more integrative estimation of leaf WUE over the life-time of the plant can be investigated using carbon isotope analysis. During carbon fixation, C₃ plants discriminate between two naturally stable carbon isotopes, ¹²C and ¹³C, with Ribulose-1,5-bisphosphate carboxylase/oxygenase (RuBisCO) discriminating against the heavier ¹³C compared to ¹²C (Farquhar *et al.*, 1989). The composition of CO₂ from combustion of plant material reveals intracellular CO₂ (C_i) carbon (C^{12}/C^{13}) ratios. C_i relates to the amount of CO₂ that enters a leaf; the gas exchange process involves water loss via transpiration as the stomata open to up-take CO₂ thus ¹²C and ¹³C ratios can be used to indicate how a plant used its water during its life-time. Plants with low C_i have higher ¹³C to ¹²C ratios as a result of RuBisCO selecting ¹³C as the amount of ¹²C depletes. Inversely, plants with higher C_i will have higher ¹²C to ¹³C ratios caused by increased levels of ¹²C. Understanding the mechanism of plant water use and performance could provide necessary information to produce crop lines that are more water use efficient in arid environments and perhaps less water use efficient in non water-limiting environments. Improved WUE could help to reduce the unsustainable current pressure on the freshwater table by reducing the need for high usage via irrigation methods and the development of more or less WUE crops which are better suited to the farming terrain within a given geographical region.

1.0.6 Stomata

Stomata are microscopic pores in the leaf epidermis which plants use to regulate gas exchange. Importantly, stomata are required to balance CO₂ uptake with water loss, with, 1-10 mmol CO₂ taken up per mole of water lost. This is achieved through a combination of altering the aperture of the stomatal pores and regulating the number of stomata that develop on the leaf surface. These changes occur in response to environmental cues and hormone signals (Casson and Hetherington, 2010).

1.0.7 Stomatal Aperture Control

Stomatal apertures are rapidly regulated by two flanking guard cells to ensure appropriate response to environmental and endogenous signals, avoiding excessive water loss (caused by open stomata) and CO₂ starvation (caused by closed stomata) (Assmann and Shimazaki, 1999). Stomatal apertures increase when an increase in osmotic concentration results in water uptake in to the guard cells. These reversible changes in turgor pressure are driven by the flow of K⁺ and Cl⁻ ions; increased levels cause guard cells to swell resulting in stomatal opening and decreased levels cause water efflux, subsequent deflation and stomatal closure. Early research suggested that increased thickening of the radial guard cell walls lead to stiffening and subsequent curling of the guard cells due to the increased turgor pressure in order to open the stomatal pore (reviewed in Araújo *et al.*, 2010). However, Carter *et al.*, (2017) recently challenged this hypothesis. Using a combination of atomic force microscopy (AFM), cell wall analysis and modelling they demonstrated that radial reinforcement is only present in mature guard cells and yet immature guard cells, lacking this radial reinforcement, still open. Therefore, they concluded that it is polar reinforcement, initiated early in guard cell maturation, which enables the observed changes in guard cell shape during opening (Carter *et*

al., 2017). Stomatal function has been intensely researched over recent years yet our knowledge of the signaling pathways that regulate guard cell function remains limited. Although research has shown how plants respond to certain environmental signals (e.g. light positively regulates stomatal function whilst CO₂ negatively regulates stomatal function), the exact mechanism remains incomplete, nor do we understand how intrinsic and extrinsic signals coordinate to affect stomatal aperture response. Further discussion of the molecular mechanisms regulating stomatal aperture control will be discussed in later sections.

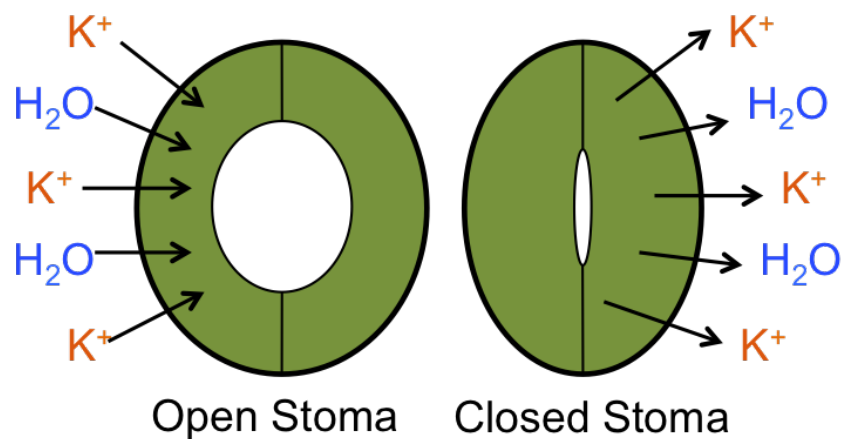


Fig.1.1 Stomatal opening and closing in response to environmental and endogenous signals. Turgor pressure within the guard cells is regulated by osmotic concentration, the movement of K⁺ and Cl⁻ ions cause swelling (open stomata) and deflation of the guard cells (closed stomata).

1.0.8 Stomatal Development

The mechanisms that regulate stomatal development have been the intense focus of research in recent years and a number of regulatory genes have been identified (reviewed in Hetherington, 2003; Israelsson, 2006; Casson and Hetherington, 2010; Zoulias *et al.*, 2018). Key differentiation steps are controlled by a set of related transcription factors, belonging to the basic helix-loop-helix (bHLH) family. These bHLH transcription factors are regulated by a signaling pathway, which includes cell surface receptors, ligands and a mitogen activated protein kinase signaling cascade (reviewed in Casson and Hetherington, 2010; Zoulias *et al.*, 2018). Environmental

signals such as light, CO₂ and temperature impact on stomatal development resulting in increases or decreases in stomatal number on developing leaves. These effects are measured using Stomatal Index (SI) and Stomatal Density (SD) values. SI, expressed as a percentage, refers to the proportion of epidermal cells that are stomata within the same given area of a leaf (SI = number of stomata/(number of stomata + other epidermal cells)). SD refers to the number of stomata per unit area of a leaf (Ticha, 1982; Lake *et al.*, 2001). Much of our current knowledge of stomatal development has come through studies in the model dicotyledonous plant, *Arabidopsis thaliana*. Despite being of little agronomic significance, *Arabidopsis* has proven very useful for studying the genetic and molecular biology of flowering plants. It possesses a number of desirable characteristics including a rapid life cycle, prolific seed production, uncomplicated cultivation, a fully sequenced and annotated diploid genome, is easily transformed and numerous genetic resources are available including a significant number of gene knockout lines. The combination of these traits and resources makes *Arabidopsis* an ideal model organism for research and in the case of stomatal development, this knowledge has informed our understanding of stomatal development in crop species. (Liu *et al.*, 2009, Chang *et al.*, 2016).

1.0.9 Stomatal Lineage Cell Division

The developmental processes leading to properly spaced stomata involve several fundamental events including coordinated signaling among cell types, asymmetric division and cell-fate specification, (Pillitteri and Tori, 2012). This process relies on successive cell divisions and cell-state transitions (Figure 1.2). Each transitional state characterises dramatic changes in morphology, transcript accumulation, and protein localisation (Pillitteri and Torii, 2012). Stomatal development initiates when a protodermal cell undergoes an asymmetric 'entry' division to produce a meristemoid mother cell (MMC). The MMC initiates the stomatal lineage via asymmetric

'amplifying' divisions regenerating a small triangular cell (meristemoid) and a larger sister cell called a stomatal-lineage ground cell (SLGC). A SLGC can terminally differentiate into a pavement cell to protect the underlying tissue layers and to ensure that, morphologically, more specialised cells are spaced correctly (Glover, 2000). SLGC can also initiate an asymmetrical spacing division to produce a satellite meristemoid which is always orientated away from any existing stomatal precursor cells. This occurs via cell-cell signaling components which ensure stomata develop at least one cell apart; this is known as the one-cell spacing rule (Pillitteri and Torii, 2012). Both meristemoid mother cells and satellite meristemoids have the ability to divide up to three times in order to regenerate a meristemoid and increase the total number of SLGCs per single lineage. Post-amplification, a meristemoid loses the ability to asymmetrically divide and undergoes cell-state transition to produce a guard mother cell (GMC). This final stomatal precursor further divides symmetrically to create two guard cells (GCs) and forms the stomatal pore. Mature GCs are terminally differentiated and do not divide further (MacAlister *et al.*, 2007; Casson and Gray, 2008). Until this final transition from GMC to GCs, stomatal development can still be aborted.

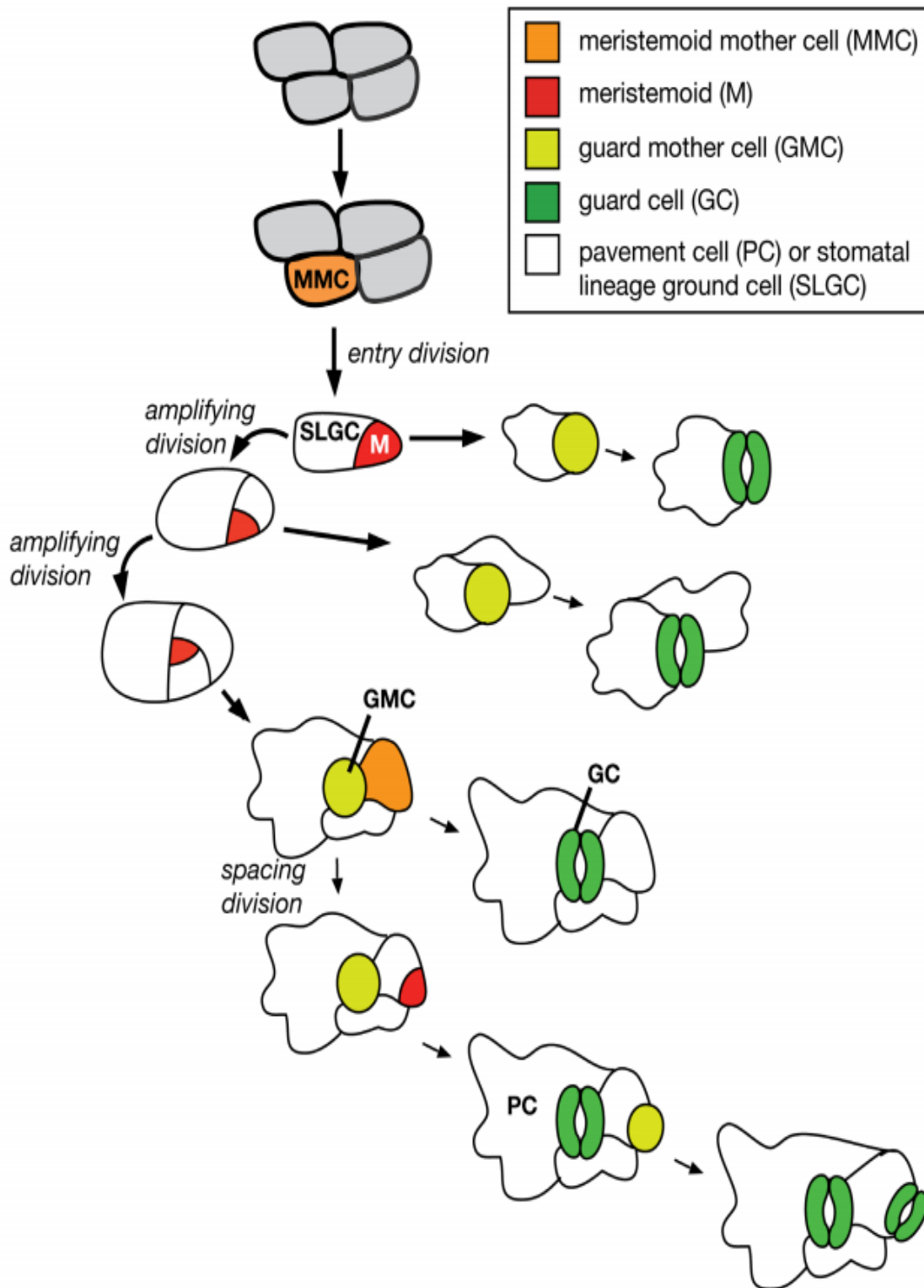


Fig.1.2 Diagram of stomatal lineage progression in Arabidopsis. (Pillitteri and Dong, 2013). A subset of protodermal cells (grey) undergo asymmetric 'entry' divisions to produce a meristemoid mother cell (MMC, orange). MMCs initiate the stomatal lineage via asymmetric 'amplifying' divisions to produce two daughter cells, a meristemoid (M, red) and a stomatal-lineage ground cell (SLGC). An SLGC can differentiate into a pavement cell (PC) or a satellite meristemoid positioned away from an existing stomatal precursor. Meristemoids can undergo a limited number of amplifying divisions, eventually transitioning into a guard mother cell (GMC, yellow). A GMC divides symmetrically to produce two guard cells (GCs, green) which flank the stomatal pore and complete the lineage.

1.1.0 Stomatal Development Genetic Pathway

Stomatal-lineage progression is positively regulated by three key bHLH transcription factors, SPEECHLESS (SPCH), MUTE and FAMA, which promote cellular transitions during stomatal development (reviewed by Torii, 2015). The bHLH domain comprises of two alpha helices individually involved in protein dimerization and DNA binding (Pillitteri and Torii, 2012).

SPCH expression correlates with the onset of post-embryonic entry and amplifying cell divisions. *SPCH* is initially expressed throughout the protoderm of the leaf primordia before localising to a few cells that are competent to undergo entry divisions. MacAlister *et al.* (2007) investigated SPCH function and showed that *spch* mutants are unable to produce stomata, with the epidermis consisting entirely of pavement cells. They also reported that *spch* mutants arrest as small, pale seedlings demonstrating that stomata are required for normal plant development (MacAlister *et al.*, 2007). *SPCHpro::nucGFP*, which is a transcriptional green fluorescence protein (GFP) reporter was shown to direct expression throughout the stomatal lineage, even in guard cells. However, the rescuing translational reporter, *SPCHpro::SPCH-GFP*, showed expression early in the stomatal lineage. This discrepancy between the transcriptional and translation reporters is because SPCH protein is rapidly degraded, showing that SPCH function is limited to the onset of entry and amplification divisions. Over-expression of SPCH in wild-type plants results in a highly divided epidermis with increased MMCs but not the overproduction of GCs that is seen in MUTE or FAMA overexpressors (MacAlister *et al.*, 2007). SPCH expression is required for the initiation of *MUTE* expression, though *MUTE* does not appear to be a direct transcriptional target of SPCH (Lau *et al.*, 2014). The transition from a meristemoid to GMC and exit from the amplifying division stage is controlled by MUTE (MacAlister *et al.*, 2007; Vaten and Bergmann, 2012). Expression of *MUTE* is strongest in the youngest meristemoids and

overexpression can lead to the conversion of the entire leaf epidermis to guard cells (MacAlister *et al.*, 2007; Pillitteri and Dong, 2013). *mute* mutants generate excessive amplifying divisions and meristemoids, which fail to progress further to a GMC or GC, so fail to produce stomata. The number of divisions in the mutant is significantly higher than wild-type with excessive division of meristemoids in an inward-spiral pattern and it is speculated that the eventual arrest of meristemoid division is due to space restriction (Pillitteri *et al.*, 2007; Pillitteri and Dong, 2013).

FAMA controls the final cell fate decision, the division and differentiation of the GMC into two GCs (Ohashi-Ito and Bergmann, 2006). *FAMA* is not expressed in meristemoid cells but strongly expressed in GMCs and in young GCs which supports the finding that *FAMA* has a role in the final stages of the stomatal development pathway. *fama* mutants develop clusters of unpaired epidermal cells which are unable to progress to the guard cell stage. Over-expression of *FAMA* results in direct differentiation of GCs but inhibits cell division; the GMC converts directly into a single guard cell, skipping cytokinesis (Ohashi-Ito and Bergmann, 2006). *FAMA* acts as a key regulator during the division and differentiation of the guard cells.

Another group of bHLH transcription factors, INDUCER OF CBF EXPRESSION 1 (ICE1)/SCREAM and SCRM2, are required for differentiation steps during stomatal development and are predicted to modulate these steps via physical interactions with SPCH, MUTE and FAMA (Kanaoka *et al.*, 2008). Kanaoka *et al.* (2008) showed that loss-of-function *SCRM* and *SCRM2* mirrored the phenotypes of *spch*, *mute* and *fama*, indicating that the amount of SCRM and SCRM2 present, determines initiation and differentiation of cells within the stomatal lineage. A gain of function mutation in *SCRM*, *scrm-D*, produced constitutive stomatal differentiation and SPCH, MUTE and FAMA are likely to heterodimerize with ICE1/SCRM2 to act as a positive feedback loop effecting each other's expression.

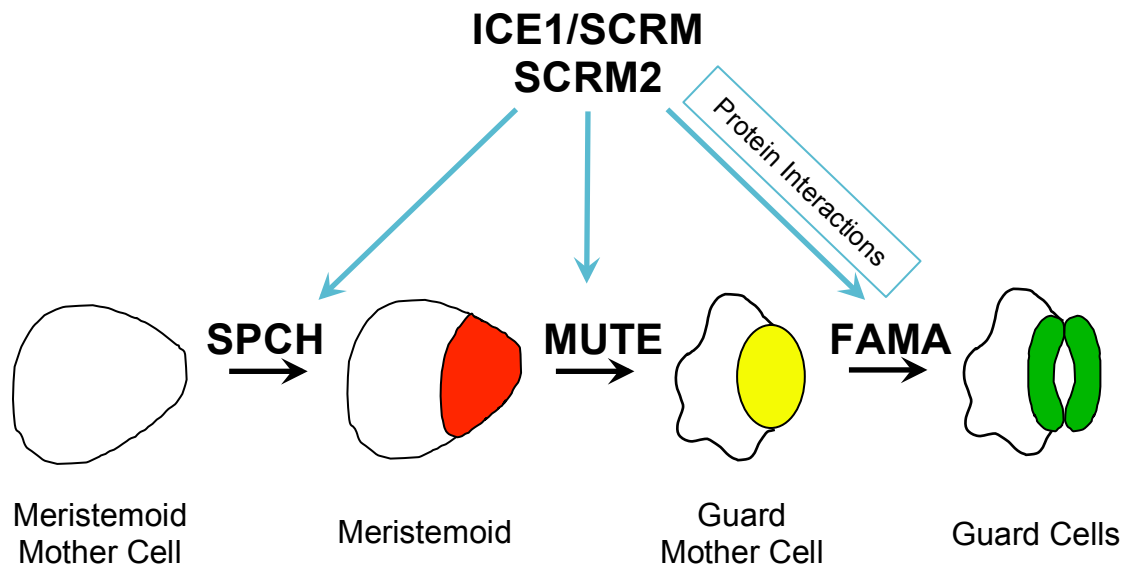


Fig.1.3 Stomatal development in Arabidopsis- transcription factor interactions. (adapted from Casson and Hetherington, 2010). The differentiation steps controlled by the bHLH transcription factors. Protein interactions are shown as blue arrows.

Acting in opposition to these bHLH stomatal promoting factors are signaling systems that limit stomatal development and establish the one-cell spacing pattern within the stomatal lineage. Secreted peptides and their receptors are key components of this system. *EPIDERMAL PATTERNING FACTOR 1* (EPF1) was identified as a peptide regulator of stomatal development (Hara *et al.*, 2007). This study screened genes predicted to encode small secreted peptides and found that plants over-expressing EPF1 had significant reductions in the number of stomata (Hara *et al.*, 2007). EPF1 is secreted by late meristemoids or GMCs, the development stages regulated by MUTE and FAMA. This suggests that EPF1 is required for the correct orientation of asymmetric divisions of secondary meristemoids (Hara *et al.*, 2007; Richardson and Torii, 2013). This hypothesis is supported by phenotypic analysis of a homozygous T-DNA insertion allele of EPF1 (*epf1-1*), which showed stomatal clustering therefore confirming a role for EPF1 in negatively regulating stomatal development to ensure correct one cell-spacing rule (Hara *et al.*, 2007). *EPIDERMAL PATTERNING*

FACTOR 2 (EPF2) is a peptide with homology to EPF1 that also acts as a negative regulator of stomatal development (Hara *et al.*, 2007; Hunt and Gray, 2009). *EPF2*promoter:GUS plants showed that *EPF2* is expressed in young leaves before being restricted to meristemoids and GMCs during leaf development. In contrast, *EPF1*pro-GUS activity occurred towards the distal leaf tip, suggesting that EPF2 is expressed earlier than EPF1 (Hunt and Gray, 2009). Two T-DNA insertion mutant lines of EPF2 (*epf2-1*, *epf2-2*) were identified and showed significant increases in SD, whilst over-expression of EPF2 showed a significant decrease in SD. EPF2 is secreted by MMC and meristemoids, the same stage as *SPCH* expression, and together with the phenotypic data supports a role in inhibiting entry in to the stomatal lineage (Hara *et al.*, 2009; Hunt and Gray 2009; Richardson and Torii, 2013). STOMAGEN/EPF9 (STOM) is a secretory cysteine-rich peptide expressed in mesophyll tissue of immature leaves, which is in contrast to the epidermal expression of *EPF1* and *EPF2* (Sugano *et al.*, 2010). Furthermore, unlike EPF1 and EPF2, STOM positively regulates stomatal development and competes with these negative regulators (EPF1 and EPF2) for receptor binding sites (see below). STOMAGEN RNAi plants with reduced *STOMAGEN* expression show decreased stomatal density, whilst over-expression caused increased stomatal density in cotyledons (Sugano *et al.*, 2010). Both phenotypes contradict the phenotypes of plants manipulated to have reduced or increased EPF1 or EPF2 expression, which showed increased SD values or decreased SD values respectively (Hara *et al.*, 2007; Hunt and Gray 2009; Hara *et al.*, 2009; Sugano *et al.*, 2010).

TOO MANY MOUTHS (TMM), one of the first components of stomatal development and patterning to be identified, promotes cell fate progression and meristemoid division in early precursor cells (Yang and Sack 1995; Nadeau and Sack 2002; Bhave *et al.*, 2009). Mutations in *TMM* result in leaves with elevated stomatal densities and stomatal clustering, which suggests that TMM plays a role in the inhibition of stomatal differentiation (Bergmann *et al.*, 2004; Bhave *et al.*, 2009).

Genetic analysis was used to show that the activity of *EPF1* and *EPF2* are dependent upon *TMM* function (Hara *et al.*, 2007; Hunt and Gray 2009). The level of stomatal clustering and increased stomatal density in *epf1 tmm* mirrored levels found in the single *tmm* mutant, which supports the hypothesis that TMM is a receptor for EPF1 (Hara *et al.*, 2007; see below). TMM is also proposed to associate with members of the ERECTA family (ER, ERL1 and ERL2) (Pillitteri and Torii, 2012). TMM encodes a putative membrane-anchored leucine-rich repeat (LRR)-containing receptor-like protein (LRR-RLP) but lacks a cytoplasmic kinase domain (Nadeau and Sack, 2002; Hara *et al.*, 2007). LRR-RLPs are suspected to form complexes with LRR-RLK (receptor like kinases), which could compensate for the lack of the kinase domain within TMM. This suggested that the one-cell spacing observed during stomatal development could be regulated by TMM-LRR-RLK interactions. The ERECTA gene family (ERf) encode putative receptor like kinases (RLK) with an extracellular ligand-binding domain capable of interacting with TMM. Pillitteri and Torii (2012), suggest TMM either positively or negatively regulates ERECTA-family signal transduction depending on the availability of ligand and/ or receptor pools. The ERECTA- family constitutes three members in Arabidopsis; ERECTA (ER), ERL1 (ERECTA-LIKE1) and ERL2 (Shpak *et al.*, 2005). 'ERECTA' originates from the short and thick inflorescence stem phenotype which made er mutants 'erect' compared to wild type plants (Torii *et al.*, 1996). Torii *et al.* (1996) showed ERECTA functioning within cell expansion process during leaf formation and is highly expressed in apical meristems. Masle *et al.* (2005) demonstrated that ER is a major regulator of transpiration efficiency due to its effects on stomatal density. ERL1 appears to inhibit meristemoid differentiation and ERL2 regulates amplifying divisions (Shpak *et al.*, 2005).

Co-immunoprecipitation (co-IP) assays were used to observe the specificity of ligand-receptor interactions of EPF1 and EPF2 against ERf and TMM receptors (Lee *et al.*, 2012). co-IP demonstrated interactions between Er or ERL1

and both EPF1 and EPF2. However, TMM-GFP failed to co-IP EPF1 although an interaction between TMM and EPF2 was observed (Lee *et al.*, 2012). This shows direct interactions between these ligands and receptors elucidating that EPF1 and EPF2 primarily associate with ERF, which contradicted previous theories that TMM was the primary receptor. It is therefore proposed that TMM likely provides specificity of this interaction to the stomatal lineage (Hunt and Gray, 2009; Lee *et al.*, 2012).

All members of the EPF family are processed from larger propeptides, which suggest that there are processing enzymes required for their cleavage. *STOMATAL DENSITY AND DISTRIBUTION 1 (SDD1)* is a subtilisin-like protease expressed in meristemoids and GMCs (Berger and Altmann, 2000). *sdd1* mutants show an increase in the stomatal index and stomatal clustering whilst over expression of *SDD1* caused a decrease in stomatal index, coupled with increased meristemoid and GMCs cell arrest (Groll *et al.*, 2002). This indicated that *SDD1* plays a role in regulating the number of entry and amplification divisions as well as orientation of spacing divisions. However, genetic analysis of both *epf1 sdd1* and *epf2 sdd1* double mutants found that their phenotypes were additive compared to the single mutants, which supports the idea that EPF1 and EPF2 function independently of *SDD1* (Hara *et al.*, 2007). *SDD1* genetically interacts in the same pathway as *TMM*, so the question remains as to what is the target of *SDD1* and which protease(s) are required for processing of the EPF1 and EPF2 peptides (Hara *et al.*, 2007). The Schroeder lab hypothesised that environmental signals mediate the control of stomatal development via EPF1, EPF2, STOM or *SDD1*. They used proteomics to analyse the subtilases, a family of subtilisin-like serine proteases of which *SDD1* is a member. Developing cotyledons showed an abundance of SBT5-2/CRSP (CO₂ Response Secreted Protease). Using *in vivo* synthesised proteins, CRSP was shown to activate EPF2 via cleavage, whilst protease inhibition showed a significant decrease in cleavage of EPF2. EPF1 and STOMAGEN/EPF9 were subjected to the

same analysis and showed no major cleavage supporting the theory that CRSP is specific to EPF2 (Engineer *et al.*, 2014).

1.1.1 MAPK Pathway

Acting downstream of these receptor-ligand interactions (TMM and ERF), is a mitogen activated protein kinase (MAPK) signaling cascade which negatively regulates stomatal development (Bergmann *et al.*, 2004). The number of Ks pertains to number of Kinases. The cascade begins with a MAPK Kinase Kinase (MAPKKK), which phosphorylates MAPKKs, which then phosphorylates MAPKs. The MAPKKK gene *YODA* (*YDA*), is a central molecular switch that controls promotion or restriction of stomatal cell fate. The loss-of-function mutant (*yda*) produced excessive stomatal formation with severe defects in the one-cell spacing rule with the constitutively active form of *YDA* resulting in a complete lack of guard cells (Bergmann *et al.*, 2004). *yda* mutants are generally seedling lethal, though some plants can progress to maturity but remain severely dwarfed in appearance (Bergmann *et al.*, 2004). Phenotypic and genetic analysis determined that *YDA* functions downstream of both *TMM* and *SDD1* to regulate stomatal development (Bergmann *et al.*, 2004). Bergmann *et al.* (2004) developed transgenic plants with a constitutively active form of *YDA* (ΔN -*YDA*) and these show a gain-of-function phenotype of no stomata, opposite to that of *tmm* and *sdd1* mutant phenotypes (Bergmann *et al.*, 2004). Plants containing a single copy of ΔN -*YDA* (ΔN -*YDA*^{+/+}) showed wild-type levels of stomata but suppressed the phenotypes of *sdd1* and *tmm* (with no clustering), indicating that *YDA* acts downstream of *SDD1* and *TMM* within the stomatal lineage (Bergmann *et al.*, 2004).

Wang *et al.* (2007) were able to identify components acting downstream of *YDA*. Plants in which *MKK4* and *MKK5* (*MKK4-MKK5RNAi*) were down-regulated, or knockouts in both *MPK3* and *MPK6* (*mpk3 mpk6*) showed severe stomatal

clustering (Wang *et al.*, 2007). RNAi gene-silencing plants of *MKK4* (*MKK4RNAi*) and *MKK5* (*MKK5RNAi*) showed a weak phenotype of clustered stomata (Wang *et al.*, 2007). *MKK4-MKK5RNAi* double mutant phenotype showed dramatic stomatal development and patterning defects with some epidermal layers composed exclusively of stomata indicating *MKK4* and *MKK5* have overlapping function in negatively regulating stomatal development and patterning (Wang *et al.*, 2007). Single loss-of-function mutants of *MPK3* and *MPK6* showed no obvious phenotype whilst the double mutant was embryo lethal (Wang *et al.*, 2007). Wang *et al.* (2007) generated an *MPK3* RNA interference construct which was transformed in to *mpk6* (*mpk6^{-/-} MPK3RNAi*) to create a no-null double mutant (Wang *et al.*, 2007). Phenotypic analysis resulted in excessive stomatal clustering indicating that *MPK3* and *MPK6* overlap in function to negatively regulate stomatal development and patterning (Wang *et al.*, 2007). Rescue of *MKK4-MKK4RNAi*, *mpk3 mpk6* and *mpk6^{-/-} MPK3RNAi* generated the same phenotypes which suggested that *MKK4/MKK5* and *MPK3/MPK6* function within the same stomatal development pathway (Wang *et al.*, 2007). Wang *et al.* (2007), generated an inducible *GVG-Nt-MEK2^{DD}* line (tobacco homolog of *Arabidopsis MKK4* and *MKK5*) which when induced suppressed the phenotypic stomatal clustering observed in the single T-DNA insertional mutant of *YDA* (*yda^{-/-}*) (Wang *et al.*, 2007). The induced double mutant (*GVG-Nt-MEK2^{DD} yda^{-/-}*) showed less clustering which suggested *MKK4/MKK5* may function downstream of *YDA* (Wang *et al.*, 2007). Using the constitutively active ΔN -*YDA*, Wang *et al.* (2007), performed in-gel kinase assay of *MPK3* and *MPK6* to demonstrate that the kinases were indeed activated and that they were likely functioning downstream of *YDA* (Wang *et al.*, 2007).

Using stomatal lineage specific promoters, Lampard *et al.* (2008), have also demonstrated roles for *MKK7* and *MKK9* in the regulation of stomatal development. This study demonstrated that the MAPK signaling regulates stomatal development

at multiple stages, though in most cases, the specific targets have yet to be identified. However, analysis of the SPCH polypeptide sequence revealed that it contains a number of consensus MAPK phosphorylation sites in a region termed the MAPK targeting domain (MPKTD), this region is absent in MUTE and FAMA, suggesting a regulatory role (Lampard *et al.*, 2008). It was demonstrated that SPCH, but not MUTE and FAMA, could be phosphorylated by MPK3 and MPK6 (Lampard *et al.*, 2008). To further analyse the role of the MPKTD in regulating SPCH function, transgenic plants (in a *spch* background) were generated that expressed SPCH variants in which either the MPKTD was deleted, or serine or threonine residues (which can be phosphorylated by MPK3/6) were mutated to non-phosphorylatable alanines (Lampard *et al.*, 2008). Plants expressing these SPCH variants showed an increased number of stomatal lineage cells similar to the 35S:*SPCH* phenotype (Lampard *et al.*, 2008). To further examine key components of the signal cascade, Lampard *et al.* (2008), expressed constitutively active YODA (*CA-YODA*) in a SPCH promoter background in MAPK-related regulator TMM, ER and SDD1 mutants. Lines expressing *sdd1* showed no significant difference, with lines that expressed *tmm* and *er* showing enhanced SPCH activity (Lampard *et al.*, 2008).

Dong *et al.* (2009) identified BREAKING OF ASYMMETRY IN THE STOMATAL LINEAGE (BASL), single mutants produced a phenotype of excessive small epidermal cells and clustered stomata indicating that BASL is required for intrinsic polarity of stomatal lineage divisions. Zhang *et al.* (2015) identified that BASL has three putative MAPK docking motifs. Mass spectrometry revealed that BASL was phosphorylated by MKK5, MPK3 and MPK6 which suggested that BASL operates within the same pathway as the MAPK cascade, this was confirmed using yeast two-hybrid system to show BASL interacts directly with YDA (Zhang *et al.*, 2015). Zhang *et al.* (2015) generated mutants GFP-tagged *basl* mutants to show that phosphorylated BASL polarizes from the nucleus to the cortical crescent and acts as

a scaffold protein to recruit the YDA MAPK cascade, including MPK3/MPK6, in order to determine the differential daughter cell fate and subsequent SPCH degradation (Zhang *et al.*, 2015).

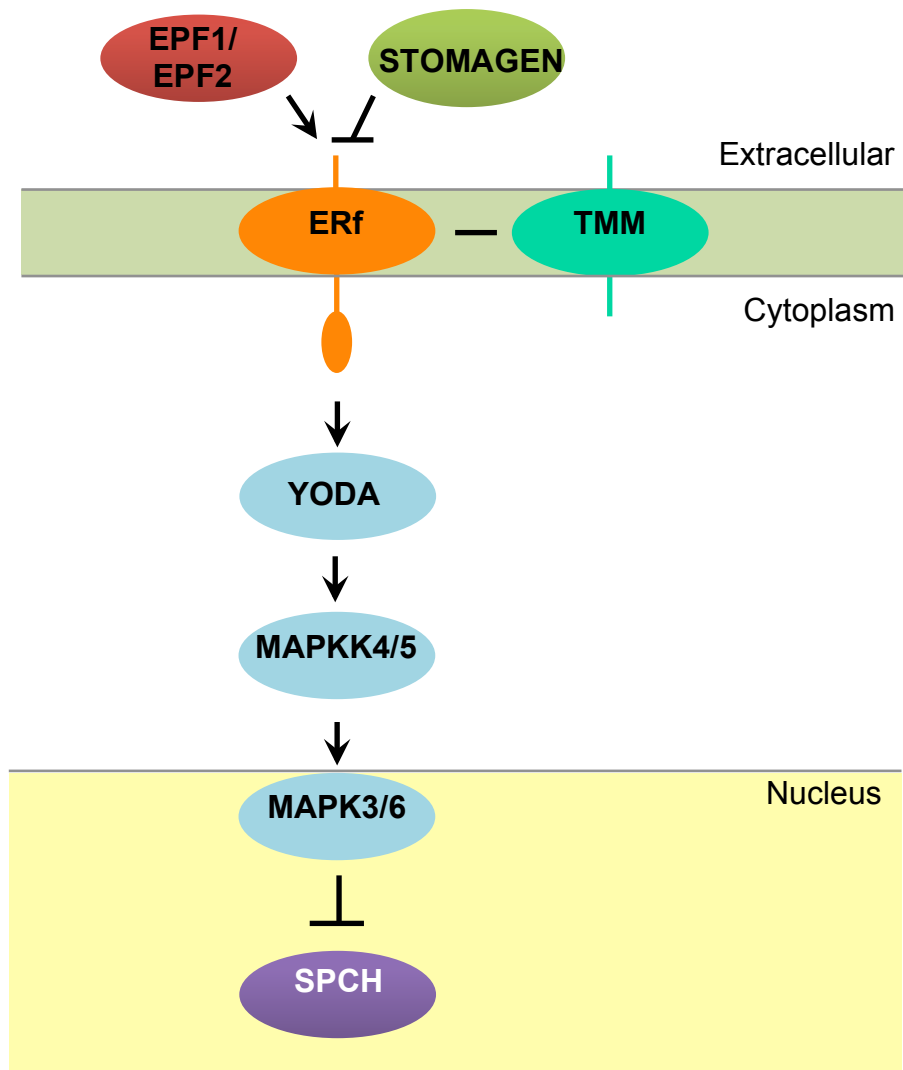


Fig.1.4 Stomatal development in Arabidopsis- Signaling cascade (adapted from Le *et al.*, 2014). EPF1 and EPF2, as negative regulators, are believed to compete with STOMAGEN, a positive regulator, for binding sites to the same ERf receptors. The signal received by ERf-TMM transduces to YODA-MAPK cascade. The YODA-MAPK cascade targets SPCH for degradation. Solid arrows represent positive regulation, closed arrow represents negative regulation and a single line represents interaction.

1.1.2 Environmental Signals and Stomata

Environmental signals such as light and carbon dioxide also regulate stomatal function and development and a number of recent advances have provided insights into the mechanisms involved (Mao *et al.*, 2005; Casson *et al.*, 2009; Kang *et al.*, 2009; Hu *et al.*, 2010; Wang *et al.*, 2010; Takemiya *et al.*, 2013; Casson and Hetherington, 2014; Engineer *et al.*, 2014; Chater *et al.*, 2015; Lee *et al.*, 2017). In the following sections, mechanisms of light and CO₂ perception and signaling will be discussed as well as their roles in regulating stomatal function and development.

1.1.3 Environment Signals: Light

Light (colour irradiance) refers to the visible light range within the electromagnetic spectrum which plants can detect via a range of particles, known as photons. Photons travel in waves which differ in size due to frequency; increased frequencies result in a shorter wavelengths (x-ray, UV) whilst lower frequencies result in longer wavelengths (infrared, radio waves). Visible light forms a small portion of the electromagnetic spectrum that ranges from approximately from 700 nanometres (red-light) to 400 nanometres (violet light). Light is essential for a plant not just because of its role as an energy source for photosynthesis but also its regulatory role in plant physiology and development. The light environment is dynamic and plants are able to perceive changes in the quality, quantity, direction and duration of light signals (Franklin *et al.*, 2005). Plants are able to perceive and respond to light ranging from ultraviolet-B to the near infrared and many of the plant developmental and physiological responses to these wavelengths are mediated by distinct families of photoreceptors. These include the red/far-red perceiving phytochromes and the blue/UV-A perceiving cryptochromes and phototropins (Christie *et al.*, 2015; Xu *et al.*, 2015; Viczián *et al.*, 2017).

1.1.4 Light Signaling Mechanisms

Phytochromes are dimeric photoreceptors with each subunit containing a polypeptide linked to the light-absorbing linear tetrapyrrole chromophore, phytochromobilin (Furuya and Song, 1994; Terry 1997). Structurally they consist of an N-terminal light-sensing domain, where the phytochromobilin is bound, and a C-terminal signaling domain. In the dark (or low light conditions) phytochromes are synthesised in the red-light absorbing Pr form, which is biologically inactive. Absorption of red light leads to photo-conversion to the active and far-red absorbing Pfr form light. This reversible photo-conversion between Pr and Pfr forms means that changes in the light environment can result in a shift in the equilibrium of the active and inactive forms (Pr:Pfr). Genetic analysis has shown that phytochromes regulate a wide range of responses from seed germination, deetiolation, flowering, circadian rhythms and shade avoidance response to stomatal development (Borthwick *et al.*, 1952; Ballaré *et al.*, 1990; Weller *et al.*, 2001; Casson *et al.*, 2009; Xu *et al.*, 2015). In *Arabidopsis* there are five phytochrome apoprotein encoding genes (phyA-E), whilst crops such as wheat and rice have only three (phyA-C) (Li *et al.*, 2015). phyA regulates gene expression and germination in response to very low intensity of UV-A to far-red light (Shinomura *et al.*, 1996). phyA is most abundant in dark grown seedlings with abundance significantly decreasing in the presence of light, making phyA the only known light liable (type I) phytochrome; the remaining phyB-phyE phytochromes are all light stable (type II) (Clack *et al.*, 1994; Sharrock and Clack, 2002; Li *et al.*, 2011). phyB is primarily required for many of the phytochrome regulated processes post-germination (Viczián *et al.*, 2017). However, analysis of single and higher order mutants in each of the phytochrome encoding genes support additive roles for phyC-E, as well as shifts in dominance depending on temperature (Franklin and Quail, 2010).

Phytochromes have been shown to regulate photomorphogenesis by two mechanisms. Firstly, following photoactivation, phytochromes have been shown to translocate to the nucleus to interact with PHYTOCHROME-INTERACTING FACTORS (PIFs) (Monte *et al.*, 2007). The PIFs are a small family (7 members in *Arabidopsis*) of bHLH transcription factors and these act in a mostly redundant manner to regulate gene expression and hence photomorphogenesis. Beyond this, PIFs are central regulators of plant growth and interact with a number of signaling pathways including hormone and temperature signaling pathways (Leivar and Monte, 2014). Interaction with active phytochromes leads to the phosphorylation, ubiquitinylation and subsequent degradation of the PIF and it has been demonstrated that in the case of PIF3, both PIF3 and phyB are degraded (Ni *et al.*, 2014).

A second mechanism by which phytochromes (and cryptochromes; see below) regulate plant responses to light is via inhibition of protein degradation by the CONSTITUTIVELY PHOTOMORPHOGENIC/DEETIOLATED/FUSCA (COP/DET/FUS) complexes (Lau and Deng, 2012). COP1 is a key regulator of light signaling and encodes an E3 ubiquitin ligase that targets key positive regulators of photomorphogenesis for degradation. This includes transcription factors such as ELONGATED HYPOCOTYL 5 (HY5), HY5-HOMOLOG (HYH), REDUCED SENSITIVITY TO FAR-RED LIGHT 1 (HFR1) and CONSTANS (CO) (Holm *et al.*, 2002; Kim *et al.*, 2002; Seo *et al.*, 2003; Mao *et al.*, 2005). Mutants in COP1 therefore resemble light grown plants when grown in the dark (Deng *et al.*, 1991).

Cryptochromes are blue/UV-A light absorbing receptors and can interact to regulate many of the same processes as phytochromes. They are therefore key regulators of photomorphogenic development, photoperiodic flowering and promote stomatal opening in a blue light-induced manner (Casal and Mazzella, 1998; Neff and Chory, 1998; Mockler *et al.*, 1999; Kang *et al.*, 2009; Chen *et al.*, 2012). Cryptochromes consist of an N-terminal photolyase-related domain and a

cryptochrome C-terminal (CCT) domain that is critical for signaling; the flavin adenine dinucleotide (FAD) chromophore is bound to the N-terminal domain (Sancar, 1994; Cashmore *et al.*, 1999; Lin and Shalitin, 2003). In *Arabidopsis* there are three cryptochrome encoding genes (*CRY1-3*), although only *CRY1* and *CRY2* have major roles in light signaling (Zuo *et al.*, 2012; Christie *et al.*, 2015). *CRY1* was first identified in a mutant screen for plants defective in blue light mediated inhibition of hypocotyl elongation (Ahmad and Cashmore, 1993). Both *CRY1* and *CRY2* are nuclear localised but *CRY2* actually undergoes blue-light mediated degradation indicating that it functions preferentially under low light conditions. It is proposed that blue light causes a conformational change and separation of the N and C-terminal domains allowing the CCT domain to interact with signaling partners (Zuo *et al.*, 2012; Christie *et al.*, 2015). This is supported by experiments in which the C-terminal domain of *CRY1* (CCT1) and *CRY2* (CCT2) was overexpressed and resulted in plants with constitutive light signaling phenotypes (Yang *et al.*, 2000).

As with phytochromes, the cryptochromes regulate photomorphogenesis by interacting with transcription factors or by inhibiting COP1 (Zuo *et al.*, 2012; Christie *et al.*, 2015). *CRY2* has been shown to regulate flowering by interacting with several bHLH transcription factors, called Cryptochrome Interacting bHLHs (CIBs). However, unlike phytochrome-PIF interactions, this interaction results in activation of the key flowering time gene, *FLOWERING LOCUS T* (*FT*; Liu *et al.* 2008). Secondly, *CRY1* and *CRY2* can inhibit COP1 degradation of regulators of light signaling. Both *CRY1* and *CRY2* were shown to directly bind COP1 via the C-terminal domain (Wang *et al.*, 2001; Yang *et al.*, 2001; Sang *et al.*, 2005). However, it has been shown more recently that *CRYs* inhibit COP1 function by disrupting the interaction between COP1 and SPA (suppressor of phyA-105) proteins (Zuo *et al.*, 2011).

Phototropins are the principal photoreceptors for blue-light phototropism as well as mediation of critical adaptive responses such as chloroplast movement and

leaf expansion. They are also the major class of photoreceptor associated with stomatal opening and are therefore important for enhancing the photosynthetic status of the plant (Briggs and Christie, 2002; Takemiya *et al.*, 2005; Boccalandro *et al.*, 2012; Sharma *et al.*, 2014; Christie *et al.*, 2015; Mawphlang and Kharshiing, 2017). There are two phototropin genes in *Arabidopsis* (*PHOT1* and *PHOT2*) and the encoded polypeptides consist of two parts; a C-terminal serine-threonine kinase domain and two light, oxygen or voltage (LOV) domains that bind flavin mononucleotides as chromophores at the N-terminus (Christie, 2007; Łabuz *et al.*, 2012). In the absence of blue light, it is proposed that the N-terminal LOV domains form a closed conformation with the C-terminal kinase domain. Blue light then causes a conformational change releasing the repression of the kinase domain (Christie *et al.*, 2015). PHOTs then undergo autophosphorylation on multiple serine residues (Christie *et al.*, 1998), which is required for PHOT mediated responses. Guard cell opening in response to blue light is discussed below however, Takemiya *et al.* (2005), showed that phototropins can also promote growth in response to low intensity blue light. Compared to plants grown solely under red light, plants grown under blue light superimposed on to red light showed a threefold increase in green tissue development (Takemiya *et al.*, 2005). The enhancement was found in *phyA phyB* and *cry1 cry2* but not in *phot1 phot2* double mutants. Further fresh weight analysis of *phot1* and *phot2* single mutants suggested that specifically *phot1* is responsible for the enhancement (Takemiya *et al.*, 2005).

1.1.5 Light Control of Guard Cell Aperture

In guard cells, *phot1* and *phot2* are the main contributors to blue light-induced stomatal opening (Kinoshita *et al.*, 2001; Inoue *et al.*, 2008; Chen *et al.*, 2012). Blue light induced autophosphorylation of the phototropins results in activation of guard cell opening signal transduction pathways, while

dephosphorylation of the serine (Ser) residues of kinases halts the signaling (Inoue *et al.*, 2008). Cytosolic Ca^{2+} is a common second messenger for phot1 and phot2 in blue light induced stomatal opening, with phot1 responsible for Ca^{+} movement under lower light and phot2 under higher blue light (Chen *et al.*, 2012). PHOT1 has been shown to activate the BLUE LIGHT SIGNALING1 (BLUS1) protein kinase, which then phosphorylates and activates the plasma membrane H^{+} -ATPase (Takemiya *et al.*, 2013). Activation of the guard cell H^{+} -ATPase results in the pumping of H^{+} outside of the guard cell membrane and this activates voltage-gated inward-rectifying K^{+} channels (Shimzaki *et al.*, 2007; Kinoshita and Hayashi, 2011; Chen *et al.*, 2012). The increase in K^{+} uptake causes the influx of water generating turgor pressure and thus opening the pore (Shimazaki *et al.*, 2007; Inoue *et al.*, 2010). Although key steps have been outlined, the complete mechanism and associated components remain largely unknown (Chen *et al.*, 2012). Cryptochromes function independently of phototropins in blue-light induced stomatal opening, with a quadruple *cry1 cry2 phot1 phot2* mutant having an additive phenotype compared to the *phot1 phot2* mutant and was virtually insensitive to blue light (Mao *et al.*, 2005). In terms of stomatal opening, cryptochromes and phototropins have been suggested to work additively to regulate blue-light response with crys functioning at higher blue-light fluence rates and phototropins function at high and low fluence rates (Talbot *et al.*, 2003; Mao *et al.*, 2005; Chen *et al.*, 2012). Mao *et al.* (2005) showed that under blue light, *cry1* and *cry2* single mutants showed a reduced stomatal aperture with the *cry1cry2* double mutant having an even further reduction in stomatal aperture indicating CRY1 CRY2 have an additive role in the regulation of stomatal opening (Mao *et al.*, 2005). The *CRY1-ovx* over-expressor line showed the widest stomatal aperture, reinforcing that cryptochromes act as positive regulators of stomatal opening (Mao *et al.*, 2005). Mao *et al.* (2005) further analysed the CRY COP1 relationship by generating a *cry1 cry2 cop1* triple mutant which produced a phenotype similar to *cop1* single mutant when grown under blue light (Mao *et al.*,

2005). This finding coupled with the resultant *cop1* single mutant dark-grown phenotype of constitutively wide stomatal apertures, showed that stomatal opening mediated by CRYs is also mediated through negative regulation of COP1 (Mao *et al.*, 2005).

Red light further promotes blue light mediated stomatal opening and this response was attributed to photosynthetic signals (Assmann and Shimazaki, 1999). However, photosynthetic rate did not appear to regulate stomatal aperture (Baroli *et al.*, 2008). Subsequently, a role for phyB was demonstrated in red light-mediated stomatal opening as well as playing an additive role with the phototropins and cryptochromes in white light-mediated stomatal opening (Wang *et al.*, 2010; Chen *et al.*, 2012). Under red-light, Wang *et al.* (2010), demonstrated that the *phyB* single mutant displayed a reduction in stomatal aperture whilst the over-expressor *PHYB-ovx* line displayed a significant increase in stomatal aperture, showing that phyB positively regulates stomatal opening under red light with similar results observed when grown in blue light but not dark-grown or infrared grown plants which showed no difference to wild-type (Wang *et al.*, 2010). Mutant analysis of *phyB cop1* double mutant showed that, although constitutively open, stomatal aperture was less than the *cop1* single mutant in dark-grown and white light-grown conditions (Wang *et al.*, 2010). This indicated that COP1 is partly involved in phyB-mediated stomatal opening and that other light signaling genes may act redundantly within the *phyb cop1* double mutant (Wang *et al.*, 2010).

1.1.6 Light Regulation of Stomatal Development

In addition to promoting stomatal opening, light also acts as a positive regulator of stomatal development. WT plants (Col-0 and Ws) showed an increased stomatal index when grown under white light; an increase in irradiance resulted in an increase in stomatal and epidermal densities showing that light is a positive regulator of cell fate (Casson *et al.*, 2009). As previously discussed, light is

perceived by photoreceptors and several studies have demonstrated the role of photoreceptors in regulating stomatal development (Casson *et al.*, 2009; Kang *et al.*, 2009; Boccalandro *et al.*, 2009; Casson and Hetherington, 2014). Casson *et al.* (2009) tested mutants defective in *phyA*, *phyB*, *phyC* and *phyD* to determine whether phytochromes are required for light-mediated changes in stomatal development (*phyE* mutants were not tested as they are only available in the stomatal defective Ler background). In white light, phenotypic analysis showed that *phyA*, *phyC* and *phyD* did not significantly contribute to light-regulated stomatal development, whereas *phyB* mutants showed significant differences in SI indicating that PHYB was the dominant photoreceptor required for light-mediated stomatal development (Casson *et al.*, 2009). Casson *et al.*, (2009) also tested mutants defective in *PIF3*, *PIF4*, *PIF5* and *PIF6* under various white light irradiances and showed that *pif4* mutants are also defective in light mediated stomatal development (Casson *et al.*, 2009). In the same work, it was also demonstrated that, under white light conditions, a *phyBpif4* double mutant responded in the same manner as the *phyB* single mutant, indicating PIF4 acts in a phyB-dependent manner to modulate stomatal development in response to light quantity (Casson *et al.*, 2009). Using an inducible *PHYB* (*i-PHYB*) plant line, Casson and Hetherington (2014) demonstrated that changes in stomatal development in young leaves was determined by phyB in mature leaves (Casson *et al.*, 2009).

Alterations in stomatal density have been shown to positively correlate with conductance and transpiration (Boccalandro *et al.*, 2009; Franks *et al.*, 2015). Boccalandro *et al.* (2009) show that white-light grown *phyB* mutant with an end-of-day FR pulse resulted in a larger leaf area and reduced transpiration rate per unit area of leaf compared to WT (Ler) (Boccalandro *et al.*, 2009). Further phenotypic analysis showed that this reduction in transpiration rate correlated with a reduction in SD and SI of *phyB* mutants grown under the same conditions. *phyA* was also

analysed but showed a wild-type phenotype further supporting the dominant role of phyB in light-mediated stomatal development. Transpiration efficiency was then estimated from isotopic discrimination data with the *phyB* mutant showing decreased carbon isotope discrimination compared with the WT (Boccalandro *et al.*, 2009). Carbon isotope discrimination analysis has been shown to be a reliable marker that negatively correlates with plant water use efficiency and so in consideration of this, it was deduced that functional phyB decreases water use efficiency (Boccalandro *et al.*, 2009). These findings help to establish a wider role for phyB in light-mediated long and short-term stomatal responses. Due to phyB showing increased stomatal density, CO₂ uptake was analysed using Infrared gas analysis. The *phyB* mutant showed reduced photosynthetic rate, reduced net CO₂ uptake and lower ratios between intracellular and ambient CO₂ concentrations compared to wild-type which indicate that there are stomatal and non-stomatal (photosynthetic machinery) effects of phyB on water use efficiency (Boccalandro *et al.*, 2009). Stomatal limitations refer to the number of stomata, size and aperture as well as the ability of CO₂ to diffuse in to sub-stomatal cavities through the mesophyll.

Cryptochromes have also been shown to regulate stomatal development. Mutant analysis of the loss-of-function double mutant *cry1cry2* in cotyledons showed that stomatal development was limited in number and size in a blue-light dependant manner; the same phenotype was observed in the *phyB* single mutant in a red-light dependant manner (Kang *et al.*, 2009). A role for COP1 in stomatal development was then shown through the analysis of *cop1* mutants (Kang *et al.*, 2009). *cop1* mutants showed increased stomatal development in the dark, as well as stomatal clustering, which indicated a clear negative role of COP1 in stomatal development and differentiation (Kang *et al.*, 2009). The same study also demonstrated that COP1 genetically acts in parallel with TMM to positively regulate YDA, which is a critical negative regulator of stomatal development and patterning (Bergmann *et al.*,

2004; Kang *et al.*, 2009; Lee *et al.*, 2017). In addition, COP10 has been shown to localise within the nucleus to interact with the COP9 signalosome and enhance COP1 function to negatively regulate stomatal development (Suzuki *et al.*, 2002). Mutant analysis of the loss-of-function *cop10* mutant displayed a phenotype similar to the *cop1* mutant, suggesting they act within the same pathway (Delgado *et al.*, 2012). Recently, it has been shown that COP1 directly interacts with ICE1 and SCRM2/ICE2 in the nuclei under dark conditions and this interaction results in ICE1 and SCRM2/ICE2 degradation to inhibit progression of the stomatal lineage (Lee *et al.*, 2017). In this study, using the same investigative techniques, COP1 was not seen to directly interact with SPCH, MUTE or FAMA (Lee *et al.*, 2017). However, unpublished data from the Casson lab that indicates that COP1 may target SPCH for degradation indicating that COP1 can target major regulators of stomatal development for degradation (James Rowe and Nicholas Zoulias, unpublished data). Therefore, one major mechanism through which phytochromes and cryptochromes regulate stomatal development is by inhibiting COP1 targeting of key bHLH transcription factors (Figure 1.5).

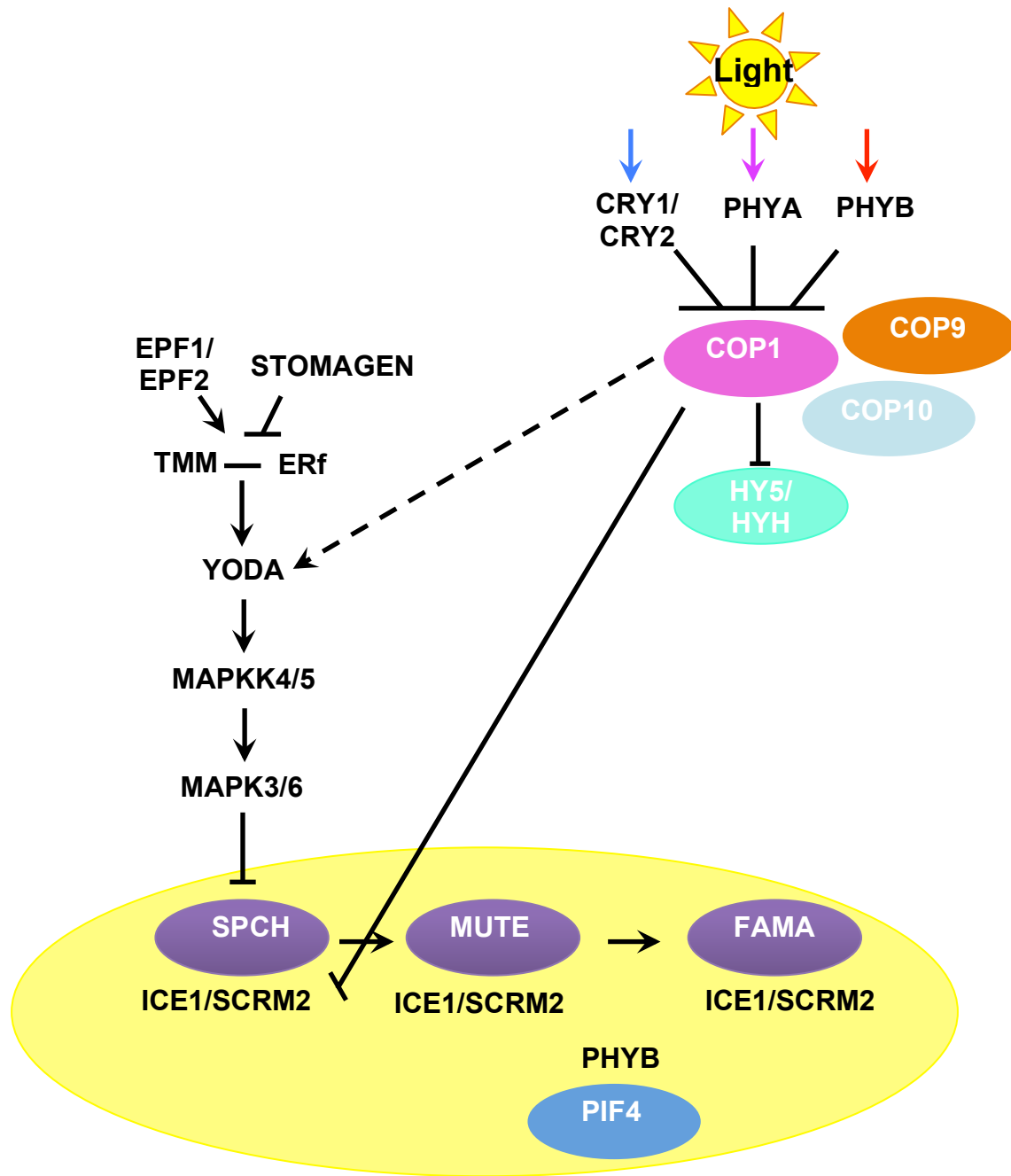


Fig.1.5 Light-mediated stomatal development in Arabidopsis. Light positively regulates stomatal development via activation of the phytochromes and cryptochromes. COP1, a negative regulator of stomatal development, acts genetically upstream of YODA and is itself negatively regulated by light signaling through phytochromes and cryptochromes. The YODA-MAPK cascade targets SPCH for degradation. Solid arrows represent positive regulation, closed arrow represents negative regulation and a single line represents interaction.

1.1.7 Environmental Signals: CO₂

Three carbon isotopes, out of a known fifteen (⁸C to ²²C), are naturally occurring; ¹²C, ¹³C and ¹⁴C. The stable ¹²C and ¹³C isotopes are analysed as a ratio and used as a proxy to determine nutrient cycling and plant water use efficiency as plants naturally discriminate towards the lighter ¹²C isotope for fixation. Widening of the stomatal aperture enables gas exchange where atmospheric CO₂ is up-taken and diffuses through sub-stomatal cavities throughout the palisade and spongy mesophyll layers to the chloroplasts for fixation within the stroma.

1.1.8 CO₂ Signaling Mechanisms

Due to the role of CO₂ within photosynthesis, plants perception of environmental CO₂ concentrations is integral. Low CO₂ concentrations trigger stomatal opening whilst ambient-high CO₂ concentrations mediate stomatal closure. At night, plant respiration occurs which causes a rapid increase of intracellular CO₂ (Hanstein *et al.*, 2001; Engineer *et al.*, 2016). In the presence of light, intracellular CO₂ can rapidly decrease as a result of increased photosynthesis. Long-term plant response to elevated CO₂ is a reduction in stomatal development (Woodward, 1987; Woodward and Kelly, 1995). The cellular sensing of changes in CO₂ concentration is integral for mediating CO₂-induced changes in stomatal movements as well as to influence stomatal development.

1.1.9 CO₂ Regulation of Stomatal Closure

In contrast to the positive role of light, CO₂ signals negatively regulate stomatal development and stomatal pore aperture (Gray *et al.*, 2000; Hashimoto *et al.*, 2006; Teng *et al.*, 2006; Young *et al.*, 2006; Gerhart and Ward, 2010). βCAs (carbonic anhydrase) bind CO₂ and accelerate its conversion into HCO₃⁻ and H⁺ to negatively effect function and development (Hu *et al.*, 2010; Engineer *et al.*, 2016). There are

several β CA genes in Arabidopsis but gene expression analysis showed that β CA1 and β CA4 are highly expressed in guard cells and/or in the mesophyll cells (Hu *et al.*, 2010). To determine if this an impact on guard cell CO₂ signalling, single and higher order mutants were analysed. *ca1ca4* double and *ca1ca4ca6* triple mutant showed strong insensitivities in CO₂-induced stomatal conductance. Lines with *ca6* showed no major role for β CA6 within the CO₂-mediated stomatal response pathway, suggesting that it is β CA1 and β CA4 that primarily regulate guard cell responses to CO₂ (Hu *et al.*, 2010). *ca1ca4* mutants show normal sensitivity to exogenous ABA, consistent with them functioning upstream of a convergence of CO₂ and ABA stomatal closure signalling pathways (Hu *et al.*, 2010). Abscisic acid (ABA) has been shown to enhance CO₂-mediated stomatal response and recent work suggests that CO₂ requires a capacity for ABA biosynthesis to mediate changes in guard cell aperture via ROS (Chater *et al.*, 2015).

HIGH LEAF TEMPERATURE 1 (HT1), which encodes a putative protein kinase, is expressed in guard cells and also functions early within in the stomatal aperture response to CO₂ (Hu *et al.*, 2010). The *ca1 ca4 ht1-2* triple mutant showed a phenotype similar to the *ht1* single mutant showing that HT1 is epistatic to β CA1 and β CA4 (Hu *et al.*, 2010). HT1 has been shown to deactivate via phosphorylation the open stomata 1 (OST1) protein kinase to induce stomatal closure (Xue *et al.*, 2011; Tian *et al.*, 2015). However, it was shown that these genes act epistatically in elevated CO₂-induced stomatal closure (Matrosova *et al.*, 2015). BiFC analysis showed direct interaction between OST1 and the slow anion Channel Associated 1 (SLAC1) to mediate stomatal response (Tian *et al.*, 2015). The same study also clarified the signalling mechanism by demonstrating that HT1 phosphorylated OST1 but not SLAC1 directly and that OST1 does not phosphorylate HT1 (Tian *et al.*, 2015). *slac1* mutant result in impaired slow (S-type) anion channels which are

activated by cytosolic Ca^{2+} and ABA to induce stomatal closure (Vahisalu *et al.*, 2008).

1.2.0 CO₂ Regulation of Stomatal Development

Woodward and Kelly (1995) analysed the effects of CO₂ concentration on stomatal density across 100 plant species (Woodward, 1987; Woodward and Kelly, 1995). The results showed that three-quarters of these species showed a reduction in stomatal density and index values when grown in elevated CO₂ (Woodward, 1987; Woodward and Kelly, 1995). Changes in CO₂ result in changes in stomatal densities, which alter the maximum capacity for conductance (Woodward, 1987; Woodward and Kelly, 1995). Stomatal density has also been shown to strongly influence plant water use efficiency indicating that growth at increased CO₂ is likely to improve WUE in many plant species (Woodward, 1987; Woodward and Kelly, 1995).

One of the first genes to be identified as having a role in CO₂ mediated regulation of stomatal development was *HIGH CARBON DIOXIDE (HIC)* (Gray *et al.*, 2000). *hic* loss-of-function mutant disrupted response to CO₂ signals and showed increased stomatal density when grown in elevated CO₂ concentrations, which suggests that HIC plays a negative role in stomatal development (Gray *et al.*, 2000). HIC encodes a 3-ketoacyl-CoA synthase, which are required for cuticular wax biosynthesis. Whilst cuticle wax has the potential to impact on plant conductance, the mechanism by which the gene mediates stomatal development within the CO₂ signal response pathway remains elusive. However, there does appear to be a link between cuticular wax and stomatal development as the same study showed that *cer1* and *cer6* mutants also show defects in stomatal development (Gray *et al.*, 2000).

More recently, the Schroeder lab identified a number of components in the pathway through which CO₂ regulates stomatal development. Having previously shown that carbonic anhydrases are required for guard cell aperture responses to CO₂ (Hu *et al.*, 2010), they were able to demonstrate that they also required for correct stomatal development (Engineer *et al.*, 2014). *ca1ca4* double mutants had been shown to display strong insensitivity to CO₂-induced stomatal closure (Hu *et al.*, 2010). In the case of stomatal development, *ca1ca4* mutants showed an increase in stomatal density in elevated CO₂, which is the opposite to the response of wild-type plants (Engineer *et al.*, 2014). They next used RNA-seq analysis to probe responses to elevated CO₂ in both wild-type and *ca1ca4* mutants. *EPF2* was found to be induced by elevated CO₂ in wild-type but not *ca1ca4* mutants suggesting it may be required for phenotypic responses to elevated CO₂. Analysis of *epf2* mutants confirmed that they are defective in their response to elevated CO₂, showing the same inverted response (increase rather than decreased stomatal index) as *ca1ca4* mutants. Using a proteomic approach they were then able to identify an extracellular protease that is required for responses to CO₂. The extracellular CO₂ RESPONSE SECRETED PROTEASE (CRSP) was targeted to cell walls to negatively regulate stomatal development in elevated CO₂ (Engineer *et al.*, 2014). The loss-of-function *crsp* mutant phenotype was less severe than that of the *epf2* mutant phenotype, which suggested that the two genes could function in the same response pathway. Further proteolytic analysis showed that CRSP cleaves the EPF2 propeptide, but not those of EPF1 or STOMAGEN (Engineer *et al.*, 2014). Cleavage by CRSP activates EPF2 to initiate the inhibition of stomatal development via the receptor kinase ER and MPK cascade (Engineer *et al.*, 2014).

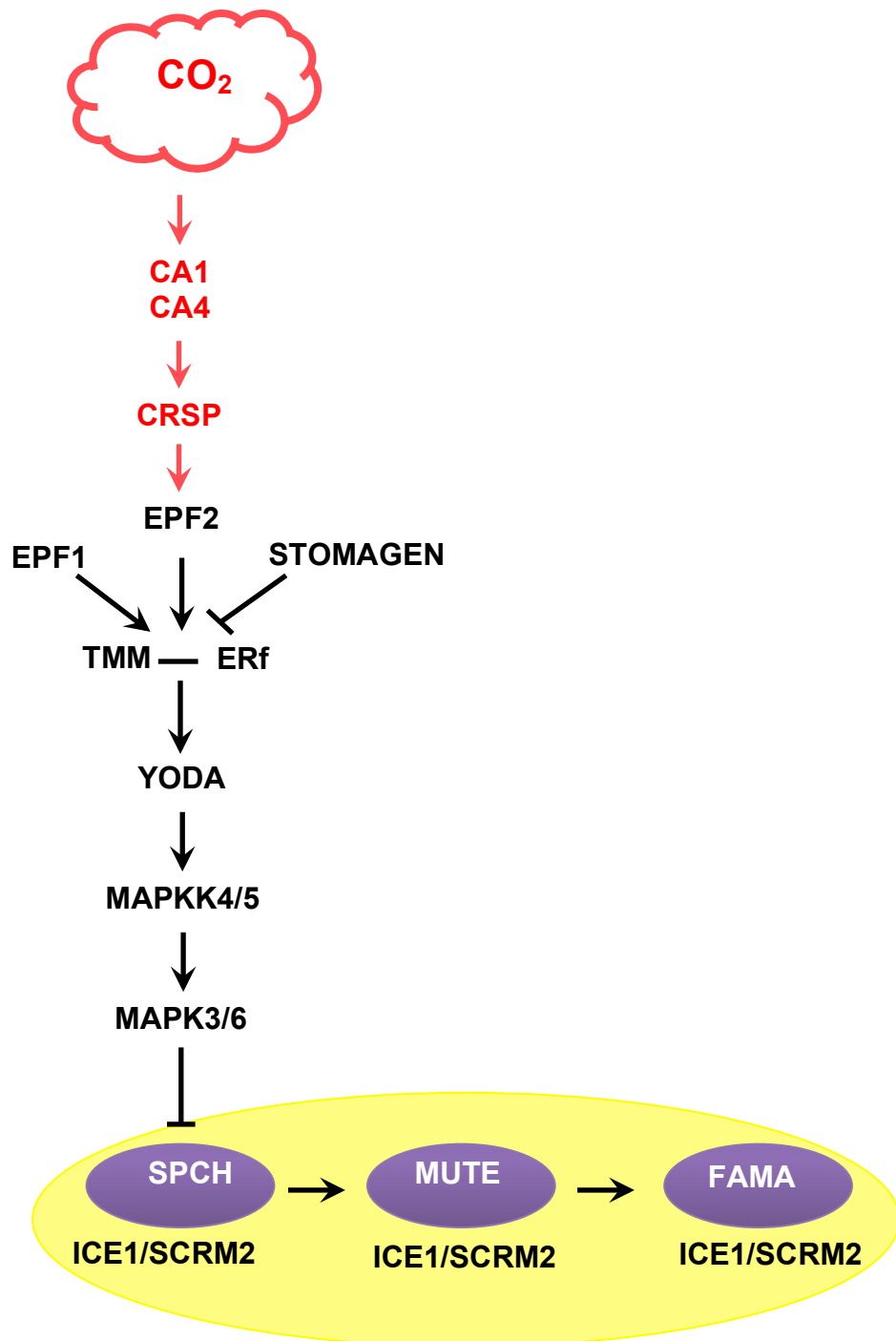


Fig.1.6 CO₂-mediated stomatal development in Arabidopsis. CO₂ negatively regulates stomatal development through CA1 and CA4, β carbonic anhydrases, which perceive intracellular CO₂ to promote CRSP, a protease, which cleaves EPF2 to activate Erf-TMM transduction to YODA-MAPK cascade. The YODA-MAPK cascade targets SPCH for degradation and negatively regulates stomatal development. Solid arrows represent positive regulation, closed arrow represents negative regulation and a single line represents interaction.

1.2.1 Environmental Signals: Hormones

Recent work has established that plant hormones including auxin, brassinosteroids (BRs) and abscisic acid (ABA) regulate stomatal development (Israelsson *et al.* 2006; Kim *et al.* 2012; Gudesblat *et al.* 2012). Auxin is a master regulator of plant development and is required for coordination of placement (phyllotaxy) and patterning of organs and cells. Le *et al.* (2014) showed that auxin pathway control is required for correct stomatal patterning and that auxin depletion in meristemoids acts as a switch resulting in a change from asymmetric meristemoid division to symmetric GMC division. Balcerowicz *et al.*, (2014b) showed that auxin controls stomatal spacing irrespective of irradiance. Transgenic and gene expression analysis showed that MONOPTEROS (MP) repressed STOMAGEN in the presence of auxin (Sugano *et al.*, 2010; Zhang *et al.*, 2014; Balcerowicz and Hoecker, 2014). Auxins may also play a role in guard cell aperture control, regulating stomatal opening by activating inward K⁺ ion channels but high concentrations result in stomatal closure (Lohse and Hedrich, 1995).

Brassinosteroids have been shown to regulate stomatal development via regulation of both SPCH and YDA. Insights into the role of BRs in the regulation of stomatal development, were determined by examination of plants with either loss-of-function or overexpression of components of the brassinosteroid signaling and biosynthesis pathways (Gudesblat *et al.*, 2012; Kim *et al.*, 2012). Brassinosteroid insensitive lines produced stomatal clusters and application of brassinolide (BL: the most active form of brassinosteroid) reduced stomatal density through SPCH, indicating that brassinosteroid acts as a negative regulator of stomatal development (Kim *et al.*, 2012). Gudesblat *et al.* (2012) demonstrated that BRASSINOSTEROID INSENSITIVE 2 (BIN2) phosphorylated SPCH activity. Mass spectrometry analysis showed that this phosphorylation occurred at specific serine and threonine residues in and outside of the MAPK target domain (Gudesblat *et al.*, 2012). These findings

resulted in Gudesblat *et al.* (2012) concluding that BRs act as positive regulators of stomatal development by inhibiting BIN2-mediated phosphorylation and subsequent inactivation of SPCH, enabling progression through the stomatal lineage (Gudesblat *et al.*, 2012). However, in opposition to this, work conducted by Kim *et al.* (2012) concluded that BRs negatively regulate stomatal development. Mutants deficient in BR perception or downstream signalling displayed a clustered stomata phenotype. The loss-of-function quadruple mutant *BSU1*-related phosphatases (*bus-q*) produced a phenotype of entirely stomata. Also, stomatal density was reduced when seedlings were treated with BRs indicating BRs negatively regulate stomatal development (Kim *et al.*, 2012). *BZR1* (*bzr1-d*) gain-of-function mutants showed normal stomatal numbers with clustering and were insensitive to BR, suggesting that *BZR1* plays no role in affecting stomatal development (Kim *et al.*, 2012). *bin2* mutants defective in the activity of serine/threonine Glycogen Synthase Kinase 3 (GSK3)/ SHAGGY-like-kinase displayed fewer stomata (Kim *et al.*, 2012). These findings suggested that GSK3-like kinases are responsible for convergence between BR and stomatal development pathways (Kim *et al.*, 2012). BIN2 was shown to bind and phosphorylate YODA resulting in a reduction in YDA-mediated phosphorylation of MKK4. So by negatively regulating YDA, BIN2 therefore promotes stomatal development (Kim *et al.*, 2012). The difference in conclusions between Gudesblat *et al.* (2012) and Kim *et al.* (2012) could be explained by the difference in tested tissues. Gudesblat *et al.* (2012) analysed hypocotyl epidermis whereas Kim *et al.* (2012) analysed cotyledons. Casson and Hetherington (2012) hypothesise that the difference in response to the BR hormone may be a result of differences in gibberellin response within each tissue, as gibberellin is required for stomatal formation in hypocotyls but not within cotyledons (Casson and Hetherington, 2012).

Abscisic Acid (ABA) regulates growth and development in response to environment signals such as drought and also plays an important role in regulating

guard cell function. Phenotypic analysis of ABA-deficient mutant (*aba2-2*) resulted in an increased number of stomata whilst the ABA-over-accumulating mutant (*cyp707a1a3*) generated a reduced number of stomatal (Tanaka *et al.*, 2013). Further work on ABA-insensitive mutants *abi1-1* and *abi2-1* showed increased stomatal development, which supports ABA as a negative regulator (Tanaka *et al.*, 2013). Expression analysis of key stomatal development genes, *SPCH* and *MUTE* in WT plants treated with exogenous ABA resulted in decreased expression (Tanaka *et al.*, 2013). *SPCH* and *MUTE* expression increased in the loss-of-function and ABA-insensitive mutants but was reduced in the gain-of-function mutant (Tanaka *et al.*, 2013). ABA inhibits entry in to the stomatal lineage by repressing *SPCH* and *MUTE* to reduce stomatal development.

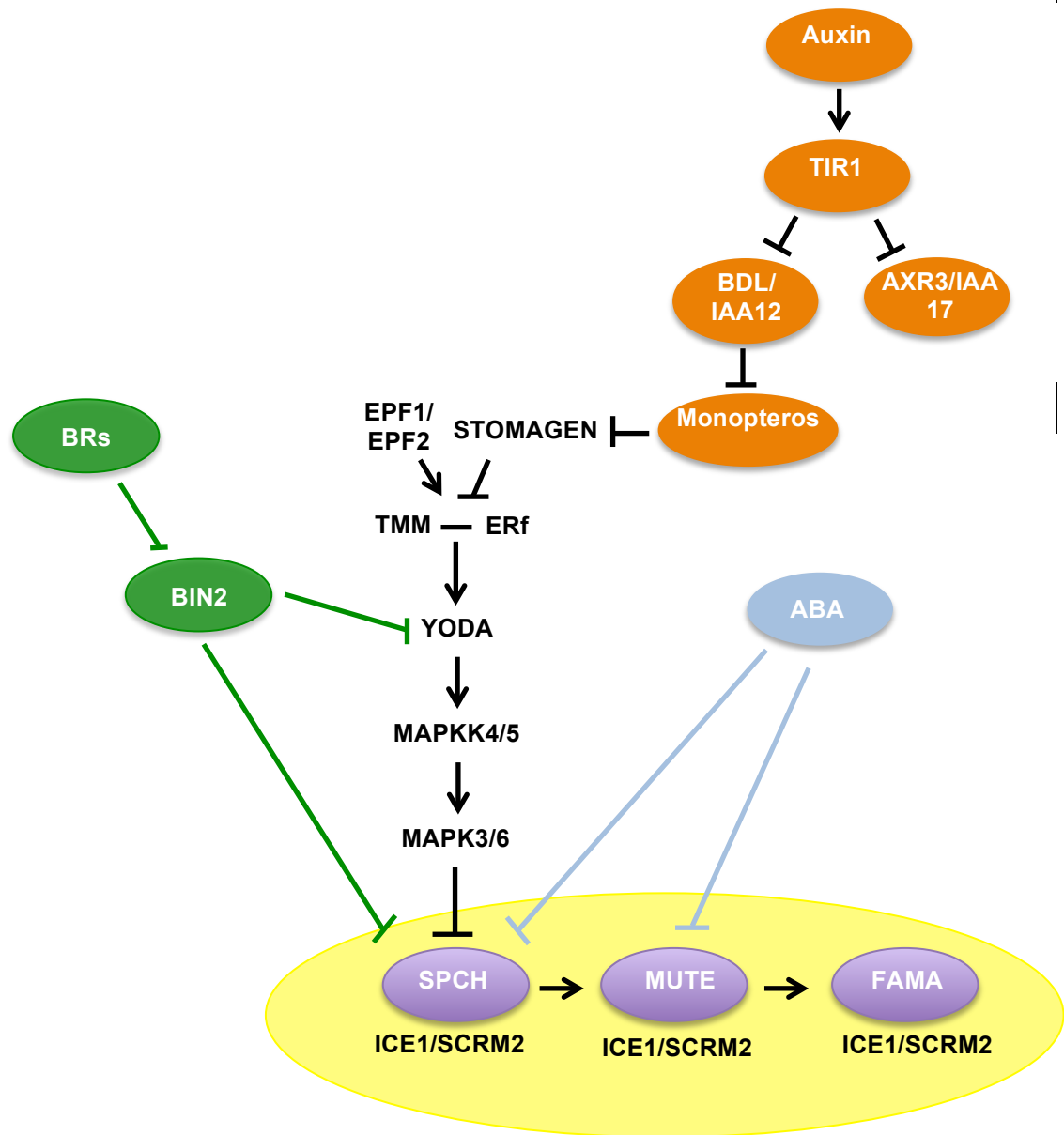


Fig.1.7 Hormone-mediated stomatal development in Arabidopsis. Auxin negatively regulates stomatal development by regulating MONOPTEROS, which negative regulates STOMAGEN expression. STOMAGEN binds to ERf receptors to inhibit YODA-MAPK cascade which enables promotion of SPCH and positively regulates stomatal development. BRASSINOSTEROIDS (BRs) can both positively and negatively regulate stomatal development through BIN2; BRs cause degradation of BIN2. BIN2 in turn can negatively regulate stomatal development by phosphorylating SPCH or positively regulate stomatal development by inhibiting YODA-MAPK cascade to promote SPCH stability. Solid arrows represent positive regulation, closed arrow represents negative regulation and a single line represents interaction.

1.2.2 Aims

An overall genetic pathway of light-controlled stomatal development has advanced the understanding of the regulatory light signal mechanism. However, it remains unknown how light signaling interacts with other environmental signals such as that of CO₂ to impact intrinsic developmental pathways. The aim of this study is to establish, *in vivo*, the impact of photoreceptor signaling on CO₂ signal response within the context of stomatal development and function.

2.0 Chapter 2:

Materials and Methods

2.0.1 General Laboratory Chemicals

All chemicals from Fisher Scientific unless stated otherwise.

2.0.2 Seed Lines

Table 2.1 Table showing the seed lines used for analysis of stomatal development.

Name	Allele	Reference
Col-0	Columbia-0	
<i>phyB</i>	<i>phyB-9</i>	NASC N6217, donated by Jason Reed. Reed <i>et al.</i> (1993)
<i>35SproPHYB::YFP</i>	<i>35SproPHYB::YFP</i> in <i>phyB-9</i>	Casson and Hetherington (2014)
<i>cry1cry2</i>	<i>cry1-304, cry2-1</i>	Mockler <i>et al.</i> (1999)
<i>phyB cry1 cry2</i>	<i>phyB-9, cry1-304, cry2-1</i>	This study
<i>hy5</i>	Salk_096651	Chen <i>et al.</i> (2008)
<i>hyh</i>	DsLox235D10	This study
<i>hy5 hyh</i>	Salk_096651, DsLox235D10	This study
<i>phyB hy5</i>	<i>phyB-9, Salk_096651</i>	This study
<i>pif4</i>	<i>pif4-101</i> (SAIL_1288_E07)	Lorrain <i>et al.</i> (2008)
STOM RNAi	<i>EPFL9RNAi-1</i>	Hunt <i>et al.</i> (2010)
<i>epf2</i>	<i>epf2-1</i> (Salk_102777)	Hunt and Gray (2009)
<i>phyB epf2</i>	<i>phyB-9, epf2-2</i>	This study
<i>crsp</i>	Salk_132812c	Engineer <i>et al.</i> (2014)
<i>phyB crsp</i>	<i>phyB-9, Salk_132812c</i>	This study
<i>ca1 ca4</i>	Salk_106570, WISCDSLOX508D11	NASC N66122, Hu <i>et al.</i> (2010)
<i>phyB ca1 ca4</i>	<i>phyB-9, Salk_106570, WISCDSLOX508D11</i>	This study

2.0.3 ½ Murashige and Skoog (MS) Media

2.2 g/L MS media (SIGMA-ALDRICH, M5519-50L). pH solution using 1 M KOH to pH 5.7 and make up to 1 L dH₂O. Weigh 0.7% (w/v) Plant Agar (Duchefa Biochemie, 1100 g/cm², P1001) in to a Duran bottle and add ½ MS media, autoclave at 121⁰C for 30 minutes.

2.0.4 Seed Sterilisation

Seeds were dehydrated for 3-5 minutes at room-temperature in 70% ethanol then aspirated. The seeds were then incubated in 1% sodium hydrochlorite (5% sodium hydrochlorite stock) and 0.1% Tween-20 for 20 minutes and washed three times with autoclaved water in a flow hood.

2.0.5 Plant Growth Conditions

All plants were grown on F2+S Levington, Everris Professional soil mixed with insecticide (NilNat) or ½ MS media and stratified at 4⁰C for 2-3 days, then placed under an 11 hour photoperiod. Experiment conditions include 250 μmol m⁻² s⁻¹ (high light), 130 μmol m⁻² s⁻¹ (optimum light), and 50 μmol m⁻² s⁻¹ (low light). Adjustments to irradiances were achieved using Lee Filters Neutral Density Filters and measured using a light meter (Apogee Model MQ-200 Quantum meter). Experimental CO₂ conditions include 200 ppm (sub-ambient [CO₂]), 500 ppm (ambient [CO₂]) and 1000 ppm (high [CO₂]). Sub-ambient [CO₂] was achieved using soda lime to scrub [CO₂] levels from ambient to 200 ppm. Ambient and high [CO₂] concentrations (500 ppm and 1000 ppm) were achieved using additive [CO₂] injections. Adjustments to [CO₂] concentrations were achieved within a controlled growth chamber. Sub-ambient [CO₂] conditions were achieved using a Conviron BDR 16 cabinet fitted with a soda-lime scrub with an additive [CO₂] injection to achieve 200 ppm. Ambient and high [CO₂] conditions were achieved using Sanyo-Gallenkamp SGC970/P/PLL with

an additive [CO₂] injection to achieve 500 ppm and 1000 ppm. Growth chamber parameters were set to day (07:00 lights on, 20⁰C, 65% RH) and night (18:00 lights off, 16⁰C, 65% RH) and were fitted with 22x Philips Master PI-L 55W/84°/4P or 48x Phillips TL4-HO 39W (fluorescent) bulbs.

2.0.6 Genomic DNA Extraction

A leaf disc (approx 1 cm diameter) or several young seedlings were ground in 400 µl Edward's Solution/ Extraction Buffer (200 mM Tris-HCl (pH 7.5), 250 mM NaCl, 25 mM EDTA, 0.5% SDS) using a pestle and centrifuged at 13500 rpm for 5-10 minutes. The supernatant was transferred to another 1.5 ml Eppendorf with 400 µl isopropanol (Fisher Scientific Laboratory Grade Propan-2-ol, 1067432), sample was mixed and centrifuged at 13500 rpm for 5-10 minutes to pellet sample. The supernatant was aspirated without disturbing the pellet and air dried for 5 minutes. The pellet was reconstituted in 100 µl sterile H₂O and vortexed to mix and stored at -20⁰C (Edwards *et al.*, 1991).

2.0.7 Polymerase Chain Reaction (PCR)

The following method has been adapted from Sigma Aldrich JumpStart™ RedTaq® ReadyMix™ PCR Reaction technical bulletin. PCR components, including autoclaved H₂O, forward and reverse primers (100µM stocks), DNA template and RedTaq (Sigma-Aldrich JumpStart™ RedTaq® ReadyMix™ PCR Reaction Mix with MgCl₂) were melted at room temperature.

Table 2.2 shows components and volumes based on required for PCR analysis.

50µl Reaction (2X)	
Component	Volume/Reaction (µl)
Primer A (100pmol/µl)	0.5
Primer B (100pmol/µl)	0.5
Sterile H ₂ O	19
RedTaq	25

Method adapted from Sigma Aldrich JumpStart™ RedTaq® ReadyMix™ PCR Reaction technical bulletin, showing the components and appropriate volumes to conduct PCR analysis.

2X master mix was prepared according to the amount of samples used. 22.5 µl of master mix was pipetted in to each PCR tube (0.2 ml). 2.5 µl of template DNA was in to each tube, mixed and briefly centrifuged to spin down the contents and eliminate air bubbles. Samples were loaded in to the thermal cycler using the set-up shown in table 2.3. Reaction volume was set to 25 µl for 35 cycles. Results were analysed by running 1% agarose gel.

Table 2.3 shows the thermal profile, incubation temperature and times, for PCR.

	Step 1	Step 2	Step 3	Step 4	Step 5	Step 6	Step 7
Temperature (°C)	95	95	55	72	Repeat	72	12
Time	3 min	30 sec	30 sec	1 min	steps 2-4 for 35 cycles	5 min	∞

Method adapted from Sigma Aldrich JumpStart™ RedTaq® ReadyMix™ PCR Reaction technical bulletin showing the incubation temperature and times required for the denaturing, annealing and elongation steps during 35 cycles required for PCR analysis.

2.0.8 Gel Electrophoresis

PCR products and RNA integrity were visualised using DNA separation in a gel via electrophoresis. X6 loading buffer (0.2% w/v bromophenol blue, 50% v/v glycerol) was added to samples up to a total volume to 10-15 µl and vortexed to mix. 1%

Agarose (Sigma Agarose Gelpowder) was mixed with 50X TAE Buffer stock (diluted to 1X with greenline H₂O): 242 g Tris Base, 57.1 ml Glacial Acetic Acid, 100 ml 0.5 M EDTA adjust to 1 L with greenline H₂O (1X TAE: 200 ml 50X TAE stock, 9.8 L greenline H₂O) and microwaved for 1-2 minutes to dissolve. Alfa Aesar Ethidium Bromide C₂₁H₂₀BrN₃ (10 mg/ml) was added to the liquid solution to act as a fluorescent indicator. The liquid solution was poured in to a transparent gel tray fitted with a comb to create wells. The gel was submerged in 1X TAE buffer and samples loaded in to each well including a DNA ladder (2.5 µl GeneRuler, DNA LadderMix ready-to-use 0.1 µg/L, 50 µg) to determine DNA fragment sizes. Gel was run at 120 V for 20-30 minutes using BioRad mini sub-cell and power supply. Gels were visualised using GelDoc-It™ system (UVP LLC) and images were taken using VisionWorks® LS analysis software (UVP LLC).

2.0.9 RNA Extraction

The protocol followed is in accordance with the Quick-RNA™ MiniPrep (Zymo Research, Cambridge Biosciences R1055a). RNA extraction also included a DNase treatment. RNA concentrations were measured at 595 nm using the 'Nucleic Acid', 'RNA-40' option on the NANODROP-8000 Spectrophotometer V1.1 (ThermoScientific). RNase-free H₂O was used as a blank, 2 µl of blanking buffer and extracts were loaded on to the reading pin.

2.1.0 cDNA Synthesis

The following protocol was adapted from Applied Biosystems High Capacity cDNA Reverse Transcription Kit. The protocol was conducted using up to 2 µg of total RNA per 20 µl reaction as specified and included an RNase inhibitor (RiboLock, Fisher Scientific 10859710). Using the table provided in the protocol manual, the volumes of each component needed to prepare the master mix were calculated in accordance the number of reactions. The RNase Inhibitor and Nuclease-free H₂O

volumes were adjusted in order to optimise the reaction. Additional reactions were factored in to the calculations to account for any loss that may occur during reagent transfers between eppendorfs.

Table 2.4 Table showing the components and volumes required for cDNA synthesis.

Component	Volume/Reaction (µL)	
	Kit <u>with</u> RNase Inhibitor	Kit <u>without</u> RNase Inhibitor
10X RT Buffer	2.0	2.0
25X dNTP Mix (100mM)	0.8	0.8
10X RT Random Primers	2.0	2.0
MultiScribe™ Reverse Transcriptase	1.0	1.0
RNase Inhibitor	0.5	-
Nuclease-free H ₂ O	3.7	4.2
Total per Reaction	10.0	10.0

Applied Biosystems High capacity cDNA Reverse Transcription kit protocol was followed to produce cDNA from template RNA for qPCR analysis.

2X RT master mix was placed on ice and mixed gently. 10 µl of 2X RT master mix was pipetted into each well of the reaction plate or individual tube. 10 µl (2 µg) of RNA sample was pipetted in to each well and the reaction plate or tubes were then sealed. The plate was briefly centrifuged to spin down the contents to eliminate any air bubbles. To perform Reverse Transcription, the thermal cycler must be programmed with the following thermal profile.

Table 2.5 Table showing the thermal profile, incubation temperature and times, for cDNA synthesis.

	Step 1	Step 2	Step 3	Step 4
Temperature (°C)	25	37	85	4
Time	10 min	120 min	5 min	∞

Applied Biosystems high capacity cDNA Reverse Transcription kit protocol showing the incubation temperature and times required for the denaturing, annealing and elongation steps required for cDNA synthesis.

Reactions were loaded into the thermal cycler and the reaction sample volume was set to 20 µl. 10 µl of the cDNA was diluted to 5 µg/ml for qPCR, remaining undiluted cDNA (stock) was stored at -20°C.

2.1.1 qPCR Analysis

The following protocol was adapted from Thermo Scientific Maxima SYBR Green/ ROX qPCR Master Mix (K0221).

Table 2.6 Components and reaction volumes required for qPCR analysis.

Component	Volume/ Reaction (µl)
X2 SYBR Green qPCR Mix	10
Primer Mix	1
Autoclaved H ₂ O	1.2
cDNA	5
MgCl ₂ solution (25mM)	2.8
Total	20

Thermo Scientific Maxima SYBR Green/ ROX qPCR Master Mix (K0221) protocol was followed to prepare cDNA templates for qPCR analysis.

The components when combined total a single reaction volume of 20 µl used for one well. Primer mix is comprised of both a forward and reverse primer used to target a gene of interest, each primer concentration was 7.5 pmol/µl and 1 µl of this primer mix was used per 20 µl reaction. 'Primer mix' refers to combined forward and reverse primers used to target a specific gene sequence, each primer concentration was 7.5 pmol and 1 µl was used per reaction. House-keeping genes, actin (ACT2) and ubiquitin (UBC21), were used as reference genes to standardise expression across the test samples as both genes are expressed uniformly and their expression is stable across a number of treatments. In order to correctly configure the BIO-RAD CFX Manager 3.1 software, BIO-RAD CFX Connect Real-Time System should be switched on prior to configuration. Ensure each well has been labelled to ease subsequent data interpretation.

Table 2.7 Thermal profile, incubation temperature and times, for qPCR analysis.

	Step 1	Step 2	Step 3	Step 4	Step 5	Step 6	Step 7
Temperature (°C)	95	95	57	72	Repeat steps 2-4 for 39 cycles	95	65
Time	2 min	15 sec	15 sec	20 sec		10 sec	5 sec

Thermal profile comprising the incubation temperature and times required for the denaturing, annealing and elongation steps required for excitation of SYBR Green fluorophores used in qPCR analysis.

Data analysis is interpreted by first establishing the baseline and threshold values, this is achieved by removing the reference gene ROX values to produce raw cycle threshold (CT) values. View the dissociation curve for the entire plate to check for anomalies and to determine relative fold change in gene expression ($2^{-\Delta C_T}$). Using excel software, the following layout was used to interpret qPCR data.

Table 2.8 Layout of excel table used to interpret qPCR data to determine the rate of expression of a sample relative to a control.

Sample Name	Threshold	Ct Value	Δ	Average Δ	$\Delta\Delta$	minus	2Ln
-------------	-----------	----------	----------	------------------	----------------	-------	--------------

Template used to analyse and interpret qPCR data to determine rate of expression of a test sample relative to a control.

Ct refers to the number of cycles required for the fluorescence signal to surpass background expression levels (threshold). Ct values are inversely proportional to the amount of target nucleic acid present within the same sample. delta (Δ) is the sample Ct value minus the control Ct value (use Actin and Ubiquitin values as controls). Average delta (average Δ) is used to find the mean value between biological and technical replicates. Delta delta ($\Delta\Delta$) normalises expression between specific test values which is then inverted to produce the opposite sign, either positive or negative. 2 Ln (natural log) is used to establish gene expression of the test sample relative to your control; zero relative expression is shown as 1.

2.1.2 Stomatal Impressions

The following protocol from was adapted from Weyer and Johansen (1985). x15 fully expanded and healthy mature leaves (three leaves from five plants, per plant line) were selected for stomatal impressions used for cell counts. Dental resin (coltene, PRESIDENT, light body dental resin) was applied to the abaxial surface of the leaves and allowed to set. Leaf material was removed and impressions coated with one layer of clear nail varnish. Clear tape was placed over the clear nail varnish and mounted on to slides for microscopic imaging.

2.1.3 Microscopy

A Leica DM IRBE Inverted Microscope with Planachromat 20x/ 0.4 ∞ / 0.17-A lens was used to image impressions. Micro-Manager 1.4 software was used to acquire

Z-stack files of 3 points on a mature leaf (base (b), middle (m) and tip (t)). A single image of a calibration slide (1 division = 0.01 mm) under the same set-up and was used to calibrate images for counting.

2.1.4 Stomatal Counting

Each Z-stack file was opened through ImageJ software, which was calibrated at the beginning of each counting session. The calibration image was used to set the scale option for counting, with a distance of 1296 pixels equating to 60 divisions on the calibration slide. $60 \times 10 \mu\text{m}$ (0.01 mm) = $600 \mu\text{m}$, which is the known distance value. The pixel aspect remained 0.1 and the unit of length was set to ' μm '. The scale option is used to establish a 400×400 pixel region of interest to begin the count. Stomata and epidermal cells with a surface area 50% or more inside the region of interest were counted separately and stored using excel. The data was analysed by calculating the SI and SD per condition or per control/mutant:

$$\text{Stomatal Index (SI)} = (\text{total stomata} / \text{total stomata} + \text{total epidermal cells}) \times 100$$

$$\text{Stomatal Density (SD)} = \text{total stomata} / \text{mm}^2$$

2.1.5 Infra-red Gas Analysis

The protocol followed is in accordance with the LI-6400XT gas analyser ver.6.2 user manual (licor.com/perm/env/LI-6400/Manual/Using_the_LI-6400XT-v6.2.pdf). Plants were grown in controlled conditions at 200 ppm (sub-ambient [CO_2]), 500 ppm (ambient [CO_2]) and 1000 ppm (high [CO_2]) under $250 \mu\text{mol m}^{-2} \text{s}^{-1}$ (high light), $130 \mu\text{mol m}^{-2} \text{s}^{-1}$ (optimum light), and $50 \mu\text{mol m}^{-2} \text{s}^{-1}$ (low light) for approximately 35 days. One expanded and healthy leaf per plant, from 7-8 plants per genotype, was measured using the LI-6400XT Infra Red gas analyser (IRGA). Each plant was measured at a constant light irradiance of $1200 \mu\text{mol m}^{-2} \text{s}^{-1}$ (PAR-photosynthetically active radiation) to maximise photosynthetic output. The leaf was

subjected to step changes in [CO₂] concentration from 500 ppm to 100 ppm (100 ppm reduction per step change), 100 ppm to 40 ppm (20 ppm reduction per step change) and then increasing from 500 ppm to 1500 ppm (100 ppm increase per step change). Plants were acclimatised at 500 ppm before each set of IRGA readings were taken. Relative humidity was kept between 65-70%, Flow was set to 300 μmol/s. Temperature was matched at 20⁰C between the leaf and block. Pressure was set at 100 kPa and the fan was set to 'fast'. The values given for the first two 500 ppm readings, shown in the above table as bold and underlined, were to acclimatise the plant and not used within data interpretation. Photosynthetic values (A) were plotted against mean intercellular [CO₂] (Ci) using GraphPad, Prism 7® to show assimilation rates versus the amount of [CO₂] absorbed and used by the leaf. Intracellular [CO₂] divided by Extracellular [CO₂] was plotted against Extracellular [CO₂] to indicate the amount being absorbed by each leaf. Assimilation (A) was divided by transpiration (E) to calculate instantaneous WUE (WUE_{inst}) and plotted against intracellular [CO₂] (Ci) to indicate the total amount of water lost via the leaves (stomata and cuticle layer).

2.1.6 Carbon Isotope Discrimination

Plants were grown in controlled conditions at 200 ppm (sub-ambient [CO₂]), 500 ppm (ambient [CO₂]) and 1000 ppm (high [CO₂]) under 250 μmol m⁻² s⁻¹ (high light), 130 μmol m⁻² s⁻¹ (optimum light), and 50 μmol m⁻² s⁻¹ (low light) for approximately 35 days. Five expanded and healthy leaves per plant, from 3 plants per genotype were dried at 60⁰C for 3 to 4 days and ground to a powder. X4 reference air samples were also collected. 1-2 mg of each sample was added to foil cups and combusted at 1800⁰C, sample components were then separated via Gas Chromatograph and subjected to a ANCA GSL 20-20 Mass Spectrometer (Sercon PDZ Europa) magnetic field to ionize and separate ¹³C and ¹²C. Carbon isotope ratios were obtained in δ-notation and calculated according to Masle *et al.* (2005).

$$\delta = R/R_{\text{standard}} - 1$$

R refers to the isotope ratio of the plant sample and R_{standard} is the isotope ratio of the VPDB standard. The $\delta^{13}\text{C}$ values were converted to $\Delta^{13}\text{C}$ using,

$$\Delta^{13}\text{C} = (\delta_a - \delta_p)/(1 + \delta_p)$$

δ_a refers to the $\delta^{13}\text{C}$ of atmospheric CO_2 from the reference sample and δ_p is the $\delta^{13}\text{C}$ of the plant material. Discrimination values were plotted using Graphpad Prism 7®.

2.1.7 Stomatal Bioassay

Plants were grown at $130 \mu\text{mol m}^{-2} \text{s}^{-1}$ (optimum light) and 500 ppm (ambient $[\text{CO}_2]$) for approximately 35 days and removed 2-3 hours in to the photoperiod for sample collection. x3 abaxial epidermal peels per genotype per treatment were floated in 10 ml opening buffer ((500 ml): 50 mM KCl (50 ml), 10 mM MES (10 ml) pH 6.2) in 6 cm petri dish and sealed using micropore tape. $[\text{CO}_2]$ treatments of $[\text{CO}_2]$ free, 500 ppm (ambient $[\text{CO}_2]$) or 1000 ppm (high $[\text{CO}_2]$) were injected through the petri dish lid and bubbled in to the opening buffer. To establish the maximum stomatal aperture of each genotype x3 epidermal peels per genotype were incubated for 2 hours in opening buffer supplemented with the fungal toxin Fusicoccin ((500 ml): 50 mM KCl (50 ml), 10 mM MES (10 ml) pH 6.2, supplemented with 500 nM fusicoccin (Sigma-Aldrich)). All samples were and incubated in the various treatments at 22°C for 2 hours at $200 \mu\text{mol m}^{-2} \text{s}^{-1}$ (Webb and Hetherington, 1997; Stout, 1988).

Epidermal peels were mounted on to slides and imaged using Olympus BX51 Light Microscope fitted with an Olympus DP70 camera under x40 objective. ImageJ software was used to establish maximum stomatal area, aperture area and GC area by taking 4 measurements (fig.2.1).

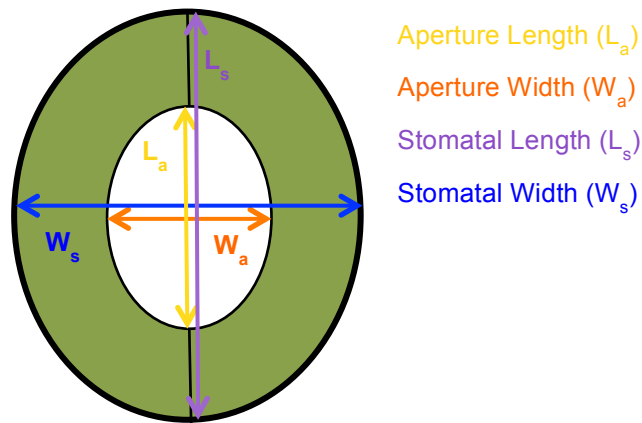


Fig.2.1 Measurements used to calculate stomatal area, aperture area and guard cell (GC) area.

Stomatal area (S) was calculated using the following equation.

$$S_{\text{area}} = \pi * (0.5 * W_s) * (0.5 * L_s)$$

W_s refers to stomatal width and L_s refers to stomatal length respectively. Stomatal aperture area (a_{max}) was calculated using aperture width (W_a) and aperture length (L_a) measurements.

$$a_{\text{max}} = \pi * (0.5 * W_a) * (0.5 * L_a)$$

Guard cell (GC_{area}) area was calculated by subtracting the aperture area from the total stomatal area.

$$GC_{\text{area}} = (\pi * (0.5 * W_s) * (0.5 * L_s)) - (\pi * (0.5 * W_a) * (0.5 * L_a))$$

2.1.8 Chlorophyll Quantification

Chlorophyll concentrations and a/b ratios were calculated according to Porra *et al.* (1989). Absorption spectra were taken on an alignment Technologies Cary 60 UV-VIS spectrophotometer. Plants were grown in controlled conditions at 200 ppm (sub-ambient [CO_2]), 500 ppm (ambient [CO_2]) and 1000 ppm (high [CO_2]) under $250 \mu\text{mol m}^{-2} \text{s}^{-1}$ (high light) and $50 \mu\text{mol m}^{-2} \text{s}^{-1}$ (low light) for approximately 35 days.

0.105 g of green leaf tissue (approx. x1 mature leaf) was ground in 1 ml dH₂O. 300 µl of chlorophyll suspension was added to 1.2 ml of 80% acetone in a 2 ml eppendorf tube and vortexed. The solution was centrifuged at 14000 rpm for 3 minutes. The acetone suspension was poured in to a quartz cuvette and absorption was measured at 750, 663 and 646 nm.

The absorption at 646 and 663 was corrected for the background at 750.

$$A_{646}^* = A_{646} - A_{750}$$

$$A_{663}^* = A_{663} - A_{750}$$

The following equations were solved for the concentrations of chlorophylls a and b (ug/ml).

$$[\text{Chl a}] = 12.25A_{646}^* - 2.55 A_{646}^*$$

$$[\text{Chl b}] = 20.31A_{646}^* - 4.91 A_{663}^*$$

Total chlorophyll concentration is [Chl a] + [Chl b] and the a/b ratio is defined as [Chl a] / [Chl b].

2.1.9 Dry Weight Measurements

x3 plants per genotype were grown at 200 ppm (sub-ambient [CO₂]), 500 ppm (ambient [CO₂]) and 1000 ppm (high [CO₂]) under 250 µmol m⁻² s⁻¹ (high light) and 50µmolm⁻²s⁻¹ (low light) to onset of bolting phase. Bolted stems were removed and rosette was separated from root structure before drying at 60°C for 3-4 days then weighed.

2.2.0 Data Analysis

All graphs produced including statistical analysis via t-test, one-way or two-way ANOVAs with a post analysis TUKEY tests to compare individual means were performed using Graphpad Prism7®. Variance was considered statistically significant when p = ≤0.05, asterisks were used to indicate significance * (p =

≤0.05), ** (p = ≤0.01), *** (p = ≤0.001), **** (p = ≤0.0001). Details of statistical tests throughout results chapters where appropriate.

2.2.1 Primer Sequences

Table 2.9 List of forward and reverse primers used for PCR and qRT-PCR of transgenes. All primers were synthesised by Sigma Aldrich.

Primer Name	Primer Type	Sequence
EFP2102777For	PCR	ACCACAAGGTAGGTCCTGTC
EFP2102777Rev	PCR	AACGGCGGAGATTCAATTGATTCAAG
CRSP132812For	PCR	TGGAGGAGTGAAGATAGTTCCG
CRSP132812Rev	PCR	CATCAATGCAACCAGGACTAG
CA1-106570For	PCR	GGCTTCAAAGAGTTTCCTACAG
CA1-106570Rev	PCR	TGGAGAACATTGTGGTGATAGG
CA4For-D11new	PCR	AGCAAGCAAACACCAGAAAC
CA4Rev-D11new	PCR	GACAGATCCTGACCGTTGG
LBp745DsLox	PCR	AACGTCCGCAATGTGTTATTAAGTTGTC
Salk Lba1	PCR	TGGTTCACGTAGTGGGCCATCG
AtUBC21Fr	qRT-PCR	GAATGCTTGGAGTCCTGCTTG
AtUBC21Rv	qRT-PCR	CTCAGGATGAGCCATCAATGC
SPCHfor3	qRT-PCR	AACGGTGTCGCATAAGATCC
SPCHrev3	qRT-PCR	CAAGAGCCAAATCTTCAAGAGC
MUTEfor1	qRT-PCR	AACGTGAAAGACCCTAAACCG
MUTErev1	qRT-PCR	TTAGCATGAGGGGAGTTACAGC
FAMAfor2	qRT-PCR	GCTGCTAGGGTTTGACGCCATGA
FAMArev2	qRT-PCR	GGAGTAGAGGACGGTTTGTTC
SCRMfor1	qRT-PCR	CACCTACACCGCAAACCTTTTC
SCRMrev1	qRT-PCR	AATGTTCACTGCTTTCCTTCC
StomagenFor1	qRT-PCR	GTTCAAGCCTCAAGACCTCG
StomagenRev1	qRT-PCR	CCTTCGACTGGAACCTTGCTC
EPF2qFor1	qRT-PCR	TCAAACGCACCACAAGAAGG
EPF2qRev1	qRT-PCR	AGCTTGATCCTGTTGGGTAC
CRSPqFor	qRT-PCR	TGCATCAGAAGGATCAGCCAG
CRSPqRev	qRT-PCR	ACGTTCTCGCATAACACAATC

betaCA1for	qRT-PCR	CGTCAAGGGTGCTTTTGAGC
betaCA1rev	qRT-PCR	AGCCACATCTTTAACAGAGCTA
betaCA4for	qRT-PCR	TCCCAAATCCTCTGCCTCATC
betaCA4rev	qRT-PCR	GCTCTTGGAAGGCTCTTCCT
ABA2-for1	qRT-PCR	GTGAGGCACTACATCGAGGA
ABA2-rev1	qRT-PCR	CCTGTGGCTCCTCCAGTGAT
NCED3-for2	qRT-PCR	TCACGACGAGAAGACATGGA
NCED3-rev2	qRT-PCR	GCTCCGATGAATGTACCGTGA
ABI1-for1	qRT-PCR	ACCGTTAATGGAGGAAGTATCT
ABI1-rev1	qRT-PCR	GATCTCCGTTCTCGGAATCTTG
HAB1-for1	qRT-PCR	CTAAAGATTCATCAACTGGGTTG
HAB1rev1	qRT-PCR	CGCAACAACCTTCGTCGATCT
OST1-for1	qRT-PCR	GCAGATCATTGCAGAAGCAAC
OST1-rev1	qRT-PCR	TCAAGATCATCAAGGTCGCTC

3.0 Chapter 3:

Investigating the effects of light and [CO₂] signal integration on stomatal development

3.1 Introduction

The impact of light and [CO₂] on long-term stomatal developmental responses are most often considered as independent signals (Fig.3.). An increase in irradiance results in an increase in stomatal index (SI) and stomatal density (SD), as well as stimulating stomatal opening. In combination, these changes (as well as other factors) enable the plant to increase photosynthetic output. By way of contrast, an increase in [CO₂] levels results in a decrease in stomatal index (SI) and stomatal density (SD), whilst encouraging stomatal closure (Chaerle *et al.*, 2005; Woodward, 1987; Woodward, 1995; Casson and Gray, 2008; Casson and Hetherington, 2010). It should be clarified that these observations are a generalisation and it has been hypothesised that different plant species have differential developmental or aperture responses to stimuli; so at one extreme some plants respond developmentally (SI and SD) but have a limited physiological (aperture) response. In contrast, others have a limited developmental response but have a highly responsive aperture response (Haworth *et al.*, 2013).

The effects of these two environmental signals have been intensely researched in recent years as isolated response pathways. My work has therefore focused on investigating how light and CO₂ signal response pathways integrate to effect stomatal development, as well as physiological responses (see chapter 5). In terms of signals that may mediate how light and CO₂ may regulate stomatal developmental responses, it is unlikely that it is simply related to photosynthetic assimilation rates. Both high light and elevated [CO₂] result in increased assimilation rates as well as sugar levels of mature leaves (Coupe *et al.*, 2005), yet light positively regulates stomatal development whilst [CO₂] negatively regulates this process. However, it also apparent from gas exchange analysis that increasing irradiance can lead to reductions in internal leaf [CO₂] (C_i) levels suggesting that light in particular can impact on the leaf CO₂ environment. It has previously been

shown that light signals regulate stomatal development through photoreceptors and in particular phyB (Casson *et al.*, 2009; Boccalandro *et al.*, 2009; Kang *et al.*, 2009). Based on preliminary findings in the Casson lab, phyB was also found to regulate stomatal development in response to [CO₂] in an irradiance dependent manner. To investigate this further, a genetic approach was employed to study interactions between light and [CO₂], focusing on mutants in either light or [CO₂] regulation of stomatal development.

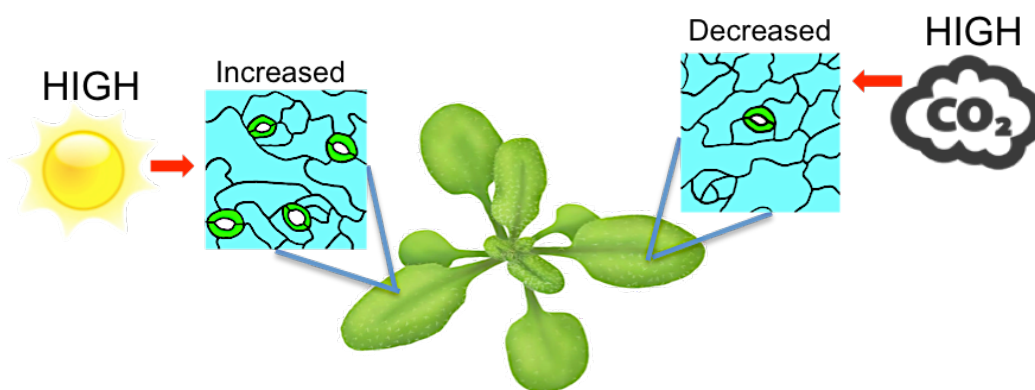


Fig.3. A schematic representation of signal regulation of stomatal development, long-term response. High light intensity results in a higher stomatal frequency and high [CO₂] levels result in a reduction of stomatal frequency.

3.2 Aims

The main aims of the research in this chapter were therefore to:

1. Use a genetic approach to investigate interactions between light and CO₂ signaling pathways and determine their impact on stomatal development.
2. Investigate what role phyB has in mediating this signal integration.

3.3 Results: Light and [CO₂] concentration effect

stomatal development

To investigate interactions between light and CO₂ signaling, a range of mutants were utilised, which are detailed in Table 3. The wild-type for these studies was Col-0, which is not defective in the *ERECTA* gene, unlike other commonly used ecotypes such as La-er. In the case of light signaling components, *phyB* and *cry1 cry2* photoreceptor mutants were included as well as mutants defective in key light signaling transcription factors (*hy5*, *hyh* and *pif4*). *HY5* in particular was chosen as this is a key transcription factor in both phytochrome and cryptochrome signaling (Christie *et al.*, 2015; Xu *et al.*, 2015). Furthermore, ChIP analysis indicates that HY5 may bind the promoter of both *EPF2* and *STOM* (Lee *et al.*, 2007). In the case of stomatal development, focus was placed on members of the EPFs, including *epf2* mutants given that they have been shown to be required for responses to [CO₂] (Engineer *et al.*, 2014), as well as a *STOM* RNAi line, as *STOM* has been implicated in responses to light and responses from photosynthetic tissue (Sugano *et al.*, 2010; Hronkova *et al.*, 2015). CO₂ signaling genes included *epf2*, *crsp* and *ca1 ca4*.

To investigate the potential mechanism of light and CO₂ signal integration in to the stomatal development pathway, a number of mutants were selected for crossing with *phyB* to produce double and triple mutants. Previous work conducted by the Casson lab showed that the red/far red light photoreceptor *phyB* was the dominant photoreceptor required for light regulated stomatal development. To confirm the genotype of these mutants, F2 seedlings were analysed. The *phyB* mutant phenotype is very distinctive with long hypocotyls and elongated petioles and this was used in many instances to identify putative F2 seedlings for analysis (when crossed with *phyB*). For T-DNA insertion mutants, primers were designed to regions flanking the insertion site. Each F2 plant was tested with this primer pair, to identify the WT locus, and then in combination with the T-DNA left border primer, to

identify a T-DNA insertion. Plants negative for the WT product but positive for the T-DNA product were designated as being a homozygous insertion mutant for that line. Genotyping of double and triple mutants generated in this study are shown in Fig.3.0. *hy5hyh* and *phyBhy5* had previously been developed in the Casson lab.

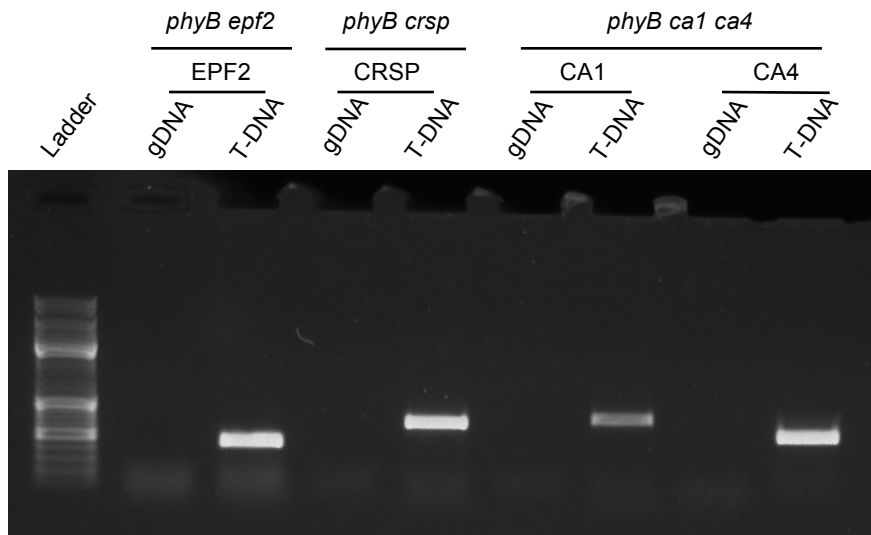


Fig.3.0 DNA gel confirming genotypes of phyB double and triple mutants.

To investigate interactions between light and CO₂, all genotypes were grown under two different light and three different [CO₂] conditions. Other factors, including photoperiod, temperature and relative humidity were constant across experiments (see plant growth conditions in materials and methods). Our conditions were: 50 μmol m⁻¹ s⁻² (low light) or 250 μmol m⁻¹ s⁻² (high light) at 200 ppm (low [CO₂]), 500 ppm (ambient [CO₂]), or 1000 ppm (elevated [CO₂]). 1000 ppm was used for high [CO₂] treatment due to the projected CO₂ emissions for 2100, 450 ppm was predicted globally for 2050 which we are forecasted to exceed (Meehl and Washington, 2006; Gerhart, 2010).

Fully expanded mature leaves were used to make impressions for counting, which took 6 - 8 weeks. Stomatal index (SI) is the percentage of stomata in a given area on the leaf divided by the total amount of other cells, including stomata and

epidermal cells. This measurement provides information on developmental decisions within the epidermis, with an increase in stomatal index normally indicating that more cells are entering the stomatal lineage and completing the transition to guard cell fate. Stomatal density (SD) corresponds to the number of stomata per unit area of a leaf, usually mm^2 and can provide information about the potential gas exchange capabilities of a leaf.

Table 3. Table showing the known mature leaf response of tested seed lines within this study, to various light and CO₂ concentrations.

Genotype	White light responses	CO ₂ responses	Light and CO ₂
phyB	<ul style="list-style-type: none"> Increased irradiance results in increased SI (steady state SI analysis 50 $\mu\text{mol m}^{-1} \text{s}^{-2}$ vs 175 $\mu\text{mol m}^{-1} \text{s}^{-2}$) – Casson <i>et al.</i>, 2009. 	<ul style="list-style-type: none"> No known published data 	<ul style="list-style-type: none"> No known published data
cry1 cry2	<ul style="list-style-type: none"> At 170 $\mu\text{mol m}^{-1} \text{s}^{-2}$ <i>cry1 cry2</i> has reduced SD compared to Col (WT) – Bocalandro <i>et al.</i>, 2012 	<ul style="list-style-type: none"> No known published data 	<ul style="list-style-type: none"> No known published data
phyB cry1 cry2	<ul style="list-style-type: none"> Developed in the Casson lab No known published data 	<ul style="list-style-type: none"> Developed in the Casson lab No known published data 	<ul style="list-style-type: none"> Developed in the Casson lab No known published data
hy5	<ul style="list-style-type: none"> No known published data 	<ul style="list-style-type: none"> No known published data 	<ul style="list-style-type: none"> No known published data
hyh	<ul style="list-style-type: none"> No known published data 	<ul style="list-style-type: none"> No known published data 	<ul style="list-style-type: none"> No known published data
hy5 hyh	<ul style="list-style-type: none"> Developed in the Casson lab No known published data 	<ul style="list-style-type: none"> Developed in the Casson lab No known published data 	<ul style="list-style-type: none"> Developed in the Casson lab No known published data
phyB hy5	<ul style="list-style-type: none"> Developed in the Casson lab No known published data 	<ul style="list-style-type: none"> Developed in the Casson lab No known published data 	<ul style="list-style-type: none"> Developed in the Casson lab No known published data
pif4	<ul style="list-style-type: none"> Increased irradiance results in reduced SI (steady state SI analysis 50 $\mu\text{mol m}^{-1} \text{s}^{-2}$ vs 175 $\mu\text{mol m}^{-1} \text{s}^{-2}$) – Casson <i>et al.</i>, 2009. 	<ul style="list-style-type: none"> No known published data 	<ul style="list-style-type: none"> No known published data
STOM RNAi	<ul style="list-style-type: none"> Reduced SI and SD compared to Col-0 when grown at 50 $\mu\text{mol m}^{-1} \text{s}^{-2}$ and 250 $\mu\text{mol m}^{-1} \text{s}^{-2}$ – Hronková <i>et al.</i>, 2014 	<ul style="list-style-type: none"> No known published data 	<ul style="list-style-type: none"> No known published data
epf2	<ul style="list-style-type: none"> No known published data 	<ul style="list-style-type: none"> increased SD and SI when grown at 150 ppm and 1000 ppm [CO₂] compared Col (100 $\mu\text{mol m}^{-1} \text{s}^{-2}$) – Engineer <i>et al.</i>, 2014 	<ul style="list-style-type: none"> No known published data
phyB epf2	<ul style="list-style-type: none"> Developed in the Casson lab No known published data 	<ul style="list-style-type: none"> Developed in the Casson lab No known published data 	<ul style="list-style-type: none"> Developed in the Casson lab No known published data
crsp	<ul style="list-style-type: none"> No known published data 	<ul style="list-style-type: none"> increased SD and SI when grown at 150 ppm and 1000 ppm [CO₂] compared Col – Engineer <i>et al.</i>, 2014 	<ul style="list-style-type: none"> No known published data

<i>phyB crsp</i>	<ul style="list-style-type: none"> • Developed in the Casson lab • No known published data 	<ul style="list-style-type: none"> • Developed in the Casson lab • No known published data 	<ul style="list-style-type: none"> • Developed in the Casson lab • No known published data
<i>ca1 ca4</i>	<ul style="list-style-type: none"> • No known published data 	<ul style="list-style-type: none"> • increased SI when grown at 150 ppm and 1000 ppm [CO₂] compared Col – Engineer <i>et al.</i>, 2014 	<ul style="list-style-type: none"> • No known published data
<i>phyB ca1 ca4</i>	<ul style="list-style-type: none"> • Developed in the Casson lab • No known published data 	<ul style="list-style-type: none"> • Developed in the Casson lab • No known published data 	<ul style="list-style-type: none"> • Developed in the Casson lab • No known published data

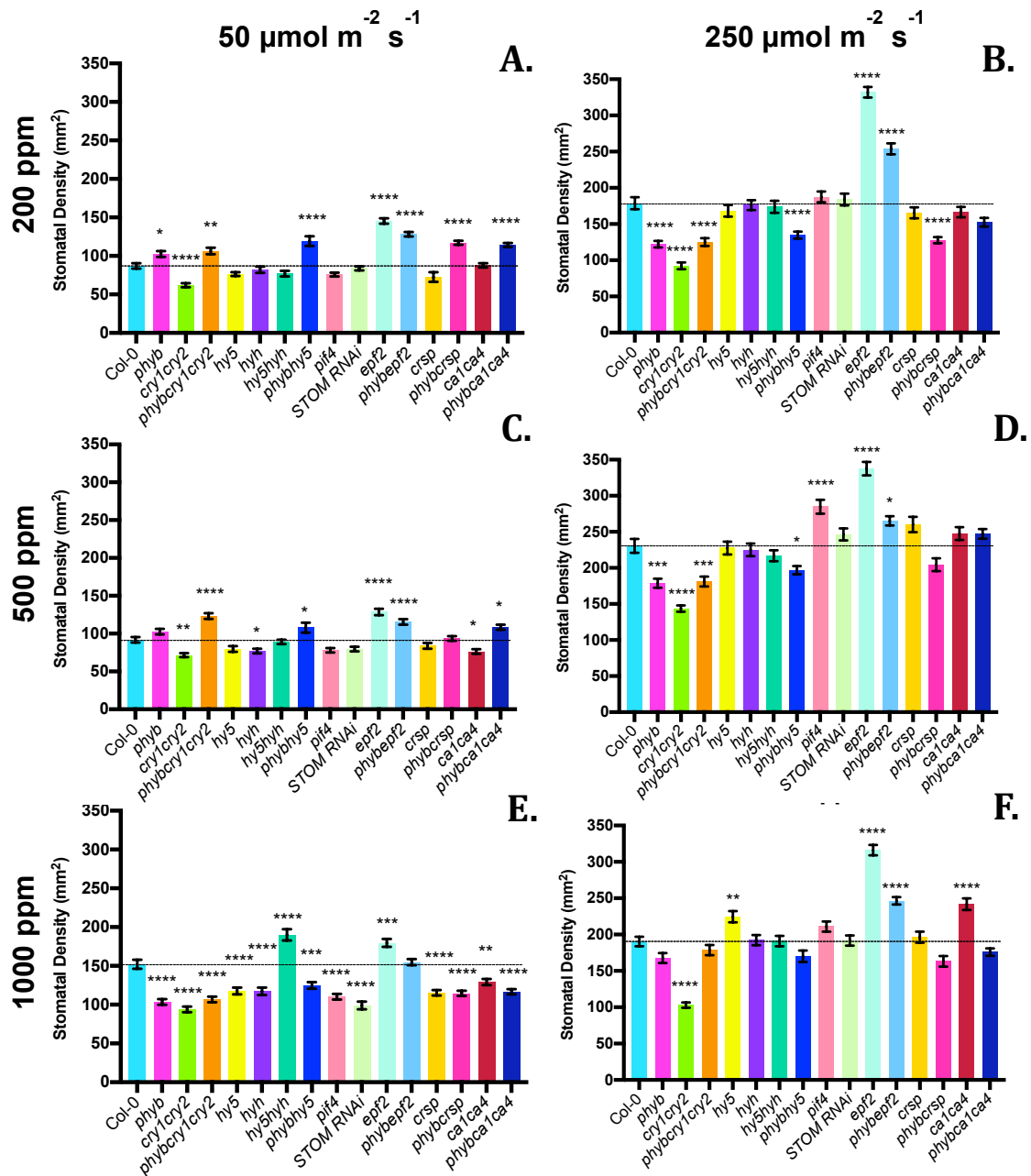


Fig.3.1 Stomatal densities (SD) of the abaxial surface of mature leaves for the indicated genotypes. Plants were grown at irradiances $50 \mu\text{mol m}^{-2} \text{s}^{-1}$ (A, C, E) or $250 \mu\text{mol m}^{-2} \text{s}^{-1}$ (B, D, F) and $[\text{CO}_2]$ concentrations of 200 ppm (A, B), 500 ppm (C, D) or 1000 ppm (E, F). Mean values are shown for each genotype ($n = 45$) with error bars indicating mean \pm SEM. Symbols indicate significant difference in SD compared with Col-0 (represented by the dotted line); one-way AVOVA with post-hoc Dunnett's test, ($p^* = \leq 0.5$, $p^{**} = \leq 0.01$, $p^{***} = \leq 0.001$, $p^{****} = \leq 0.0001$).

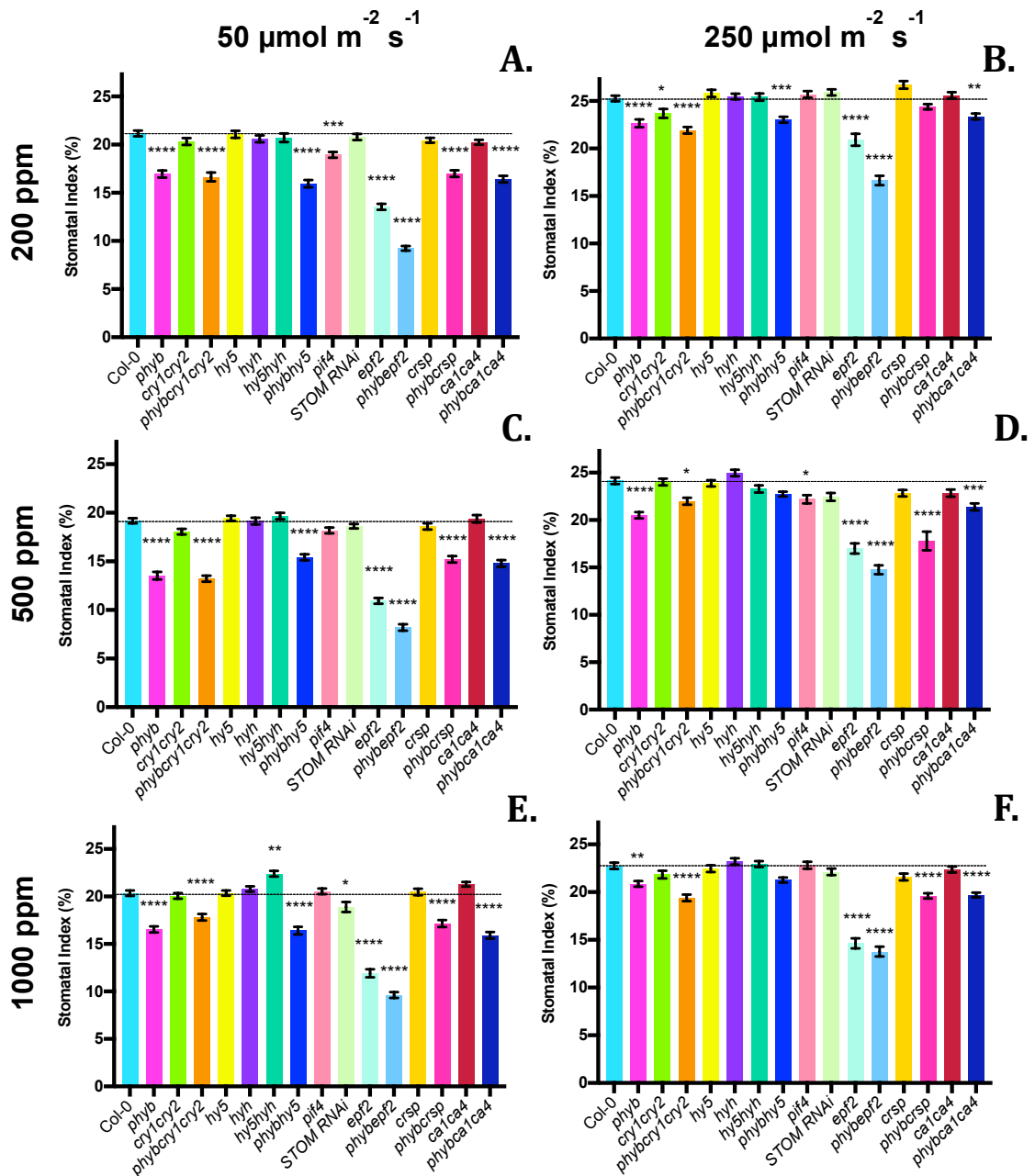


Fig.3.2. Stomatal indices (SI) of the abaxial surface of mature leaves for the indicated genotypes. Plants were grown at irradiances $50 \mu\text{mol m}^{-2} \text{s}^{-1}$ (A, C, E) or $250 \mu\text{mol m}^{-2} \text{s}^{-1}$ (B, D, F) and $[\text{CO}_2]$ concentrations of 200 ppm (A, B), 500 ppm (C, D) or 1000 ppm (E, F). Mean values are shown for each genotype ($n = 45$) with error bars indicating mean \pm SEM. Symbols indicate significant difference in SI compared with Col-0 (represented by the dotted line); one-way AVOVA with post-hoc Dunnett's test, ($p^* \leq 0.5$, $p^{**} \leq 0.01$, $p^{***} \leq 0.001$, $p^{****} \leq 0.0001$).

3.4 Light regulation of stomatal development

Increases in irradiance have previously been shown to positively regulate stomatal development (reviewed in Casson and Gray, 2008). Data will be examined in terms of light response before considering responses to CO₂, light/CO₂ interactions and the role of *phyB* in mediating light/CO₂ interactions. Data for all genotypes and conditions are shown in Fig.3.1 and Fig.3.2, however, data has been extracted from these graphs and displayed in different formats through this chapter to facilitate interpretation.

In the WT, Col-0, it is clear that both SI and SD show significant increases at the higher irradiance, irrespective of [CO₂] levels (Fig.3.3.A and Fig.3.4.A). So, as expected, growth at higher light levels promotes stomatal development. The general trend for the light signaling mutants is that SI and SD increase at the higher radiance further supporting that higher light levels positively regulate stomatal development. However, some of these responses are dependent on [CO₂] levels, which will be discussed in later sections. Whilst these photoreceptor mutants are responding to light and show increases in SI and SD at higher irradiances, the actual SI and/or SD for *phyB*, *cry1 cry2* and *phyB cry1cry2* are consistently lower than Col-0. So, the SI of *phyB* mutants is consistently lower than Col-0 under most conditions indicating that *phyB* mutants have a reduced basal level of stomatal development (Fig.3.2; Fig.3.4.A and B). This increase in SI and SD of *phyB* at the higher irradiance suggests that either there is redundancy with other photoreceptors or an alternative mechanism/s confers sensitivity to changes in irradiance.

In the case of *cry1 cry2* mutants, SD is generally lower than Col-0 (Fig.3.1; Fig.3.3.A and C). However, in the case of SI, there is no significant difference compared to Col-0. This is different to observations made previously (Kang *et al.*, 2009), though those experiments utilised blue rather than white light. This may indicate that *cry1 cry2* plays more of a roll in cell division and expansion rather than

specifically regulating stomatal development under these conditions (Fig.3.3 and Fig.3.4).

Given the potential redundancy of *phyB* in mediating sensitivity to increased irradiance, a *phyBcry1cry2* was examined. The triple mutant appears to generally show that *phyB* is epistatic to *cry1 cry2*, though this is not definitive across all conditions. The *phyBcry1cry2* SD response is *phyB*-like, both in terms of trend and actual SD (Fig.3.3.B and D). The general trend in SI again appears more *phyB*-like, though this is not so apparent at elevated [CO₂] (Fig.3.4.B and D). Similar to *phyB*, the fact that the triple mutant still shows sensitivity to higher irradiance suggests that there are other photoreceptors or mechanisms that act redundantly to positively regulate changes in SI and SD. As stated earlier, the basal level of stomatal development in the *phyB* genotypes are however lower.

The role of other components of light signaling was then examined. HY5 is a key transcription factor in both phy and CRY signaling and can function redundantly with the related HYH (Christie *et al.*, 2015; Xu *et al.*, 2015). However, under these experimental conditions *hy5*, *hyh* and *hy5hyh*, in general, behaved like Col-0 (Fig.3.1; 3.2; 3.7 and 3.8). Despite ChIP analysis indicating that HY5 may bind the promoters of EPF2 and STOM as well as evidence of HY5 acting downstream of *phyB* and CRY1 CRY2 to control light regulated gene expression (Lee *et al.*, 2007; Christie *et al.*, 2015; Xu *et al.*, 2015), there appears to be no major role for these transcription factors in stomatal development, at least in terms of long-term phenotypic analysis. This suggests that they are unlikely to be regulating the expression of core stomatal regulatory genes and unlikely to be the factors that coordinate *phyB* and CRY regulation of stomatal development. PIF4 has previously been shown to be defective in light-mediated stomatal development (Casson *et al.*, 2009). In this study, there was phenotypic variation across the different conditions in terms of both SD and SI (Fig.3.1; 3.2; 3.7 and 3.8). Unlike *phyB* however, over most conditions, *pif4* mutants did not consistently have lower SIs suggesting that it

may act redundantly with other PIFs or is not a major regulator of light-mediated stomatal development. A number of reports have linked PIF4 to temperature responses in plants (reviewed in Quint *et al.*, 2016). Therefore, it cannot be discounted that these experimental conditions were not within the relevant temperature range to observe major *pif4* responses.

The role of STOM and EPF2 was also examined, particularly given that STOM is proposed to link photosynthetic tissue to epidermal development and is reported to be light regulated (Kondo *et al.*, 2010; Sugano *et al.*, 2010; Hronková *et al.*, 2015). Whilst the STOM RNAi line used here has previously been reported to have a significantly reduced SI and SD (Hunt and Gray, 2010), in most conditions there was not a significant difference in comparison with Col-0 making interpretation of the role of STOM in light responses difficult (Fig.3.1 and Fig.3.2). Mutations in EPF2 should result in increased STOM-mediated inhibition of the MPK pathway. Across all conditions *epf2* mutants had increased SD but reduced SI. This may be because of increased SPCH stability as a result of STOM inhibiting the MPK pathway resulting in an increase in amplifying divisions, a phenotype observed in SPCH variants engineered to be resistant to MPK phosphorylation (Lampard *et al.*, 2008). However, despite reduced SIs, *epf2* mutants do respond to increased irradiance but the magnitude of change was often greater than that observed for other genotypes (this is also the case for SD) (Fig.3.3 and Fig.3.4). Therefore, manipulating the EPFs may alter sensitivity to light suggesting that SPCH stability (or other MPK targets) may be a factor that determines both the basal level of stomatal development as well as the sensitivity to a change in irradiance.

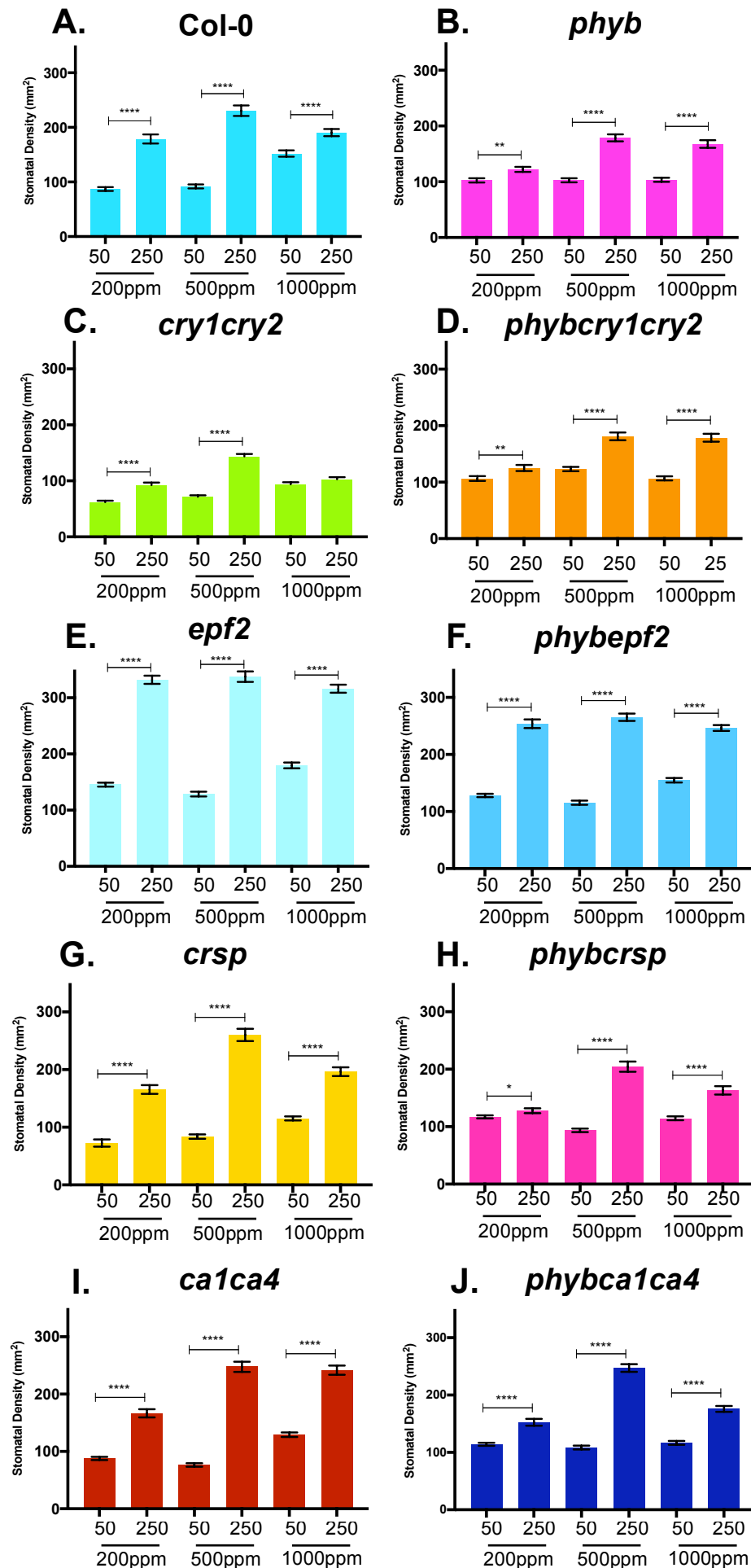


Fig.3.3. Stomatal density of individual genotypes under different light and [CO₂] conditions. Data is extracted from Figure 3.1 and shows the SD of Col-0 (A), *phyB* (B), *crycry2* (C), *phyB cry1 cry2* (D), *epf2* (E), *phyB epf2* (F), *crsp* (G), *phyB crsp* (H), *ca1 ca4* (I) and *phyB ca1 ca4* (J). Symbols indicate significant differences; one-way AVOVA with post-hoc Dunnett's test, (p* = ≤ 0.05, p** = ≤ 0.01, p*** = ≤ 0.001, p**** = ≤ 0.0001).

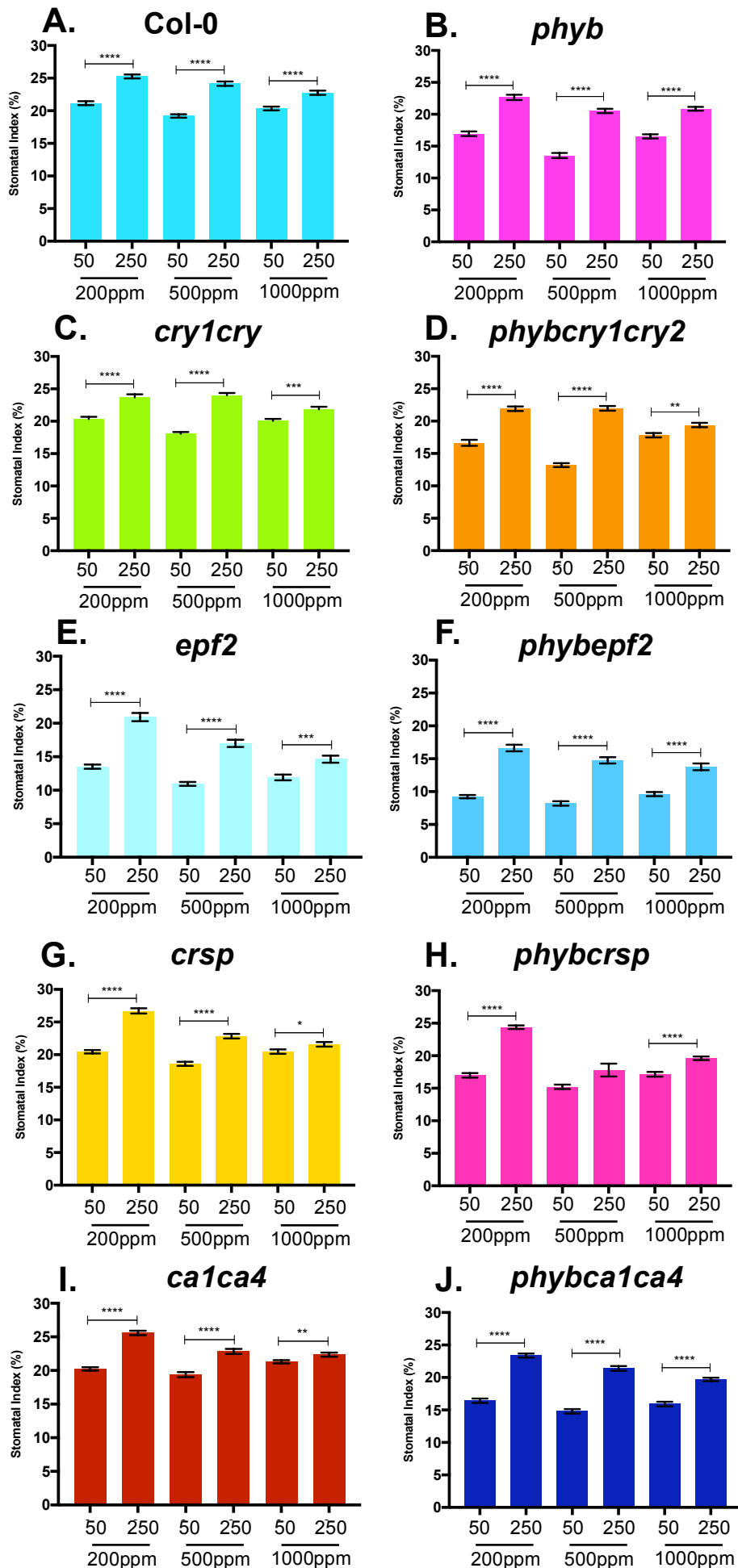


Fig.3.4. Stomatal indices of individual genotypes under different light and [CO₂] conditions. Data is extracted from Figure 3.2. and shows the SI of Col-0 (A), *phyB* (B), *crycry2* (C), *phyB cry1 cry2* (D), *epf2* (E), *phyB epf2* (F), *crsp* (G), *phyB crsp* (H), *ca1 ca4* (I) and *phyB ca1 ca4* (J). Symbols indicate significant differences; one-way AVOVA with post-hoc Dunnett's test, (p* = ≤ 0.5, p** = ≤ 0.01, p*** = ≤ 0.001, p**** = ≤ 0.0001).

3.5 [CO₂] regulation of stomatal development

In contrast to light, increases in [CO₂] are reported to negatively regulate stomatal development in many plant species, though variation in this has been observed (Woodward, 1987). One hypothesis put forward to explain this variation in response to [CO₂] is that both physiological (aperture) and developmental (SI and SD) responses exist and that different species fall on different spectrums; so one plant species may not respond developmentally but guard cell aperture control will be very sensitive to [CO₂] (Haworth *et al.*, 2013). In examining responses to [CO₂], in this section, focus will be placed on the results of genotypes grown at 250 $\mu\text{mol m}^{-2} \text{s}^{-1}$ (Fig.3.5 and Fig.3.6), as light/CO₂ interaction will be considered in the following section.

In the WT, Col-0, SD increases from 200 ppm to 500 ppm [CO₂] but then decreases between 500 ppm to 1000 ppm (Fig.3.5.A); this is a trend observed in several other genotypes at 250 $\mu\text{mol m}^{-2} \text{s}^{-1}$. In contrast to SD, there is a stepwise reduction in SI from 200 ppm – 500 ppm – 1000 ppm, which is consistent with the literature that [CO₂] negatively regulates stomatal development (Fig.3.6.A). Considering both SD and SI together, it appears that there is no strict coupling of developmental decisions of cell division and cell expansion. Total cell densities (stomata and all other cells) were greatest at 500 ppm (mean 155.9 cells/mm²) compared with 200 ppm (113.2 cells/mm²) and 1000 ppm (134.3 cells/mm²). Given that only two irradiances were examined, it cannot be ruled out that this does not also occur in an irradiance dependent manner. Interestingly, *cry1 cry2* mutants also show an uncoupling between SD and SI, with consistently lower SD but not SI compared with Col-0.

This study also included several mutants that have previously been characterised as being defective in either their development or physiological responses to [CO₂] (or both). Regards SI; *epf2*, *crsp* and *ca1 ca4* mutants are

reported to show an increase in SI from 150 ppm to 500 ppm (16 hour day, 100 $\mu\text{mol m}^{-2} \text{s}^{-1}$, 21°C; Engineer *et al.*, 2014). It is not reported how they respond to a further increase in $[\text{CO}_2]$. However, during our analysis of *epf2*, *crsp* and *ca1 ca4* mutants, with occasional exceptions, there was no observation of the phenotypes previously reported at either 50 $\mu\text{mol m}^{-2} \text{s}^{-1}$ or 250 $\mu\text{mol m}^{-2} \text{s}^{-1}$ (Fig.3.1; 3.2; 3.5 and 3.6; E, G, I). At 250 $\mu\text{mol m}^{-2} \text{s}^{-1}$ both *epf2* and *crsp* respond in the same manner as Col-0 in terms of SI, with a stepwise decrease in SI from 200 ppm – 500 ppm – 1000 ppm (Fig.3.6; E, G). In the case of *epf2*, the SI response appeared to be even hypersensitive to increases in $[\text{CO}_2]$, as was the case with light. However, the SD of *epf2* mutants did not significantly change from 200 ppm – 500 ppm – 1000 ppm (Fig.3.5.E). Coupled to the SI data, this indicates that *epf2* mutants have increased non-stomatal cell densities at higher $[\text{CO}_2]$ levels. Whilst not aligning to the literature, *ca1ca4* mutants do appear to be insensitive to $[\text{CO}_2]$ between 500 ppm – 1000 ppm, both in terms of SI and SD (Fig.3.5.I and Fig.3.6.I). They do however respond in a WT manner between 200 ppm – 500 ppm. In conclusion, both *EPF2* and *CA1 CA4* may influence responses to $[\text{CO}_2]$, both in terms of cell division/expansion and stomatal developmental responses. However, a clear role for CRSP could not be identified.

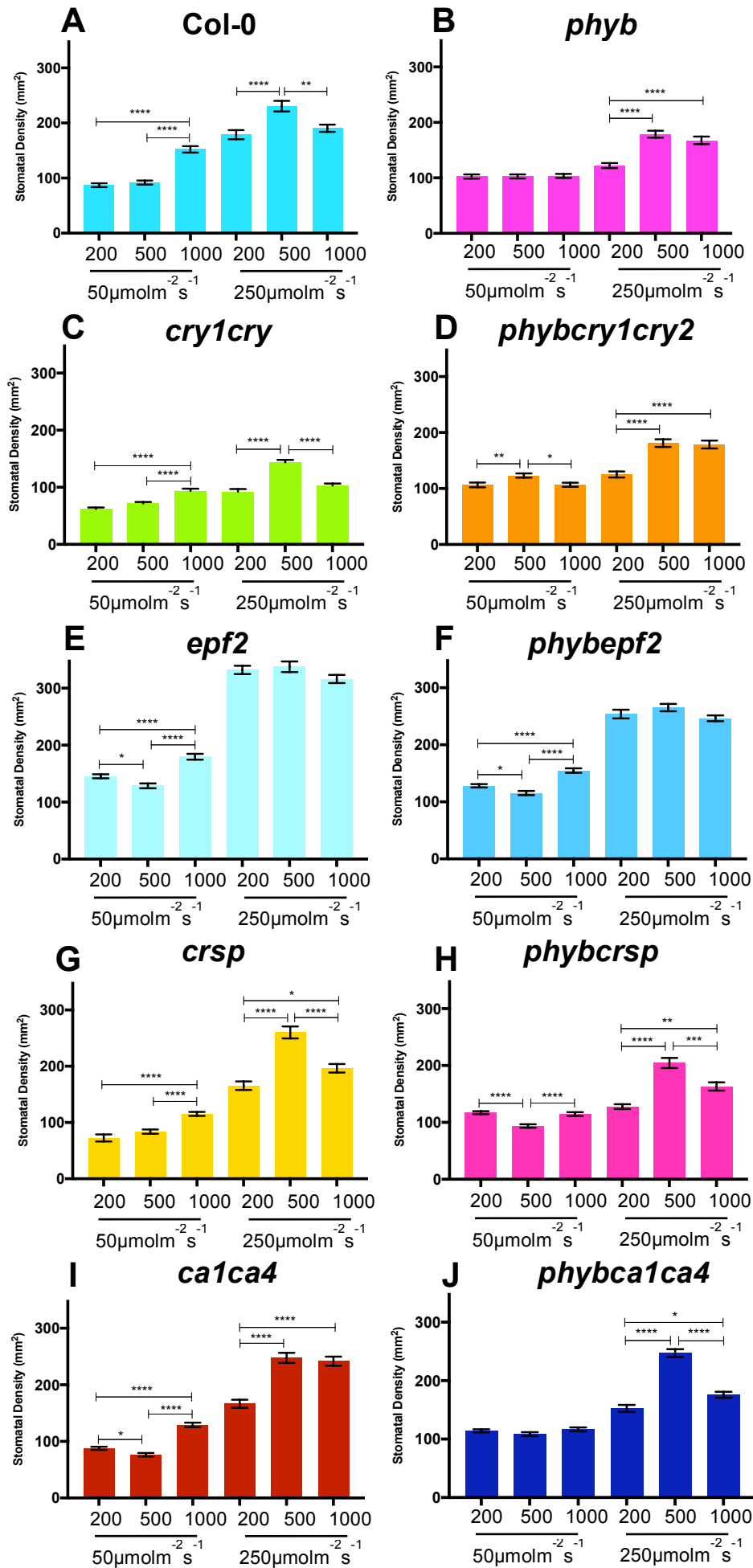


Fig.3.5 Stomatal density of individual genotypes under different light and [CO₂] conditions. Data is extracted from Figure 3.1 and shows the SD of Col-0 (A), *phyB* (B), *cry1cry2* (C), *phyB cry1 cry2* (D), *epf2* (E), *phyB epf2* (F), *crsp* (G), *phyB crsp* (H), *ca1 ca4* (I) and *phyB ca1 ca4* (J). Symbols indicate significant differences; one-way AVOVA with post-hoc Dunnett's test, (p* = ≤ 0.05, p** = ≤ 0.01, p*** = ≤ 0.001, p**** = ≤ 0.0001).

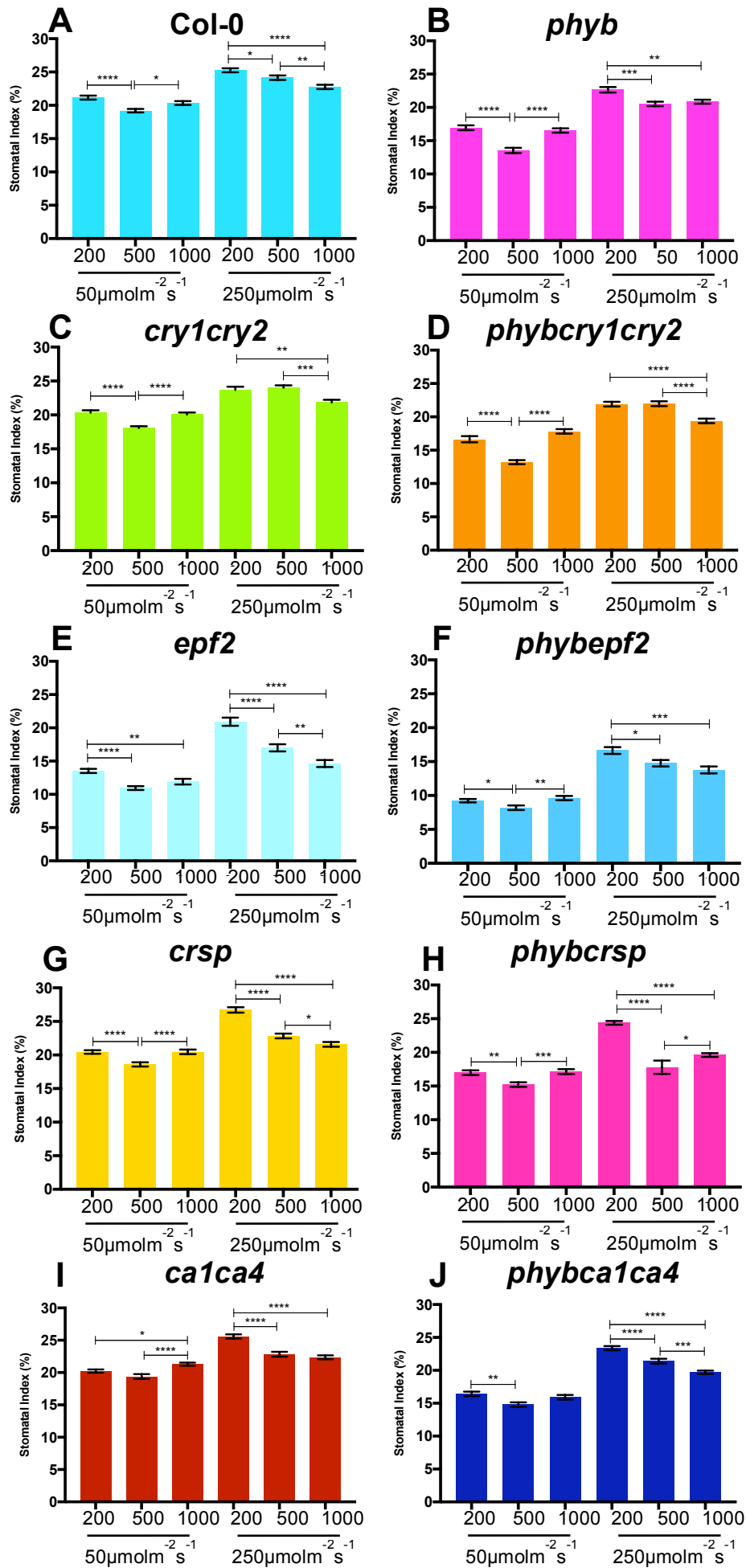


Fig.3.6 Stomatal indices of individual genotypes under different light and [CO₂] conditions. Data is extracted from Figure 3.2 and shows the SI of Col-0 (A), *phyB* (B), *cry1cry2* (C), *phyB cry1 cry2* (D), *epf2* (E), *phyB epf2* (F), *crsp* (G), *phyB crsp* (H), *ca1 ca4* (I) and *phyB ca1 ca4* (J). Symbols indicate significant differences; one-way AVOVA with post-hoc Dunnett's test, ($p^* \leq 0.5$, $p^{**} \leq 0.01$, $p^{***} \leq 0.001$, $p^{****} \leq 0.0001$).

3.6 Light and CO₂ interactions during stomatal development

In this section, the role, if any, of light in regulating SD and SI responses to CO₂ was examined. If, for example, light does not interact with CO₂, then the expected response of a genotype would follow the same pattern irrespective of the irradiance. The SD and SI [CO₂] response of Col-0 at a growth irradiance of 50 $\mu\text{mol m}^{-2} \text{s}^{-1}$, showed a difference in response compared to the higher irradiance of 250 $\mu\text{mol m}^{-2} \text{s}^{-1}$ (Fig.3.5.A and Fig.3.6.A). For SD, under the lower irradiance, there is no significant change in SD between 200 ppm and 500 ppm (SD $\sim 90 \text{ mm}^2$) but then a significant increase at 1000 ppm ($\sim 150 \text{ mm}^2$). At 250 $\mu\text{mol m}^{-2} \text{s}^{-1}$, an increase was observed in SD between 200 ppm and 500 ppm then a decrease between 500 ppm and 1000 ppm (Fig.3.5.A). Examining SI, also reveals differences in responses between the two light conditions. As discussed, growth at high irradiance results in stepwise reductions in SI between 200 ppm and 1000 ppm, whereas at the lower irradiance there is a decrease between 200 ppm and 500 ppm but then there is an increase in SI between 500 ppm and 1000 ppm. It is therefore clear that light modulates [CO₂] responses and that this interaction must impact both on stomatal developmental responses as well as cell division and cell expansion. An examination of light and [CO₂] responses to SD and SI also reveals an interesting point. In the case of light, increased light always results in more stomata both in terms of SD and SI (e.g. Fig.3.3.A and Fig.3.4.A). However, for [CO₂], an increase in SD does not always correlate with an increase in SI (e.g. Fig.3.5.A and Fig.3.6.A). For example, if you compare the SD and SI of Col-0 grown at 50 $\mu\text{mol m}^{-2} \text{s}^{-1}$ and 200 ppm or 1000 ppm [CO₂]; the SD increases but the SI is slightly reduced. Similarly, at 250 $\mu\text{mol m}^{-2} \text{s}^{-1}$, and 200 ppm and 500 ppm, SD increases but SI decreases (Fig.3.5.A and Fig.3.6.A). So, at least under these conditions, light elicits

coordination between cell division, expansion and stomatal cell fate decisions, whilst [CO₂] can act differentially on these processes to mediate changes in the epidermis.

The role of *phyB* in regulating responses to [CO₂] will be considered in the next section so here the focus will be on other light signaling factors. In the case of *cry1cry2* the SD response across the different [CO₂] concentrations and irradiances shows a similar pattern to that of Col-0, though the actual SD are lower (Fig.3.3.C and Fig.3.5.C). However, in the case of SI, at 250 $\mu\text{mol m}^{-2} \text{s}^{-1}$, *cry1 cry2* mutants appear insensitive to [CO₂] changes; at 50 $\mu\text{mol m}^{-2} \text{s}^{-1}$, the responses follow those observed for Col-0 (Fig.3.6.C).

Under the higher irradiance, *cry1 cry2* total cell densities (all cells other than stomata) were greatest at 500 ppm (mean 73.1 cells/mm²) compared with 200 ppm (mean 46.7 cells/mm²) and 1000 ppm (mean 59.7 cells/mm²). *cry1 cry2* showed a stepwise reduction in total cell densities which correlated with a reduction in [CO₂] when grown under low light (mean 60.5 cells/mm² at 1000ppm; mean 51.7 cells/mm² at 1000ppm; mean 38.9 cells/mm² at 1000ppm). This epidermal data in addition to SI and SD of *cry1 cry2* mutants show an uncoupling between SD and SI, with consistently lower SD but not SI compared with Col-0. This is therefore the first indication that photoreceptors can modulate stomatal developmental responses to [CO₂] under specific conditions.

Analysis of the *hy5*, *hyh* and *hy5 hyh* mutants found that in general, their individual responses showed a similar pattern to that observed in Col-0, though there were some condition specific differences (Fig.3.1 and Fig.3.2). Considering each mutant in isolation but across all conditions, *hy5* mutants grown at 250 $\mu\text{mol m}^{-2} \text{s}^{-1}$, did not show a decrease in SD between 500 ppm and 1000 ppm [CO₂] (SD 227.5 mm² vs 224.5 mm²; P-value >0.99) observed in Col-0. The also *hyh* mutant behaves as Col-0, both within each condition but also showing a reduction in SD between 500 ppm and 1000 ppm at 250 $\mu\text{mol m}^{-2} \text{s}^{-1}$ (SD 216.8 mm² vs 191.1 mm²; p-value 0.0598). The *hy5hyh* double mutant shows the same insensitivity as *hy5*

between these conditions, though this is not as pronounced suggesting additive interactions with *hyh*. The SI data also suggests additive as opposed to epistatic interactions between *HY5* and *HYH* under the higher irradiance. For example, *hyh* mutants appear insensitive to [CO₂] from 200 ppm to 500 ppm (SI 25.47% vs 24.96%; p-value 0.86); *hy5* and *hy5hyh* mutants respond as Col-0 between these conditions. This is similar to what is observed for *cry1 cry2* though the absolute SI values are different between these mutants. However, it is the double mutant that appears insensitive between 500 ppm to 1000 ppm, though neither single mutant is (SI 23.3% vs 22.9%; p-value 0.99). As with the cryptochrome mutants, this suggests that light signaling components can modulate condition-specific responses to [CO₂], though there is no predictable pattern.

A similar picture is apparent when *pif4* mutants are analysed. The SD response across all conditions follows a similar trend to Col-0, though again the absolute SDs are different. Where *pif4* mutants do appear to differ is in the range of 200 ppm - 500 ppm [CO₂] at the higher irradiance. In this instance, there is a major drop in SI between these two [CO₂] concentrations, which is then not apparent at 1000 ppm (SI 200 ppm - 500 ppm - 1000 ppm; 25.7% - 22.2% - 22.8%). This may suggest hypersensitivity between 200 ppm – 500 ppm as opposed to insensitivity to 1000 ppm. As with other light signaling factors, the responses appear limited to a particular set of conditions as opposed to a consistent change in responsiveness.

3.7 The role of phyB in light and [CO₂] signal integration

A number of light signaling and CO₂ signaling mutants were selected for crossing with *phyB* to produce double and triple mutants in order to investigate interactions between *phyB* and CO₂ signaling in the stomatal development pathway. As shown

in Fig.3, the genotypes of these crosses were confirmed either in this study or previously.

In this section, comparisons will be made using *phyB* to analyse the response of the *phyB* double and triple mutants outlined in Table 3, (Figs. 3.7; 3.8; 3.9 and 4 will be analysed). As discussed in section 3.5, unfortunately under the growth conditions of this study, replication of published results could not be achieved therefore comments could only be made on the interactions as observed. The general trend at low light of *phyB* is that SD values remain consistent ($\sim 100 \text{ mm}^2$) across $[\text{CO}_2]$ concentrations; whilst other genotypes consistently show an increase between 500 ppm and 1000 ppm, this is not seen in *phyB*. Similarly, at the higher irradiance, whilst several genotypes including Col-0 show a decrease in SD between 500 ppm to 1000 ppm, *phyB* mutants show no change (Fig.3.5). This indicates that *phyB* mutants may be defective in responses to elevated $[\text{CO}_2]$. The SI data partly supports this conclusion, though only under the higher irradiance conditions. In the lower irradiance conditions the response is similar to that of Col-0 (Fig.3.6).

Interestingly, when analysing the response of the crosses between *phyB* and the CO_2 signaling mutants, in the majority of cases and conditions, the double and triple mutants were very similar to the *phyB* single mutant (this was also mostly observed for *phyB hy5*). Thus, in most cases, *phyB* appeared to be epistatic to *crsp* and *ca1ca4* in both SD and SI (Fig.3.9 and Fig.4). The single exception to this is the *phyB ca1 ca4* at high light and 500 ppm which shows a *ca1 ca4*-like increase in SD, though this is partly evident at 200 ppm as well. In summary, this shows that under these conditions, *phyB* function is epistatic to *CRSP*, *CA1* and *CA4* function further supporting that *phyB* plays an important role in stomatal development whilst showing *CRSP* and *CA1* and *CA4* don't appear to be integral to light/ CO_2 integration under our experimental conditions (Fig.3.9).

More interesting was the analysis of the *phyB epf2* double mutant (Figs 3.9 and 4). *epf2* mutants consistently have higher SD but lower SI than both Col-0 and *phyB* mutants. Comparison of *phyB*, *epf2* and *phyB epf2* would suggest that these two components are acting additively to control these traits. The SD of the double mutant is consistently intermediate between *phyB* and *epf2*. In all conditions, except for high light and 1000 ppm, the SI of the *phyB epf2* double mutant is reduced compared with the *epf2* mutant. The likely additive nature of this interaction would therefore support a model whereby phyB and EPF2 regulate stomatal development by separate pathways. However, it should also be added that in terms of trends, the SD phenotype of the *phyB epf2* double is similar to that of the *epf2* mutant, whereas SI is similar to *phyB* (Fig.3.9.B, E and F; Fig.4.B, E and F).

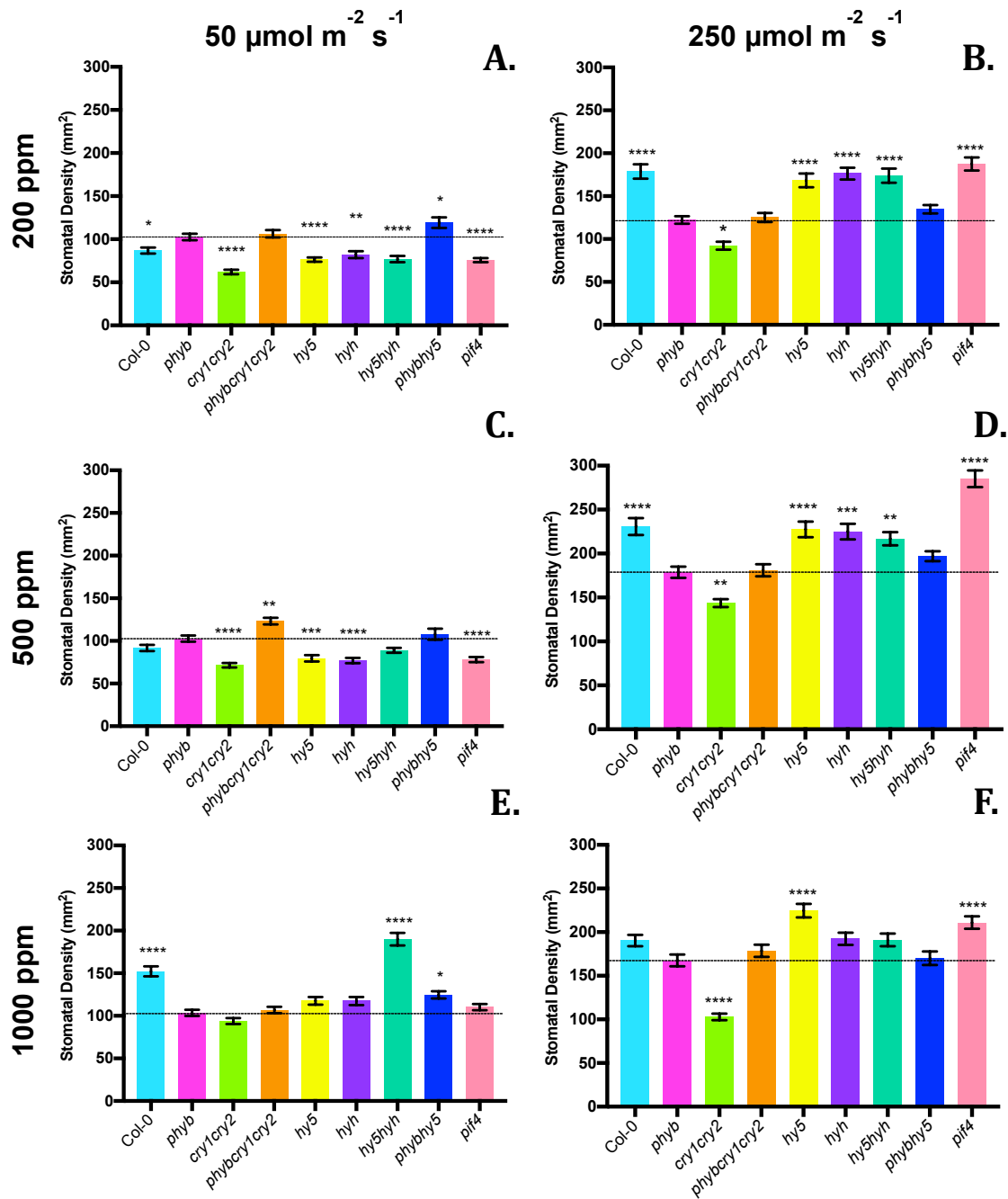


Fig.3.7 Interactions between *phyB* and components of light signalling (Stomatal Density). This data is extracted from Fig 3.1 and focuses on *phyB* and the genetic interactions with components of light signalling. Symbols indicate significant difference in SD compared with *phyB* (represented by the dotted line); one-way AVOVA with post-hoc Dunnett's test, ($p^* \leq 0.5$, $p^{**} \leq 0.01$, $p^{***} \leq 0.001$, $p^{****} \leq 0.0001$).

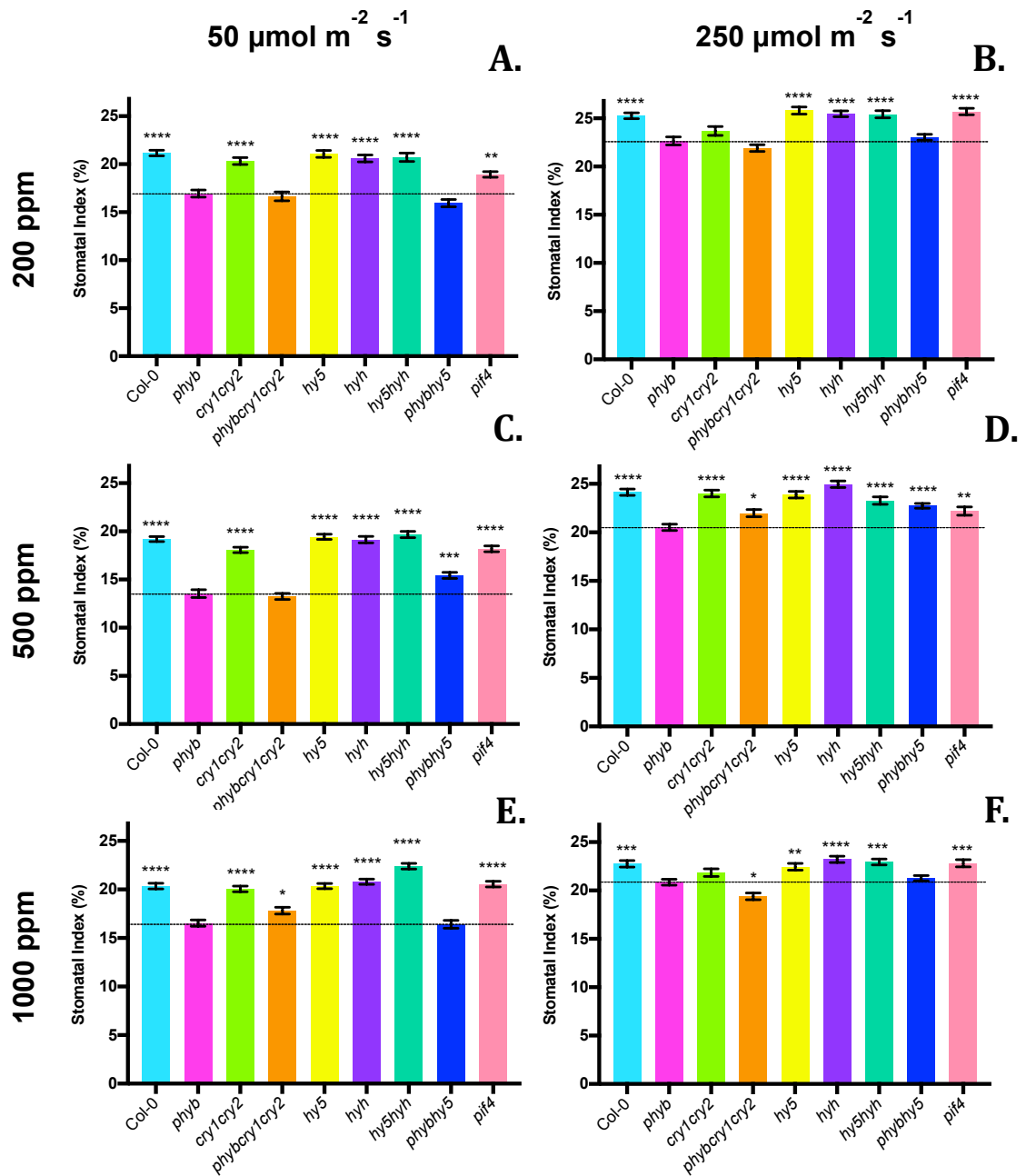


Fig.3.8 Interactions between *phyB* and components of light signalling (Stomatal Index). This data is extracted from Fig 3.2 and focuses on *phyB* and the genetic interactions with components of light signalling. Symbols indicates significant difference in SI compared with *phyB* (represented by the dotted line); one-way AVOVA with post-hoc Dunnett's test, (p* = ≤ 0.05, p** = ≤ 0.01, p*** = ≤ 0.001, p**** = ≤ 0.0001).

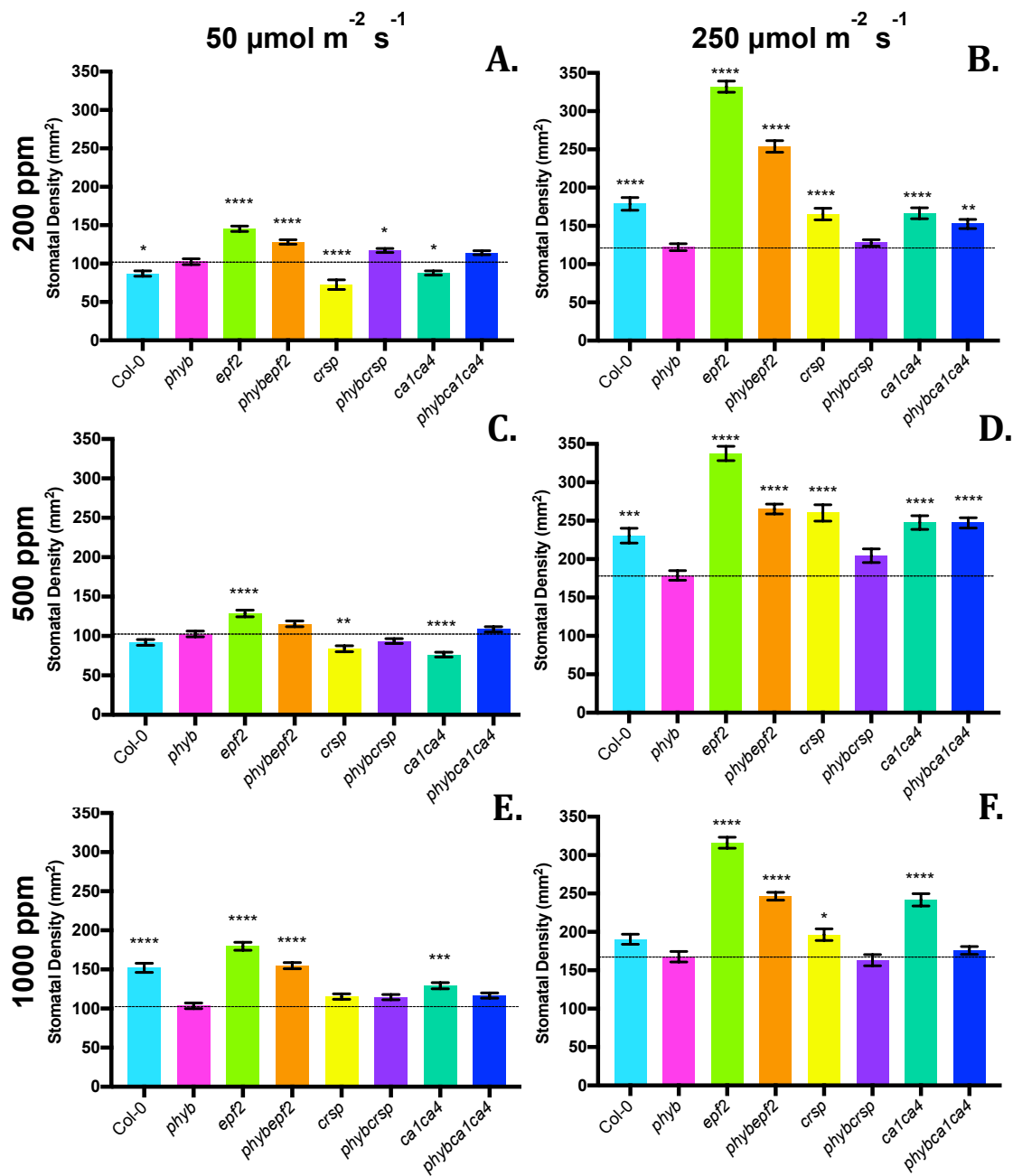


Fig.3.9 Interactions between *phyB* and components of CO₂ signalling (Stomatal Density). This data is extracted from Figure 3.2 and focuses on *phyB* and the genetic interactions with components of light signalling. Symbols indicate significant difference in SD compared with *phyB* (represented by the dotted line); one-way AVOVA with post-hoc Dunnett's test, (p* = ≤ 0.5 , p** = ≤ 0.01 , p*** = ≤ 0.001 , p**** = ≤ 0.0001).

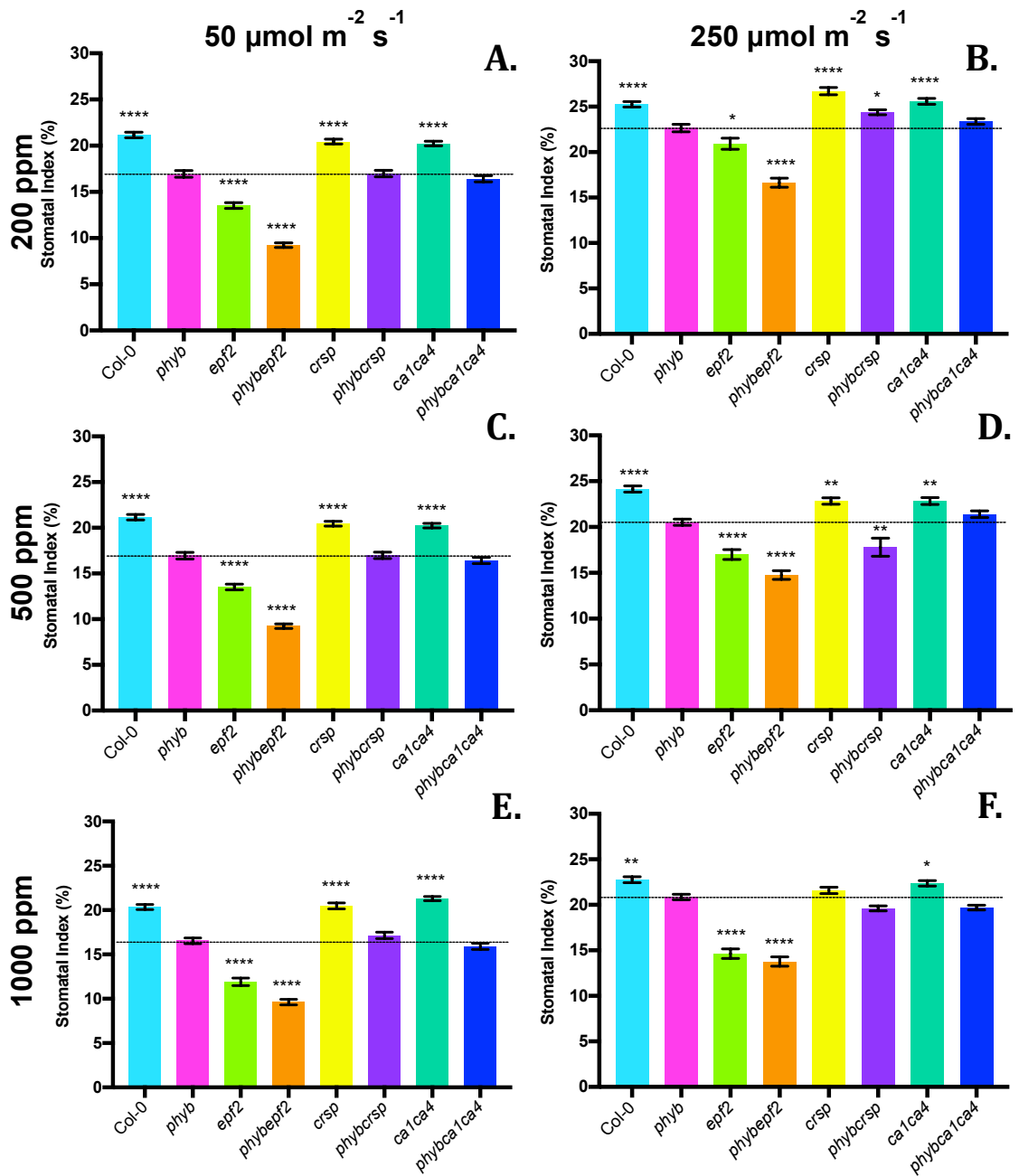


Fig.4 Interactions between *phyB* and components of CO₂ signalling (Stomatal Index). This data is extracted from Figure 3.2 and focuses on *phyB* and the genetic interactions with components of light signalling. Symbols indicates significant difference in SI compared with *phyB* (represented by the dotted line); one-way AVOVA with post-hoc Dunnett's test, ($p^* \leq 0.5$, $p^{**} \leq 0.01$, $p^{***} \leq 0.001$, $p^{****} \leq 0.0001$).

3.8 Discussion

Generally, an increase in irradiance almost always led to an increase in both SD and SI indicating that light promotes cell division (epidermal cell numbers also increase across irradiances; data not shown) over cell expansion and promotes stomatal development. Although the photoreceptor mutants showed consistently lower SD and SI values compared to WT, they were not insensitive to changes in irradiance. The increased SD and SI values at the higher irradiance shows that they maintain responsiveness, this could be due to a number of factors. The first explanation could be that there is extensive redundancy across the photoreceptors and so the single, double and triple mutants used in this study may not have been sufficient to achieve insensitivity. It may be that the photoreceptors promote stomatal development additively and by removing a key photoreceptor, such as phyB, the basal number of stomata decreases but in a linear manner. A possible solution for this could be the use/analysis of higher order mutation including many of the phys and crys in order to achieve complete insensitivity to irradiance. It is also possible that other mechanisms may be interacting to regulate responsiveness to light and there is unpublished data from the Casson lab indicating that there is a non-photoreceptor regulated pathway.

Despite strong evidence suggesting HY5, and potentially HYH, as key transcriptional regulators within phytochrome and cryptochrome signalling, my data does not support any major role for HY5 in terms of light or CO₂-regulated stomatal development. This may be an indication that the photoreceptors are actually regulating stomatal development post-transcriptionally rather than at the transcriptional level, which has been proposed in the literature (Christie *et al.*, 2015; Xu *et al.*, 2015; Lee *et al.*, 2007). Further evidence for a post-transcriptional mechanism of photoreceptor-regulated stomatal development has recently been proposed. Lee *et al.* (2017) demonstrated that COP1 directly interacts with and

targets ICE1 and SCRM2/ICE2 (but not SPCH, MUTE or FAMA directly) within the nucleus for degradation and thus inhibiting stomatal initiation (Lee *et al.*, 2017). However, analysis carried out within the Casson lab shows that COP1 may actually target SPCH directly indicating that COP1 can target major regulators of stomatal development for degradation (data unpublished, Jim Rowe and Nicholas Zoulias). Therefore, it appears likely that the major mechanism through which phyB (and cryptochromes) regulates stomatal development is via inhibition of COP1, promoting SPCH, ICE1 and SCRM2/ICE2 activity.

The increased SD and reduced SI seen in my analysis of *epf2* mutant lines could be due to increased SPCH stability resulting from increased levels of STOM inhibiting the MPK pathway, the resulting phenotype is increased amplifying cell divisions (Lampard *et al.*, 2008). The additive phenotype of phyB and EPF2 may suggest that either COP1 is able to degrade some of this stable SPCH or that COP1 degradation of ICE1 results in SPCH being less active (as it forms dimers with ICE1), therefore enabling progression through the stomatal lineage.

In terms of light/CO₂-mediated stomatal development, the general trend is that a number of light-signaling components impact on [CO₂] signal response, although this is in a condition specific manner (such as *cry1 cry2*). In terms of SD, phyB appears to regulate sensitivity to [CO₂] concentration across both irradiances as the *phyB* mutant is generally unresponsive to changes [CO₂] concentration between 500 ppm and 1000 ppm. Exceptions to this are between 200 ppm and 500 ppm at the higher irradiance (SD) and SI at the lower irradiance level.

Based on this result, as well as bioassay data, which shows that *phyB* seems insensitive to elevated [CO₂] in terms of stomatal development (possibly controls the basal level of stomata in response to light) whilst showing hypersensitivity to elevated [CO₂] in terms of aperture (see chapter 5, Fig.5.0.6). To build upon the idea that plants may have differential development and aperture

responses to stimuli (Haworth *et al.*, 2013), I propose that phyB could be key to determining developmental and/or physiological response to [CO₂] signals.

3.9 Key findings:

- Photoreceptor mutants showed consistently lower SD and SI values compared to WT, however, there was not insensitivity to changes in irradiance.
- Despite strong ChIP data suggesting HY5, and potentially HYH, are key transcriptional regulators within phytochrome and cryptochrome signalling, the data within this study did not support any major role for either in terms of light or CO₂-regulated stomatal development.
- Based on the data within this chapter, it appears likely that the major mechanism through which phyB (and cryptochromes) regulate stomatal development is via inhibition of COP1 and thus promoting SPCH, ICE1 and SCR2/ICE2 activity to positively regulate stomatal development.
- Analysis of *epf2*, *crsp* and *ca1 ca4* mutants, with occasional exceptions, did not reflect the phenotypes previously reported.
- The additive phenotype of phyB and EPF2 may suggest that either COP1 is able to degrade some of this stable SPCH or that COP1 degradation of ICE1 results in SPCH being less active (as it forms dimers with ICE1), therefore enabling progression through the stomatal lineage.
- In terms of SD, phyB appears to regulate sensitivity to [CO₂] concentration across both irradiances as the *phyB* mutant is generally unresponsive to changes [CO₂] concentration between 500 ppm and 1000 ppm.

4.0 Chapter 4:

Photoreceptor regulation of stomatal development in response to [CO₂]

4.1 Introduction

Photoreceptor signaling pathways are regulated by key transcriptional regulators such as HY5 or PIFs, with regulated proteolysis also a major mechanism (Christie *et al.*, 2015; Xu *et al.*, 2015). With regards phytochrome and cryptochrome signaling, HY5, and potentially HYH, have previously been shown as key transcriptional regulators. However, the data in chapter 3 doesn't support a major role for HY5 in terms of light or CO₂-regulated stomatal development. This could suggest that rather than a transcriptional control mechanism; photoreceptors may regulate stomatal development via post-transcriptional mechanisms. Lee *et al.* (2017) provided further evidence supporting a post-transcriptional mechanism of photoreceptor-regulated stomatal development, showing that COP1 directly interacts and targets for degradation ICE1 and SCRM2/ICE2 (but not directly with SPCH, MUTE or FAMA). Work carried out in the Casson Lab shows that COP1 may also target SPCH directly, indicating that COP1 is able to target master regulators for degradation within the stomatal development pathway (data unpublished, Jim Rowe and Nicholas Zoulias). Based on this, it therefore seems likely that the major mechanism by which photoreceptors (phyB and cry1cry2) regulate stomatal development is via inhibition of COP1 to promote SPCH, ICE1 and SCRM2/ICE2 activity. The analysis of gene expression patterns could clarify whether phyB and/or cry1cry2 regulate key stomatal development genes such as SPCH, MUTE, FAMA and STOM in response to changes in [CO₂] concentration.

Another mechanism for regulating stomatal development is via the EPFs, with competition for receptor binding by EPF2 and STOM regulating the MPK pathway that directly targets SPCH (Lee *et al.*, 2015). EPF2 has obviously previously been shown to be involved in CO₂ regulation of stomatal development (Engineer *et al.*, 2014). Interestingly, SPCH has been shown to directly regulate *EPF2* expression, with an increase in *SPCH* correlating with an increase in *EPF2*

expression, therefore there is potential for negative feedback (Lau *et al.*, 2014). SPCH has also been shown to directly regulate or interact with other regulators of stomatal development such as BASL, ICE1 and SCRM2/ICE2 (Kanaoka *et al.*, 2008; Lau *et al.*, 2014). Given SPCH central role in regulating stomatal development, controlling SPCH activity appears to be a major regulatory mechanism (Lampard *et al.*, 2008). Altering SPCH stability has a major impact on the stomatal lineage; whilst increased SPCH activity increases initiation, overexpression inhibits stomatal development via successive dividing cells with no progression to guard cell stage (Lampard *et al.*, 2008).

Another mechanism for light and CO₂ signal integration could be via auxin. Previous research has shown that *STOM* expression is negatively regulated by the auxin response MONOPTEROS (MP); therefore an increase in auxin results in stabilisation of MP and inhibition of *STOM* expression, (Sugano *et al.*, 2010; Zhang *et al.*, 2014; Balcerowicz and Hoecker, 2014). A link has also been shown between auxin and plant sugar status with an increase in auxin biosynthesis positively linked with soluble sugar availability (Sairanen *et al.*, 2012). Due to increased [CO₂] leading to increased carbon fixation and soluble sugars, this may be a link to CO₂ response (Teng *et al.*, 2006). Furthermore, recent research has provided further indication that photoreceptors regulate auxin signaling (Xu *et al.*, 2017).

4.2 Aims

The main aims of the research in this chapter were therefore to:

1. Identify whether light receptors regulate key stomatal development genes in response to changes in [CO₂] concentration.
2. Investigate how phyB and EPF2 may interact to regulate changes in stomatal development in response to elevated [CO₂].

4.3 Results: *cry1cry2* regulates the expression levels of CO₂-signal response genes at low [CO₂].

Based on our stomatal index data (discussed in chapter 3), *cry1cry2* appears to be insensitive to [CO₂] between 200 and 500 ppm at 250 μmol m⁻² s⁻¹ (Fig. 3.6 C). Under the same conditions, Col-0 responds with a reduction in SI between 200 ppm and 500 ppm [CO₂], indicating suppression of stomatal development. The stomatal density response of both genotypes is similar in that both show an increase in SD between 200 ppm to 500 ppm [CO₂], though actual SD in *cry1 cry2* mutants are significantly reduced compared with Col-0.

To analyse this response at the molecular level, gene expression profiles were investigated under these two [CO₂] conditions at high light. Tissue from 10-day-old seedlings (grown at 250 μmol m⁻² s⁻¹ in 500 ppm [CO₂]) were transferred from 500 ppm to 200 ppm [CO₂] for 6 hours with controls maintained at 500 ppm [CO₂]. Seedling tissue was used for analysis due to key stomatal development genes (e.g. *SPCH*, *MUTE* and *FAMA*) being expressed in their highest levels at this development stage (Pillitteri and Dong, 2013). Growing plants under the different [CO₂] regimes could lead to plants being at different developmental stages (growth at lower [CO₂] inhibits growth rates). Therefore, we a transfer experiment was conducted to investigate how the system responds to a dynamic change in [CO₂] levels. The 6 hours time point was chosen as experiments within the Casson lab have previously found that there are robust changes in stomatal regulatory gene expression within 6 hours of other treatments (e.g. light transfers). Throughout the experiments described in this chapter, 500 ppm [CO₂] was chosen as our control and hence transfers were from this concentration. Reciprocal experiments (200 ppm – 500 ppm and 1000 – 500 ppm [CO₂]) could reveal further information regarding the role of photoreceptor responses to [CO₂].

Fig. 4.1 shows the analysis of genes that are associated with the stomatal development pathway. *SPCH*, *MUTE* and *FAMA* are associated with each of the key stages of stomatal development. Col-0 shows slight reductions in expression of *SPCH* (Fig.4.1 A; RE 0.78; SEM 0.116; P-value 0.01), *MUTE* (Fig.4.1 B; RE 0.9; SEM 0.08; P-value <0.5) and *FAMA* (Fig.4.1 C; RE 0.7; SEM 0.09; P-value 0.08). This small reduction in expression on transfer to 200 ppm correlates more with the reduction in SD at this [CO₂] condition as opposed to the increased SI (Fig.3.7 A and Fig.3.8 A). In each of these instances, the *cry1cry2* mutant shows a very similar response and hence the transcriptional analysis of these genes does not provide any major indication of the mechanism regulating the SI insensitivity of *cry1 cry2*.

Col-0 and *cry1 cry2* do however show a differential response when the expression of *ICE1*, *STOM* and *EPF2* was examined (Figs. 4.1 D to F). On transfer to 200 ppm, Col-0 shows an up-regulation of *ICE1*, whereas a significant change in *ICE1* expression is not observed in *cry1 cry2* mutants. *ICE1* dimerises with *SPCH*, *MUTE* and *FAMA* to positively regulate their function and promote progression through the stomatal lineage. *STOM* is up-regulated in Col-0 when transferred from 500 ppm to 200 ppm (Fig.4.1.E), whilst *cry1 cry2* mutants show elevated *STOM* expression at 500 ppm, which is then reduced at 200 ppm; so an opposite response to Col-0. There is no significant change in *EPF2* expression across these [CO₂] conditions in Col-0, however, in *cry1 cry2* mutants *EPF2* expression is elevated at 500 ppm and reduced at 200 ppm (Fig.4.1.F). In this case, both *STOM* and *EPF2* expression follows a similar trend in *cry1 cry2*. In the case of Col-0, it may be that this differential increase in *STOM* expression at 200 ppm, coupled with an increase in *ICE1* accounts for the increased SI under these conditions and that in *cry1 cry2*, the balance between *STOM* and *EPF2* is maintained under both [CO₂] conditions (though RE levels are different) and this accounts for the lack of change in SI.

Another group of genes that were investigated were the CO₂-response genes previously shown to regulate stomatal development (Engineer *et al.*, 2014).

Col-0 shows no change in expression of *CRSP* or *CA4* (or *EPF2*) in response to these changes in [CO₂] concentration (Fig.4.2 A, B and D). However, there is an up-regulation in *CA1* in Col-0 when transferred to 200 ppm (Fig.4.2 C). In contrast, these genes show altered regulation in *cry1cry2* mutants. *CRSP* expression is increased at 500 ppm, compared with Col-0 and is then down-regulated on transfer to 200 ppm (Fig.4.2 A). This expression pattern mirrors the pattern observed for *EPF2* in *cry1 cry2* mutants (Fig.4.1 F). Interestingly, *cry1cry2* shows up-regulation of *CA1* and *CA4* when transferred to 200 ppm. The *CA1* response does follow the same trend as Col-0, however, the basal levels of expression are lower in *cry1cry2*. Therefore, analysis of these particular CO₂ related genes; it can conclude that at least in Col-0, *CA1* expression is modulated by CO₂ in this timeframe. *cry1 cry2* has altered profiles of both *CA1* and *CRSP*, suggesting that it has an altered response to [CO₂], however, unlike the stomatal genes, neither offers an obvious explanation for the insensitivity of stomatal development in this mutant.

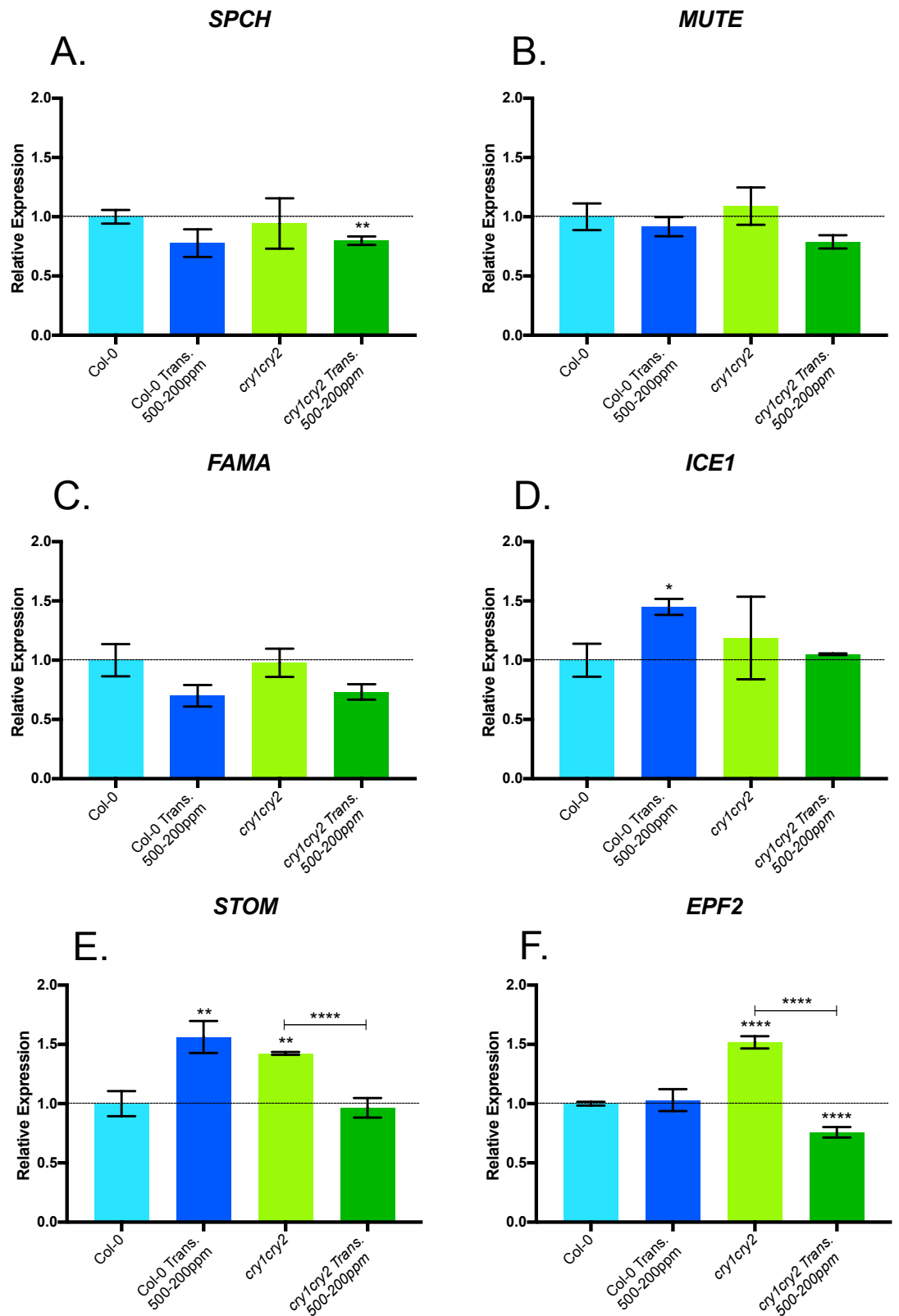


Fig.4.1 Shows stomatal development gene expression analysis for Col-0 and *cry1cry2*. Plants were grown at $250 \mu\text{mol m}^{-2} \text{s}^{-1}$ and 500 ppm $[\text{CO}_2]$ for 10 days then transferred from 500 ppm to 200 ppm $[\text{CO}_2]$. Data was normalised using house-keeping gene *UBC21* and expression values are relative to Col-0 (relative expression level of 1). A) shows *SPCH* expression levels. B) shows *MUTE* expression levels. C) shows *FAMA* expression levels. D) shows *ICE1* expression levels. E) shows *STOM* expression levels. F) shows *EPF2* expression levels. Mean values are shown for each genotype (n= 3; with 3 technical repeats) with error bars indicating mean \pm SEM. Symbols indicate significant difference in expression compared with Col-0; t-test ($p^* \leq 0.05$, $p^{**} \leq 0.01$, $p^{***} \leq 0.001$, $p^{****} \leq 0.0001$).

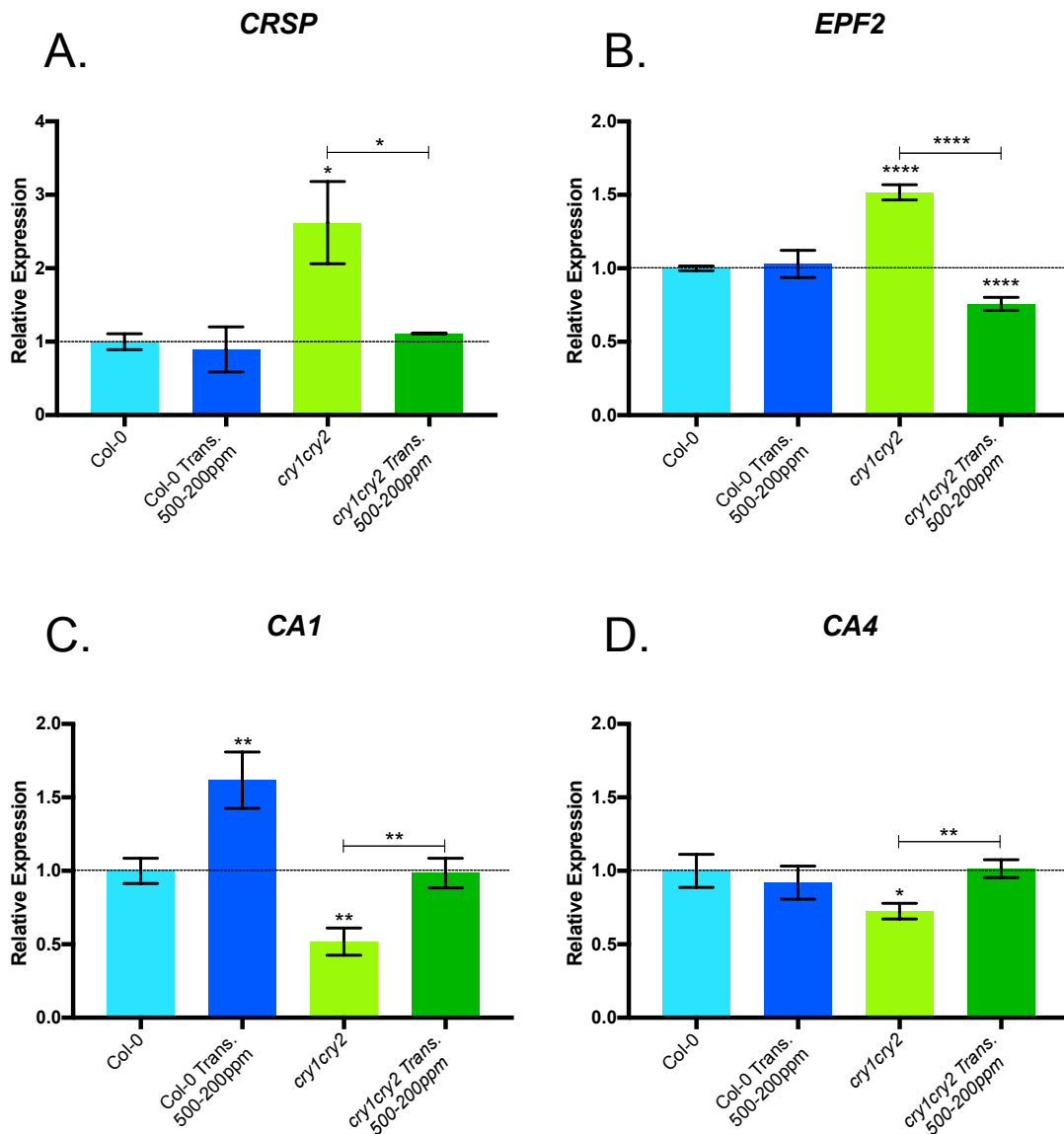


Fig.4.2 Shows gene expression analysis of CO₂ signal response genes for Col-0 and *cry1cry2*. Plants were grown at 250 $\mu\text{mol m}^{-2} \text{s}^{-1}$ and 500 ppm [CO₂] for 10 days then transferred from 500 ppm to 200 ppm [CO₂]. Data was normalised using house-keeping gene *UBC21* and expression values are relative to Col-0 (relative expression value of 1). A) shows *CRSP* expression levels. B) shows *EPF2* expression levels. C) shows *CA1* expression levels. D) shows *CA4* expression levels. Mean values are shown for each genotype (n= 3; with 3 technical repeats) with error bars indicating mean +/- SEM. *EPF2* expression data has been included for ease of comparison (Fig.4.1). Symbols indicate significant difference in expression compared with Col-0; t-test (p* = ≤ 0.05 , p** = ≤ 0.01 , p*** = ≤ 0.001 , p**** = ≤ 0.0001).

4.4 phyB regulates key stomatal development and CO₂-signal response gene expression.

Whereas an increase from 500 ppm to 1000 ppm down-regulates stomatal development in WT plants, *phyB* mutants appear to be insensitive to [CO₂] concentrations in this range based on both our stomatal index and density results, particularly at high light (discussed in chapter 3; Figs 3.5 and 3.6). We therefore took the same approach as described above but in this case, seedlings were transferred from 500 ppm to 1000 ppm for 6 hours, with controls maintained at 500 ppm.

Col-0 showed no significant difference in *SPCH* or *MUTE* expression when transferred to 1000 ppm (Fig.4.3 A and B). *FAMA*, *ICE1* and *STOM* expression levels are up-regulated when transferred to 1000 ppm (Fig.4.3 C to E). This is unusual given that the increase in [CO₂] negatively regulates stomatal development genes. However, the up-regulation of *EPF2* in Col-0 when subjected to 1000 ppm may negate the slight up-regulation of the positive regulators of stomatal development to cause a reduction in stomata overall (Fig.4.3 F). The expression of *SPCH* is reduced under both conditions in *phyB*, however *ICE1* expression is still up-regulated. One significant difference with Col-0 is with regards *STOM* and *EPF2*, with the expression of these genes not changing in *phyB* mutants. Again, there is therefore the possibility that maintaining the balance of *STOM/EPF2* may account for the insensitivity of *phyB* mutants to elevated [CO₂]. The data would therefore suggest that *phyB* is required for mediating these changes in these EPFs following transfer to elevated [CO₂].

In terms of CO₂ signal response genes, Col-0 shows down-regulation of *CRSP* when transferred to 1000 ppm which doesn't correlate with the literature which has previously showed up-regulation in WT, though in this case there was no transfer and so represented steady state levels (Fig.4.4 A; Engineer *et al.*, 2014). As

discussed above, Col-0 does show up-regulation of *EPF2* when transferred to 1000 ppm, which supports CO₂ negatively regulating stomatal development (Fig.4.4 B). However, Col-0 shows no changes in expression of *CA1* or *CA4* when transferred to 1000 ppm (Fig.4.4 C and D). Given that *CA1* is regulated in response to a reduction in [CO₂] (Fig. 4.2 A) this may suggest that there is differential responsiveness of *CA1* to [CO₂], or that this timeframe is not interrogating this response.

In contrast to Col-0, *phyB* shows no change in *CRSP* expression when transferred to elevated [CO₂] (1000 ppm) but does show some down-regulation of *CA1*. As discussed, *phyB* appears to be insensitive to [CO₂] with regards the regulation of *EPF2*. As with *cry1 cry2* above, it would appear that analysis of these CO₂ regulatory genes is less informative than stomatal developmental genes in determining a mechanism for *phyB* insensitivity to elevated [CO₂].

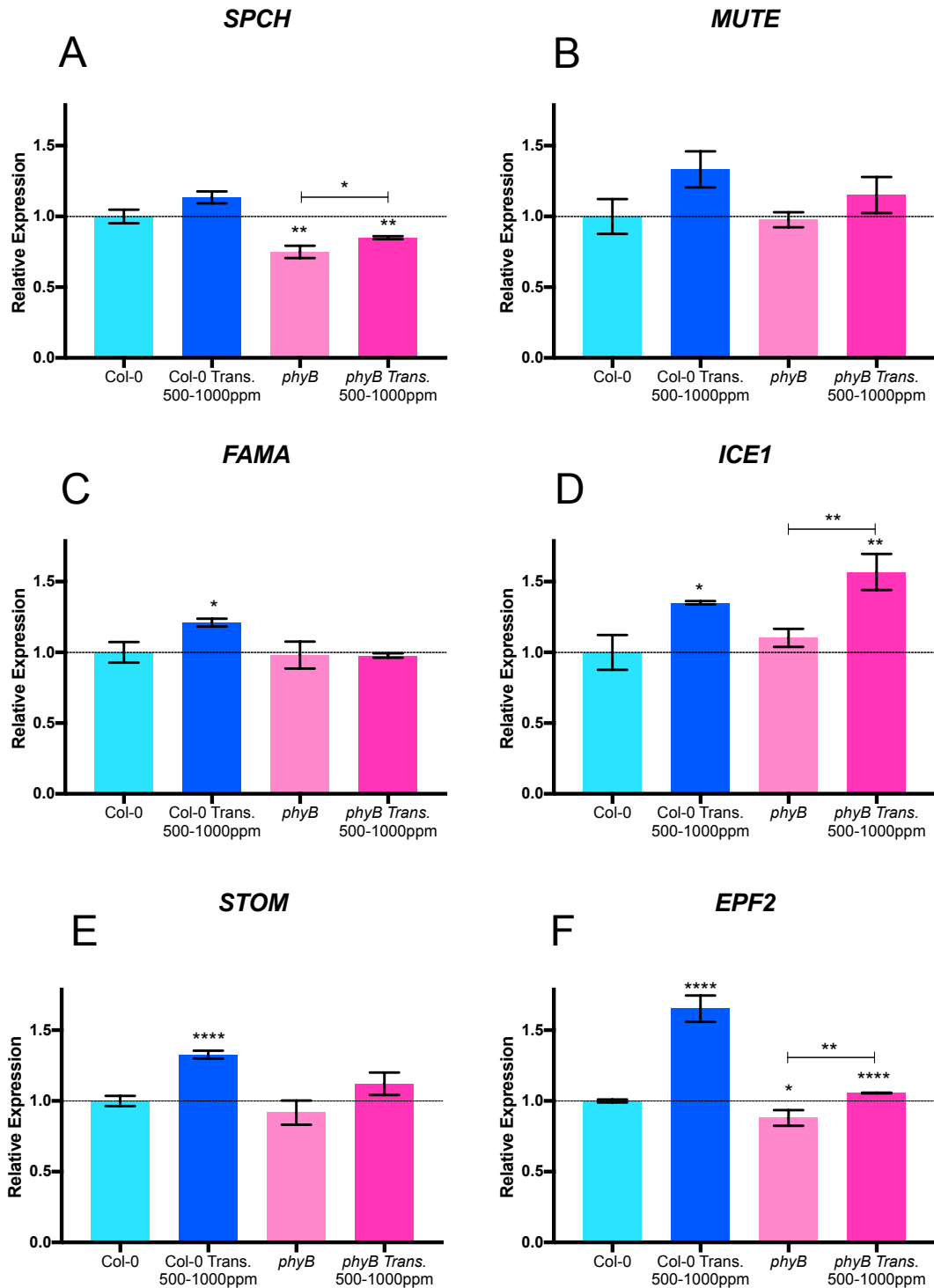


Fig.4.3 Shows stomatal development gene expression analysis for Col-0 and *phyB*. Plants were grown at 250 $\mu\text{mol m}^{-2} \text{s}^{-1}$ and 500 ppm $[\text{CO}_2]$ for 10 days then transferred from 500 ppm to 1000 ppm $[\text{CO}_2]$. Data was normalised using house-keeping gene *UBC21* and expression values are relative to Col-0 (relative expression value of 1). A) shows *SPCH* expression levels. B) shows *MUTE* expression levels. C) shows *FAMA* expression levels. D) shows *ICE1* expression levels. E) shows *STOM* expression levels. F) shows *EPF2* expression levels. Mean values are shown for each genotype (n= 3; with 3 technical repeats) with error bars indicating mean \pm SEM. Symbols indicate significant difference in expression compared with Col-0; T-Test ($p^* = \leq 0.05$, $p^{**} = \leq 0.01$, $p^{***} = \leq 0.001$, $p^{****} = \leq 0.0001$).

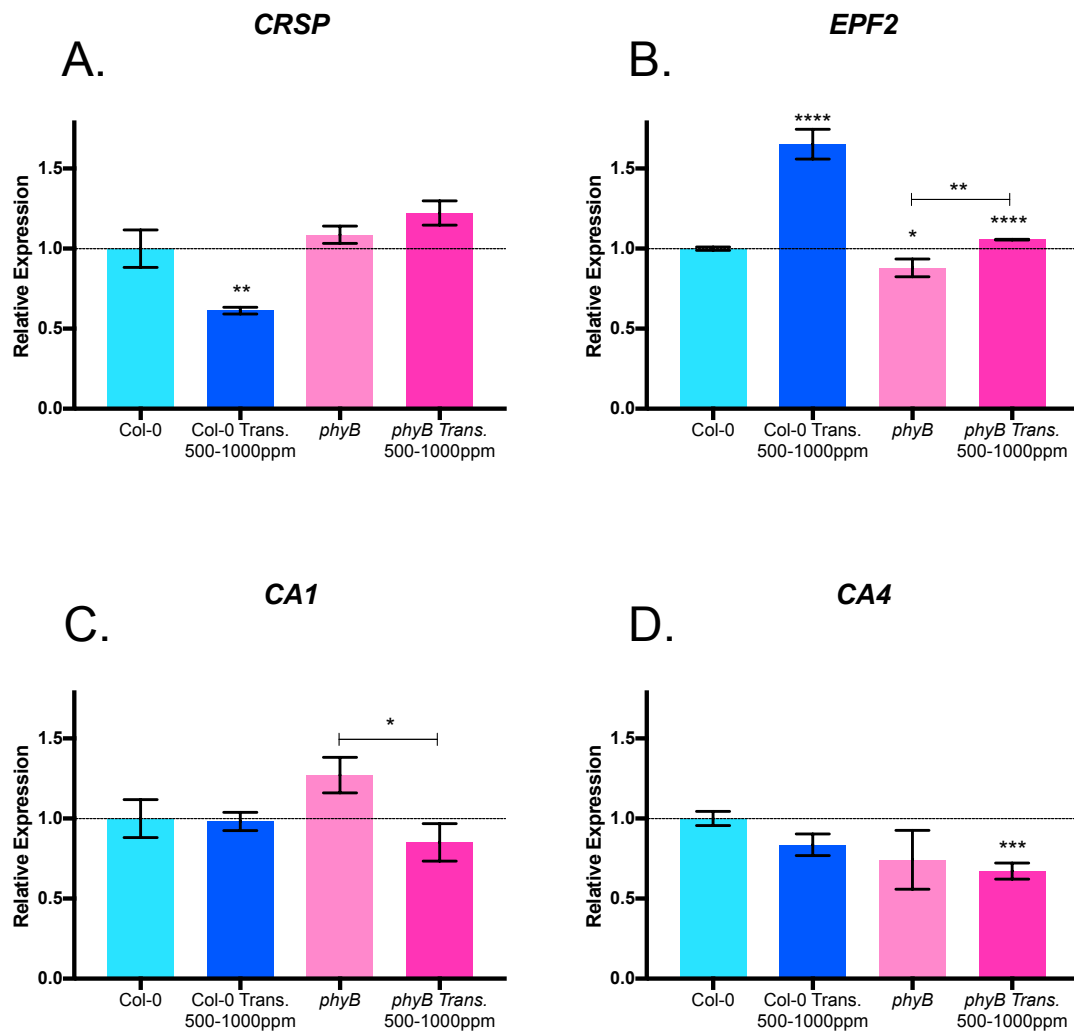


Fig.4.4 Shows gene expression analysis of CO₂ signal response genes for Col-0 and *phyB*. Plants were grown at 250 $\mu\text{mol m}^{-2} \text{s}^{-1}$ and 500 ppm [CO₂] for 10 days then transferred from 500 ppm to 1000 ppm [CO₂]. Data was normalised using house-keeping gene *UBC21* and expression values are relative to Col-0 (expression value of 1). A) shows *CRSP* expression levels. B) shows *EPF2* expression levels. C) shows *CA1* expression levels. D) shows *CA4* expression levels. *EPF2* expression data has been included for ease of comparison (Fig.4.3). Mean values are shown for each genotype (n= 3; with 3 technical repeats) with error bars indicating mean +/- SEM. Symbols indicate significant difference in expression compared with Col-0; T-Test (p* = ≤ 0.05 , p** = ≤ 0.01 , p*** = ≤ 0.001 , p**** = ≤ 0.0001).

4.5 *phyB* acts additively with *epf2* to regulate key stomatal development genes.

To further investigate the additive phenotype of *phyB* and *epf2* at 250 $\mu\text{mol m}^{-2} \text{s}^{-1}$ (discussed in chapter 3) gene expression analysis was performed on *phyB*, *epf2* and *phyBepf2* mutants (grown at 250 $\mu\text{mol m}^{-2} \text{s}^{-1}$ in 500 ppm) that had been subjected to a 6-hour transfer from 500 ppm to 1000 ppm [CO_2]. It was proposed that the additive phenotype could be due to increased COP1 activity targeting either SPCH or ICE1, coupled to the fact that *epf2* mutants are likely to have reduced MPK targeting of SPCH (and hence more stable SPCH). The result under most growth conditions was that the *phyB epf2* double mutant had further reductions in SI compared with either parent.

epf2 shows increased levels of *SPCH*, *FAMA*, *ICE1* and *STOM* compared to *phyB* at 500 ppm. The detection of EPF2 transcript in the *epf2-1* background is likely due to the qPCR primer sites being upstream of the T-DNA insertion site. The expression levels of these genes do not change in *epf2* when transferred to 1000 ppm (Fig.4.5). This result correlates with the proposed mechanism and may also explain the increased basal level of stomata in *epf2* mutants observed across all conditions compared with *phyB*. The additive effects of *phyB* and *epf2* are also reflected in the gene expression patterns of *phyBepf2*, particularly with regards *SPCH* and *ICE1* (Fig.4.5 A, C, D and E). Interestingly, *phyB* appears to be epistatic to *epf2* when regulating *CRSP* expression (fig.4.6 A). *epf2* shows down-regulation in *CRSP* when transferred to 1000 ppm, however, *phyBepf2* shows increased expression which remains unchanged when subjected to 1000 ppm (Fig.4.6.A). *phyB* and *epf2* show no changes in *CA1* or *CA4* expression levels (Fig.4.6 C and D).

Taken together, the additive interactions observed with the stomatal counts data are partly evident in this molecular analysis. However, these gene expression

analyses would not be predictive of the SI data for *phyB epf2* compared with the parental lines but is more in line with the SD data. Under most instances, the double mutant has an SI that is lower than either parent and yet expression of *SPCH* and *EPF2* is intermediary. Given that both pathways ultimately regulate protein activity and stability, a detailed analysis of *SPCH* (and *ICE1*) target genes would be required to analyse this interaction.

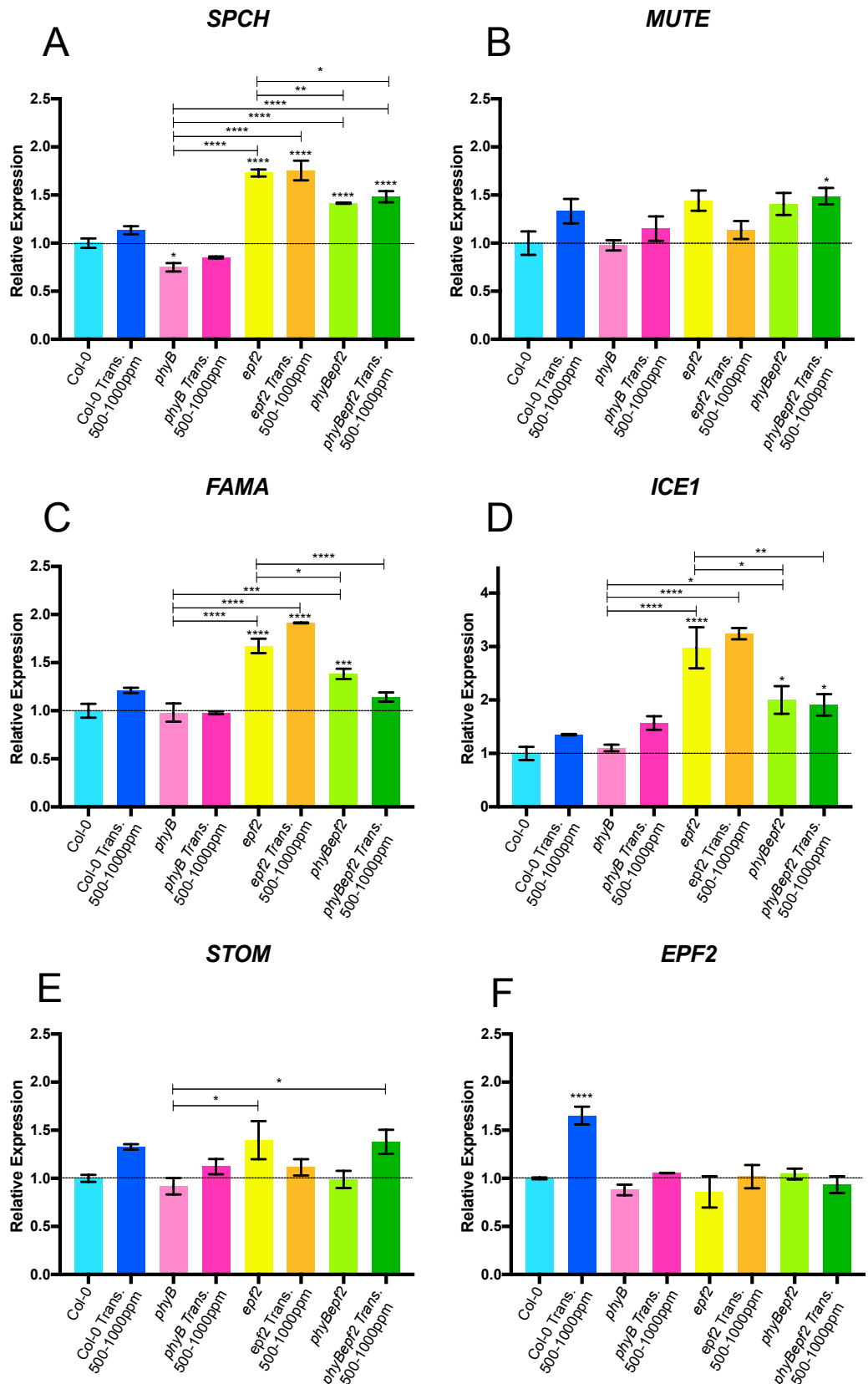


Fig.4.5 Shows stomatal development gene expression analysis for Col-0, *phyB*, *epf2* and *phyBepf2*. Plants were grown at 250 $\mu\text{mol m}^{-2} \text{s}^{-1}$ and 500 ppm $[\text{CO}_2]$ for 10 days then transferred from 500 ppm to 1000 ppm $[\text{CO}_2]$. Data was normalised using house-keeping gene *UBC21* and expression values are relative to Col-0 (relative expression value of 1). A) shows *SPCH* expression levels. B) shows *MUTE* expression levels. C) shows *FAMA* expression levels. D) shows *ICE1* expression levels. E) shows *STOM* expression levels. F) shows *EPF2* expression levels. Mean values are shown for each genotype (n= 3; with 3 technical repeats) with error bars indicating mean \pm SEM. Symbols indicate significant difference in expression compared with Col-0; One-way ANOVA ($p^* \leq 0.05$, $p^{**} \leq 0.01$, $p^{***} \leq 0.001$, $p^{****} \leq 0.0001$).

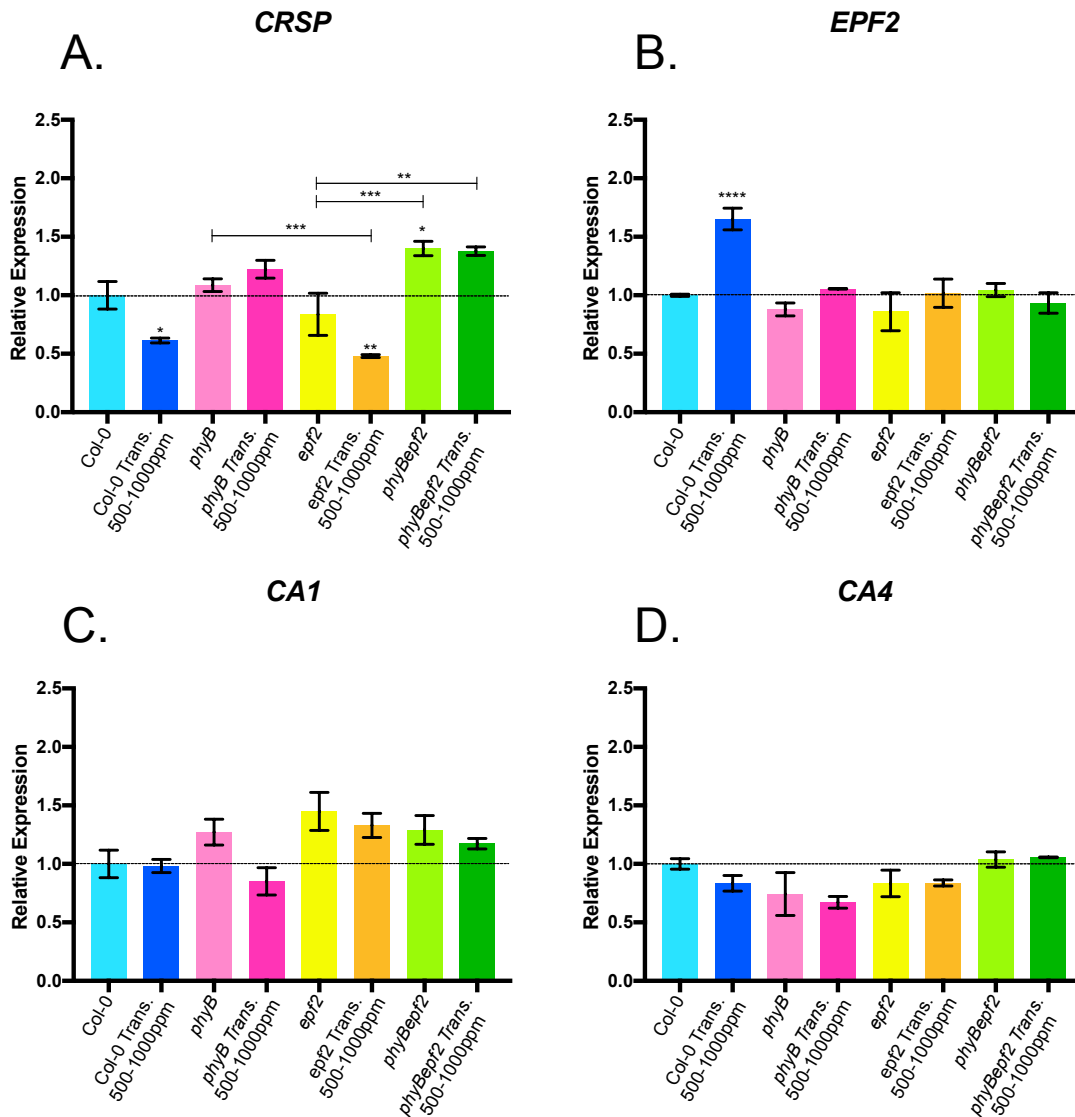


Fig.4.6 Shows gene expression analysis of CO₂ signal response genes for Col-0, *phyB*, *epf2* and *phyBepf2*. Plants were grown at 250 $\mu\text{mol m}^{-2} \text{s}^{-1}$ and 500 ppm [CO₂] for 10 days then transferred from 500 ppm to 1000 ppm [CO₂]. Data was normalised using house-keeping gene *UBC21* and expression values are relative to Col-0 (expression value of 1). A) shows *CRSP* expression levels. B) shows *EPF2* expression levels. C) shows *CA1* expression levels. D) shows *CA4* expression levels. *EPF2* expression data has been included for ease of comparison (Fig.4.5). Mean values are shown for each genotype (n= 3; with 3 technical repeats) with error bars indicating mean +/- SEM. Symbols indicate significant difference in expression compared with Col-0; One-way ANOVA (p* = ≤ 0.05 , p** = ≤ 0.01 , p*** = ≤ 0.001 , p**** = ≤ 0.0001).

4.6 Discussion

Our results show that *cry1cry2* is required to mediate CO₂-signaling gene expression to regulate stomatal development in response to low [CO₂]. The expression patterns of key regulators of stomata development, *SPCH*, *MUTE* and *FAMA* do not appear to be directly regulated by *cry1cry2* in a [CO₂] dependent manner. However, functional CRY1 and CRY2 do appear to be required for the correct regulation of *STOM*, a positive regulator, as well as *EPF2* and *CRSP*, negative regulators, in response to 200 ppm. The insensitivity of the *cry1 cry2* mutant to sub-ambient [CO₂] (200 ppm) may reflect a maintained balance of *STOM* and *EPF2*. In WT plants, it appears that an increase in *STOM* may account for increased stomatal development under these lower [CO₂] conditions. At present, little is known about the regulation of *STOM* expression (or processing of the propeptide). CRYs are associated with regulating gene expression either via inhibition of COP1 or by interacting with cryptochrome-interacting basic-helix-loop-helix proteins (CIBs; reviewed in Liu *et al.*, 2011). One of the known targets of COP1 is HY5 but given that our data shows no role for HY5 in regulating stomatal development, it seems unlikely that this accounts for the differences observed here. *STOM* expression has previously been shown to be regulated by the auxin response factor, MONOPTEROS (MP; Zhang *et al.*, 2014). Therefore, increased auxin concentration leads to stabilisation of MP and inhibition of *STOM* expression. It has been shown that there is a link between the sugar status of the plant and auxin with increased auxin biosynthesis positively correlating with soluble sugar availability (Sairanen *et al.*, 2012). Here, there could be a link to CO₂, given that increased [CO₂] does lead to increased carbon fixation and soluble sugars (Teng *et al.*, 2006). How could this relate to the CRYs and the mis-regulation of *STOM*? One possibility is via PIFs, which are known to regulate auxin biosynthesis and be negatively regulated by CRYs (Franklin *et al.*, 2011; Pedmale *et al.*, 2016).

Unfortunately, whilst this might provide a mechanism, it would be predicted that an increase from 500 ppm to 1000 ppm would have a similar outcome and yet *cry1cry2* mutants are not insensitive in this range.

phyB mutants are however insensitive to these higher [CO₂] concentrations and do appear to be required for the correct regulation of *STOM* expression between 500 ppm and 1000 ppm. In the WT however, there is a small but significant increase in *STOM* expression after transfer to 1000 ppm, which does not fit with the hypothesis presented above, as you might expect a further increase in soluble sugars and hence auxin. *EPF2* expression is significantly up-regulated in WT seedlings and shifting the balance between *STOM* and *EPF2* is therefore a potential mechanism for elevated [CO₂] to inhibit stomatal development, in line with previous work (Engineer *et al.*, 2014). *phyB* appears to be required for the elevated [CO₂] increase in *EPF2* given that there is no increase in *phyB* mutants. As indicated, *phyB* is known to inhibit COP1 which has now been shown to target ICE1 for degradation (Lee *et al.*, 2017), and potentially SPCH (unpublished data). SPCH is known to directly regulate the expression of *EPF2* and hence increases in SPCH activity can present as increased *EPF2* expression (Lau *et al.*, 2014). We don't see any evidence for transcriptional control of *SPCH*, therefore any change would be at the protein level and the increase in *EPF2* would then feedback to inactivate this. Further time points would be required to investigate whether such a feedback loop is in operation here and the final balance. It would also be beneficial to investigate the expression of other SPCH targets, such as *BASL*, to determine the nature of the active SPCH pool here. Whilst increasing SPCH activity may seem counterintuitive to negative regulation of stomatal development it should be pointed out that overexpression of SPCH does lead to an epidermis of small dividing cells (Lampard *et al.*, 2008). Whilst SPCH is critical for stomatal development, the ability to remove SPCH is also of importance.

This point may therefore be of relevance when considering the *phyB epf2* mutant and the additive phenotype compared to the parental lines. The gene expression data for *SPCH* and *ICE1* is intermediary between the two parental lines, yet the SI is generally lower for the double mutant. If *SPCH* is stabilised in *epf2* mutants (due to STOM inhibiting the MPK pathway), then the question is how the removal of *phyB* further inhibits progression through the pathway. Altering *ICE1* levels does impact on progression through stomatal development (Kanoaka *et al.*, 2008). So, a combination of stable *SPCH* and a reduction in *ICE1* may inhibit the ability of cells to exit early stages of development. Again, it would be useful to examine the expression of other targets of *SPCH* to determine more precisely the active pool of *SPCH* in the double mutant.

Overall, there is evidence to suggest that *phyB* is involved responsible for regulating both stomatal development and physiological responses to changes in $[CO_2]$ with *cry1cry2* playing a role at low $[CO_2]$ concentrations. In consideration of the affects of *phyB* on stomatal number, it would be interesting to investigate the extent of which *phyB* controls physiological response to light/ CO_2 signals.

4.7 Key findings:

- *cry1cry2* is required to mediate CO₂-signaling gene expression to regulate stomatal development in response to low [CO₂].
- *CRY1* and *CRY2* appear to be required for the correct regulation of *STOM*, a positive regulator, as well as *EPF2* and *CRSP*, negative regulators, in response to 200 ppm.
- *phyB* acts additively with *epf2* to regulate key stomatal development genes.

5.0 Chapter 5:

Physiological effects of phyB on plant water use efficiency.

5.1 Introduction

Current issues surrounding climate change, food security and fresh water scarcity have meant that the investigation of plant water use efficiency (WUE) has become increasingly important within crop research in recent years. WUE refers to the balance of gains (in this instance, moles of [CO₂] assimilated) and costs (conductance - water lost) (Medrano *et al.*, 2014). It is important to clarify that although improved water use efficiency can improve productivity and reduce water stress under drier conditions, the term differs in meaning from 'drought-tolerance', which is a plants ability to survive or recover from a prolonged period of water scarcity. In the short-term, plants can improve WUE by reducing stomatal apertures and thus reduce conductance (physiological response) (Franks *et al.*, 2015). A more long-term response of plants is to reduce stomatal density, which reduces the maximum rate of stomatal conductance in order to improve WUE (developmental response) (Franks *et al.*, 2015). Genetic and physiological analysis of *EPF* mutants and transgenic lines showed that genetic manipulation of stomatal density (SD) directly impacts on plant WUE, with a reduced SD resulting in improved WUE (Franks *et al.*, 2015). There are limitations to improving WUE via reductions in SD as the uptake of CO₂ can be limited by a reduction of stomatal apertures potentially effecting photosynthetic capacity and possibly reducing overall biomass.

Previous work, along with data in earlier chapters, has shown that phyB regulates stomatal development with impacts on SD (Casson *et al.*, 2009; Boccalandro *et al.*, 2009). An end of day pulse of FR light was shown to reduce SD in WT (Ler) *Arabidopsis* plants and that conductance rates correlated positively with SD; increased SD resulted in increased transpiration (Boccalandro *et al.*, 2009). It was demonstrated that this response was regulated by phyB and that as a result, phyB negatively regulates WUE (i.e. *phyB* mutants have improved WUE compared with WT plants). Under the experimental conditions used in this study, mutations in

phyB were shown to negatively impact on assimilation rates and also resulted in stomatal limitations to CO₂ uptake (Boccalandro *et al.*, 2009). The study did not determine whether these limitations were purely due to the developmental role of *phyB* in regulating stomatal development or whether *phyB* also regulates stomatal responses, nor did they investigate whether non-stomatal limitations account for some of these changes.

5.2 Aims

1. Understand the role of *phyB* in mediating plant WUE.
2. Determine whether *phyB* controls stomatal aperture response to changes in [CO₂].

5.3 Results: *phyB* improves water use efficiency

(WUE_i)

Based on the stomatal density results (discussed in chapter 3), *phyB* is necessary for light-mediated stomatal development but also seems to play a role in regulating responses $[CO_2]$, particularly between 500 ppm to 1000 ppm. Although, in terms of stomatal density, *phyB* seems insensitive to elevated $[CO_2]$ its epistatic function to *CA1 CA4*, responsible for CO_2 -mediated stomatal closure, suggests that *phyB* may play a regulatory role in both short and long-term stomatal responses to light/ CO_2 integration. To investigate whether *phyB* effects CO_2 uptake and plant performance compared to wild-type plants, gas exchange analysis was performed using the Li-6400XT Infra Red gas analyser. We focused on $[CO_2]$ responses in this instance as opposed to light response curves. All plants were grown under three light conditions and two $[CO_2]$ conditions. Other factors, including photoperiod, temperature and relative humidity were constant across experiments. Experimental conditions were; $50 \mu mol m^{-2} s^{-1}$ (low light), $130 \mu mol m^{-2} s^{-1}$ (medium light) or $250 \mu mol m^{-2} s^{-1}$ (high light) in medium $[CO_2]$ (500 ppm) or high $[CO_2]$ (1000 ppm) for 35 days. One expanded and healthy leaf per plant was subjected to saturating light and step-wise changes in $[CO_2]$ concentration (see methods). Intrinsic WUE (WUE_i), refers to the ratio (A/g_s) of assimilation of CO_2 (A) and conductance (g_s) to indicate the level of conductance via stomata.

In Fig.5.0.1, the *phyB* mutant (shown as pink symbols) shows a general trend of improved WUE_i compared to wild-type, Col-0 (shown as blue symbols). These improvements in the WUE_i of *phyB* mutants are most evident for plants grown at 500 ppm $[CO_2]$ and then when leaves are exposed to $[CO_2]$ concentrations greater than 500 ppm. Whilst there is variability, the light growth conditions do not appear to change this trend (Fig.5.0.1.A, C and E). However, when grown at 1000 ppm $[CO_2]$, in general, there is no significant difference in the WUE_i of *phyB*

compared with Col-0 (Fig.5.0.1. B, D and F). *phyB* mutants do show improved WUE_i at $[CO_2]$ concentrations greater than 1200 ppm but this is only significant for those plants grown in the low light conditions (Fig.5.0.1.B). Therefore, mutations in *phyB* can result in improved WUE_i but this is dependent on the $[CO_2]$ growth conditions. This dampened WUE response of 1000 ppm compared to 500 ppm grown plants, is likely due to the 1000 ppm grown plants being acclimatised to the higher range of $[CO_2]$ concentrations used within this experiment.

To better understand the factors driving the differences in WUE_i , the data was segregated in to its constituent parts of assimilation (A) and conductance (g_s). The aim of analysing separate components was to investigate whether stomatal, non-stomatal (photosynthetic) or a combination of factors contribute to the improved WUE_i of *phyB* mutants. Fig.5.0.2 shows A/C_i curves for Col-0 and *phyB* grown under the different light and $[CO_2]$ conditions; A refers to the net $[CO_2]$ uptake within a leaf, whilst C_i refers to the internal $[CO_2]$ concentration within a leaf. *phyB* mutants show reduced assimilation (approx. half) compared with Col-0 if they have been grown under the low light conditions and both 500 ppm and 1000 ppm (Fig.5.0.2.A and B). Similarly, this is also observed for plants grown at high light in 1000 ppm, (Fig.5.0.2.F). When grown under the remaining conditions (e.g. 500 ppm $[CO_2]$ and $130 \mu\text{mol m}^{-2} \text{s}^{-1}$), there was no difference in assimilation rates between *phyB* and Col-0. However, in all cases, $[CO_2]$ levels (C_i) within the leaves of *phyB* mutants were consistently reduced compared with Col-0; this becomes more pronounced at higher external $[CO_2]$ concentrations. This would suggest there may be stomatal limitations to CO_2 uptake across a range of plant growth conditions, whilst non-stomatal limitations effecting photosynthetic ability are particularly apparent for *phyB* mutants grown at low light. Interestingly, assimilation rates for both Col-0 and *phyB* grown at high light and 1000 ppm $[CO_2]$ are comparable to those of low light grown plants and may indicate that growth under these conditions suppresses photosynthesis (Fig.5.0.2.A, B and F).

The A/C_i curves suggest that there are stomatal limitations to CO_2 diffusion in *phyB* mutants. Fig.5.0.3 shows conductance rates of *phyB* and Col-0, which refers to specific stomatal conductance levels and does not include cuticular conductance (similar results were observed for calculated stomatal transpiration). *phyB* has a consistently lower conductance rate compared to Col-0 across all plant growth conditions. This has to be considered alongside the stomatal density data in chapter 3, since conductance will be determined by both stomatal density as well as stomatal aperture. Whilst *phyB* mutants have reduced SDs compared with Col-0 under high light conditions ($250 \mu\text{mol m}^{-2} \text{s}^{-1}$), this is not always evident at low light. Indeed at growth conditions of 500 ppm [CO_2] and $50 \mu\text{mol m}^{-2} \text{s}^{-1}$, there is no difference in SD between Col-0 and *phyB*. Therefore, this would suggest that SD differences alone cannot account for these observed reductions in conductance and suggest that there may be further differences in pore aperture (see below). In addition to this, there is a further interesting observation. Increased [CO_2] is known to cause stomatal closure (Engineer *et al.*, 2016). This response to [CO_2] is evident in reduced conductance rates at higher concentrations of [CO_2] (Fig.5.0.3.C to F), however, it is significantly limited when plants of both genotype are grown at low light (Fig.5.0.3.A and B). Whilst again, the lower SD of low light grown plants is likely a factor, this may also indicate that stomatal aperture sensitivity to [CO_2] may be regulated by the light conditions during growth.

In combination with the analysis of conductance, stomatal limitations can be more directly examined by plotting A/C_i response within a leaf compared to extracellular [CO_2] concentration (or ambient [CO_2]; Fig.5.0.4). A nonsynchronous response would indicate that stomata are limiting the diffusion of CO_2 into the leaf (g_s is limiting A) and thus effecting differences in WUE_i (McAusland *et al.*, 2016; Farquhar and Sharkey, 1982).

Stomatal limitations appear to be an influencing factor to differences in WUE_i in plants grown at $50 \mu\text{mol m}^{-2} \text{s}^{-1}$ under both [CO_2] conditions (500 ppm and 1000

ppm) as well as $250 \mu\text{mol m}^{-2} \text{s}^{-1}$ and 500 ppm (Fig.5.0.4.A, B and E). However, there do not appear to be apparent stomatal limitations effecting plants that were grown at $130 \mu\text{mol m}^{-2} \text{s}^{-1}$ at 500 ppm or 1000 ppm or plants grown at $250 \mu\text{mol m}^{-2} \text{s}^{-1}$ and 1000 ppm [CO_2] (Fig.5.0.4.C, D and F).

Under low light, stomatal and non-stomatal limitations play a role in driving a difference in WUE_i as both assimilation and conductance levels are lower in *phyB* compared to Col-0 (Fig.5.0.1.A and B; Fig.5.0.2.A and B; Fig.5.0.3.A and B; Fig.5.0.4.A and B). Stomatal limitations specifically play a role at high light and 500 ppm, the change in WUE_i is driven solely by a reduction in conductance levels of *phyB*, assimilation does not appear to be significantly different compared to Col-0 (Fig.5.0.1.E; Fig.5.0.2.E; Fig.5.0.3.E; Fig.5.0.4.E).

Strict uncoupling of stomatal and non-stomatal limitations may be aided by longer exposure time to changes in [CO_2] during IRGA analysis. The 2 to 3 minutes experimental exposure time may not have been sufficient for stomata to acclimate optimally to [CO_2] increments.

The total chlorophyll content of leaves was therefore determined (Fig.5.0.5). Across all growth conditions, chlorophyll levels are continually lower in *phyB* compared to Col-0. This may in part explain differences in photosynthetic ability of *phyB* compared with Col-0 but given the growth condition specific difference, further analysis of photosystem efficiency could provide further insights in to the full extent of *phyB*-photosynthetic limitations. Other factors considered to be stomatal limitations include number (stomatal density), aperture and size.

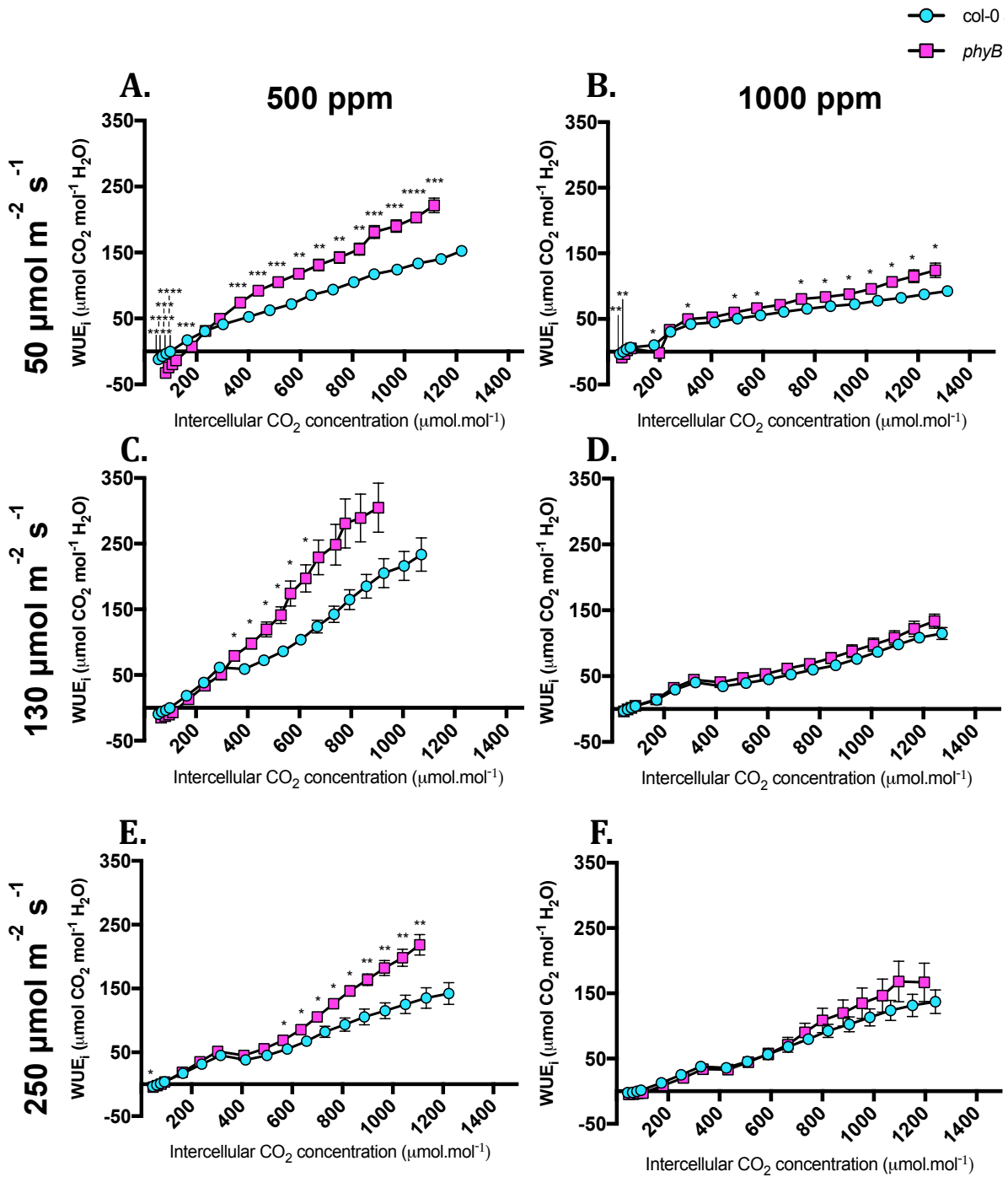


Fig.5.0.1 Water use efficiency (WUE_i) of mature leaves for Col-0 and *phyB*. Plants were grown at irradiances $50 \mu\text{mol m}^{-2} \text{ s}^{-1}$ (A, B), $130 \mu\text{mol m}^{-2} \text{ s}^{-1}$ (C, D) or $250 \mu\text{mol m}^{-2} \text{ s}^{-1}$ (E, F) and $[\text{CO}_2]$ concentrations of 500 ppm (A, C, E) or 1000 ppm (B, D, F). Mean values are shown for each genotype ($n = 8$) with error bars indicating mean \pm SEM. Symbols indicate significant difference in WUE_i compared with Col-0; t-test, ($p^* = \leq 0.05$, $p^{**} = \leq 0.01$, $p^{***} = \leq 0.001$, $p^{****} = \leq 0.0001$).

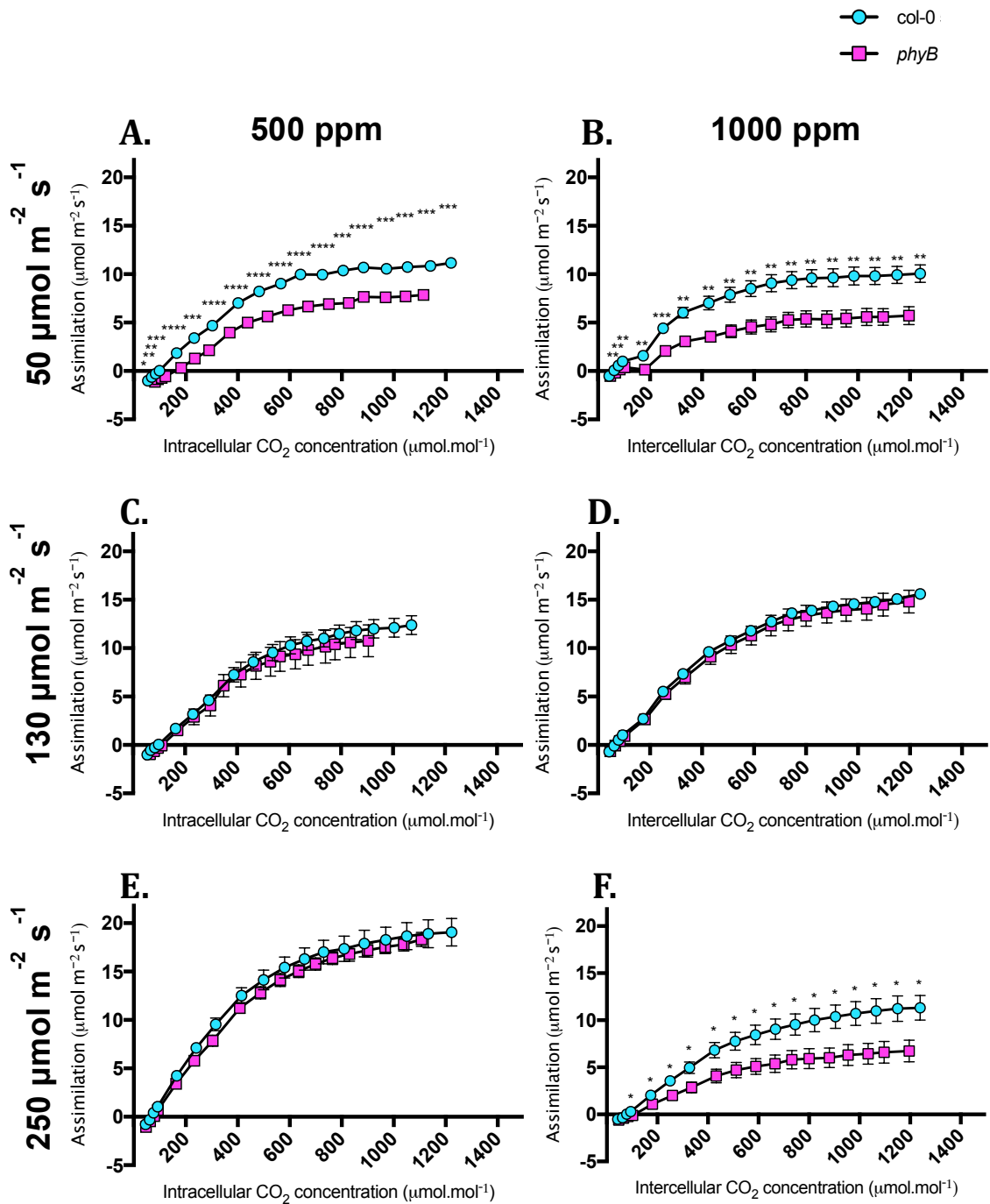


Fig.5.0.2 A/Ci curves showing Assimilation (A) of mature leaves for *Col-0* and *phyB* plotted against intracellular $[\text{CO}_2]$ (C). Plants were grown at irradiances $50 \mu\text{mol m}^{-2} \text{s}^{-1}$ (A, B), $130 \mu\text{mol m}^{-2} \text{s}^{-1}$ (C, D) or $250 \mu\text{mol m}^{-2} \text{s}^{-1}$ (E, F) and $[\text{CO}_2]$ concentrations of 500 ppm (A, C, E) or 1000 ppm (B, D, F). Mean values are shown for each genotype ($n = 8$) with error bars indicating mean \pm SEM; t-test, ($p^* = \leq 0.05$, $p^{**} = \leq 0.01$, $p^{***} = \leq 0.001$, $p^{****} = \leq 0.0001$).

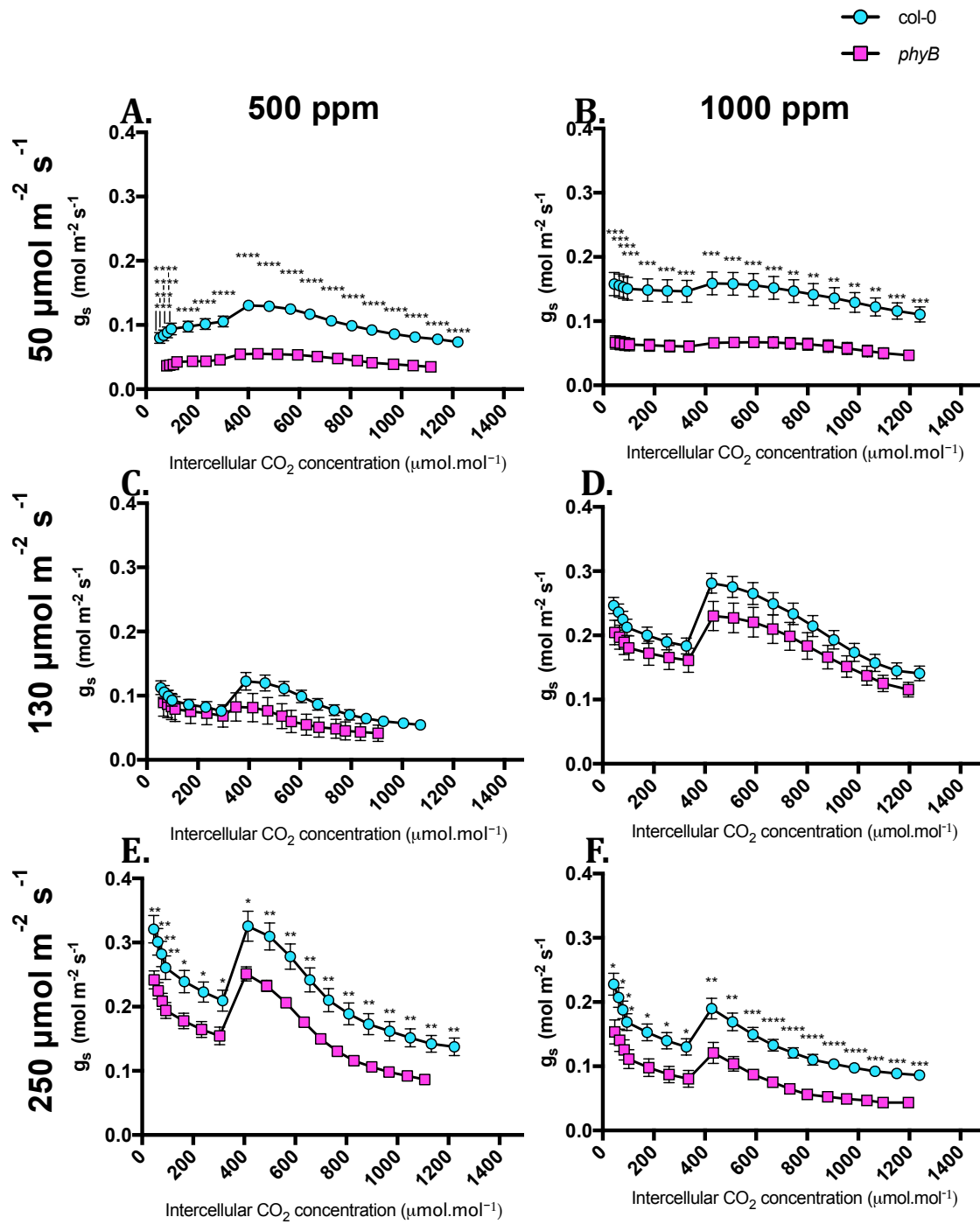


Fig.5.0.3 Conductance rates (g_s) of mature leaves for Col-0 and *phyB* plotted against intracellular $[CO_2]$ (C). Plants were grown at irradiances $50 \mu\text{mol m}^{-2} \text{s}^{-1}$ (A, B), $130 \mu\text{mol m}^{-2} \text{s}^{-1}$ (C, D) or $250 \mu\text{mol m}^{-2} \text{s}^{-1}$ (E, F) and $[CO_2]$ concentrations of 500 ppm (A, C, E) or 1000 ppm (B, D, F). Mean values are shown for each genotype ($n = 8$) with error bars indicating mean \pm SEM. Symbols indicate significant difference in WUE compared with Col-0; t-test, ($p^* = \leq 0.05$, $p^{**} = \leq 0.01$, $p^{***} = \leq 0.001$, $p^{****} = \leq 0.0001$).

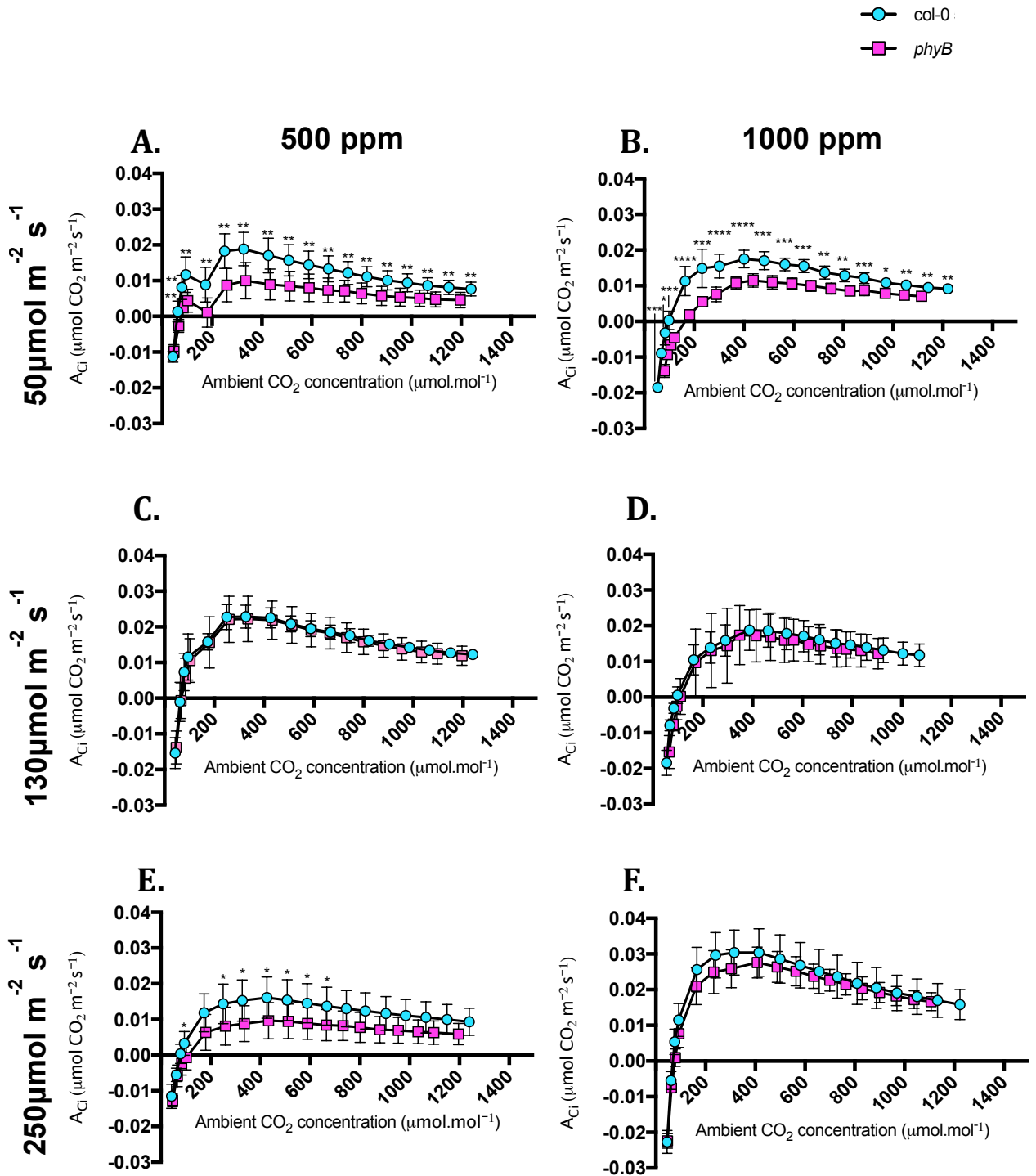


Fig.5.0.4 Stomatal limitation showing A/C_i (Assimilation against intracellular $[\text{CO}_2]$ C_i) of mature leaves for Col-0 and *phyB* plotted against extracellular/ambient $[\text{CO}_2]$ (C_a). Plants were grown at irradiances 50 $\mu\text{mol}\cdot\text{m}^{-2}\cdot\text{s}^{-1}$ (A, B), 130 $\mu\text{mol}\cdot\text{m}^{-2}\cdot\text{s}^{-1}$ (C, D) or 250 $\mu\text{mol}\cdot\text{m}^{-2}\cdot\text{s}^{-1}$ (E, F) and $[\text{CO}_2]$ concentrations of 500 ppm (A, C, E) or 1000 ppm (B, D, F). Mean values are shown for each genotype ($n = 8$) with error bars indicating mean \pm SEM. Symbols indicate significant difference in C_i compared with Col-0; t-test, ($p^* = \leq 0.05$, $p^{**} = \leq 0.01$, $p^{***} = \leq 0.001$, $p^{****} = \leq 0.0001$).

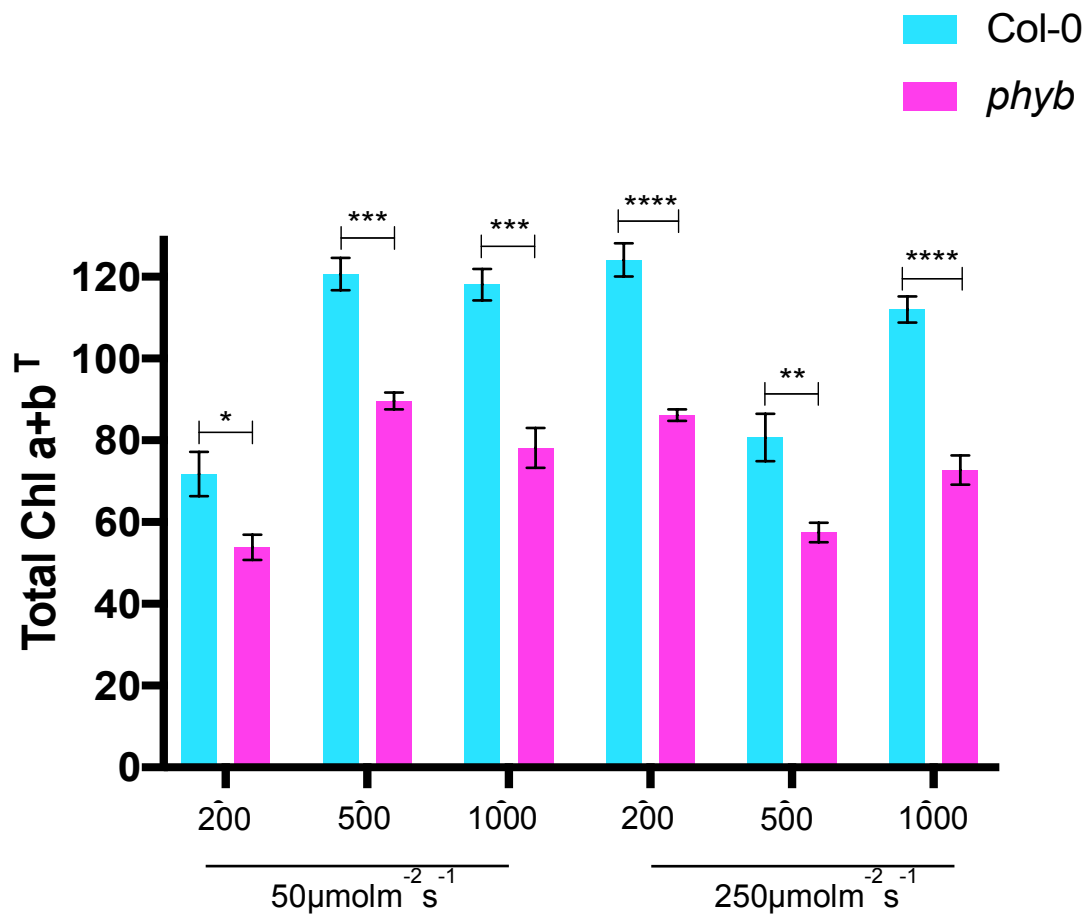


Fig.5.0.5 Total chlorophyll concentrations of mature leaves for Col-0 and *phyB*. Plants were grown at irradiances of 50 $\mu\text{mol m}^{-2} \text{s}^{-1}$ or 250 $\mu\text{mol m}^{-2} \text{s}^{-1}$ and $[\text{CO}_2]$ concentrations of 200 ppm, 500 ppm or 1000 ppm. Mean values are shown for each genotype ($n = 5$) with error bars indicating mean \pm SEM. Symbols indicate significant difference in chlorophyll concentrations compared with Col-0; two-way AVOVA with post-hoc Tukey test, ($p^* \leq 0.05$, $p^{**} \leq 0.01$, $p^{***} \leq 0.001$, $p^{****} \leq 0.0001$).

5.4 phyB controls aperture response to elevated

[CO₂]

In order to investigate the extent of stomatal limitations to [CO₂] in *phyB* mutants, a [CO₂] bioassay was performed. Epidermal peels from mature 35-day-old plants (grown at 130 μmol m⁻² s⁻¹ in 500 ppm [CO₂]) were subjected to [CO₂] free, 500 ppm or 1000 ppm [CO₂] treatments to induce stomatal closure, testing the dynamics of stomatal response to [CO₂]. In addition to Col-0 and *phyB*, a 35S*phyB* over-expressor line was analysed to further investigate the role of phyB in sensing changes in [CO₂]. *ca1 ca4* and *phyB ca1 ca4* mutants were analysed because of the role CA1 and CA4 play in [CO₂]-mediated stomatal closure (Hu *et al.*, 2010). Previously, the stomatal development response of *phyB ca1 ca4* showed a *phyB*-like response to elevated [CO₂] suggesting phyB function is epistatic to CA1 CA4 in terms of light/CO₂ signal integrated stomatal development.

Fig.5.0.6.A shows the stomatal aperture of the five genotypes when subjected to the various [CO₂] concentrations. *phyB*, 35S*phyB*, *ca1 ca4* and *phyB ca1 ca4* have a reduced stomatal aperture compared to Col-0 at each condition with *phyB* having the smallest aperture across all genotypes within each treatment. This suggests that *phyB* stomata are either less open or that stomatal complexes are smaller, both of which would reduce conductance and thus have the potential to increase WUE (assuming no major detrimental impact on assimilation). Stomatal size (guard cell area determined by total stomatal area minus total aperture area) was therefore calculated following treatment of epidermal peels with fusicoccin, a fungal toxin that opens stomatal pores. This demonstrated that *phyB* had a highly significant reduction in guard cell area (0.0362 μm²; SEM 0.0065; P-value <0.0001) compared to that of Col-0 (0.0909 μm²; SEM 0.0015) meaning that in addition to a reduced stomatal aperture that actual size of stomata are smaller in the *phyB* mutant (Fig.5.0.7.A and B).

Fig.5.0.6.B shows the same data from Fig.5.0.6.A plotted per genotype instead of per treatment. Col-0 has a higher aperture area in [CO₂] free injection, which shows that stomata are open the widest under this condition as expected. Col-0 shows a step-wise reduction in stomatal aperture area with increased [CO₂] concentrations, which correlates with the literature that [CO₂] induces stomatal closing (Fig.5.0.6.B). *phyB* shows a step-wise reductions in stomatal aperture area with a substantially reduced aperture at 1000 ppm [CO₂] suggesting that guard cells of the *phyB* mutant may be hypersensitive to [CO₂] between 500 ppm and 1000 ppm (Fig.5.0.6.B and C). Further support for *phyB* regulating responses to [CO₂] in this range is shown when examining the response of the 35SphyB transgenic line. Unlike the *phyB* mutant, 35SphyB guard cells show reduced sensitivity to 1000 ppm [CO₂] compared to 500 ppm (Fig.5.0.6.B and C). The *ca1 ca4* loss of function mutant that had previously been shown have reduced sensitivity to changes in [CO₂] as determined by both gas exchange and bioassay analyses (Hu *et al.*, 2010). In our conditions, *ca1 ca4* shows a step-wise decrease in stomatal aperture area as [CO₂] concentration is increased (Fig.5.0.6.B and C). The step-wise response suggests that either the mutant phenotype is weaker than previously thought, that there is possible redundancy with other CO₂ signal receptors, or that our growth conditions contribute to changes in response. Analysis of the *phyB ca1 ca4* triple mutant suggest potential interactions between both guard cell size and sensitivity to elevated [CO₂]. Total pore area of the triple mutant is reduced compared with *ca1 ca4* mutant and may suggest an additive interaction with *phyB* which regulates guard cell size. The proportional response to elevated [CO₂] is also intermediary between the two parental genotypes but does show the enhanced sensitivity of the *phyB* mutant. This could be interpreted as either epistasis or an additive interaction but certainly indicates that mutations in *phyB* enhance sensitivity to elevated [CO₂] irrespective of CA1 and CA4 activity.

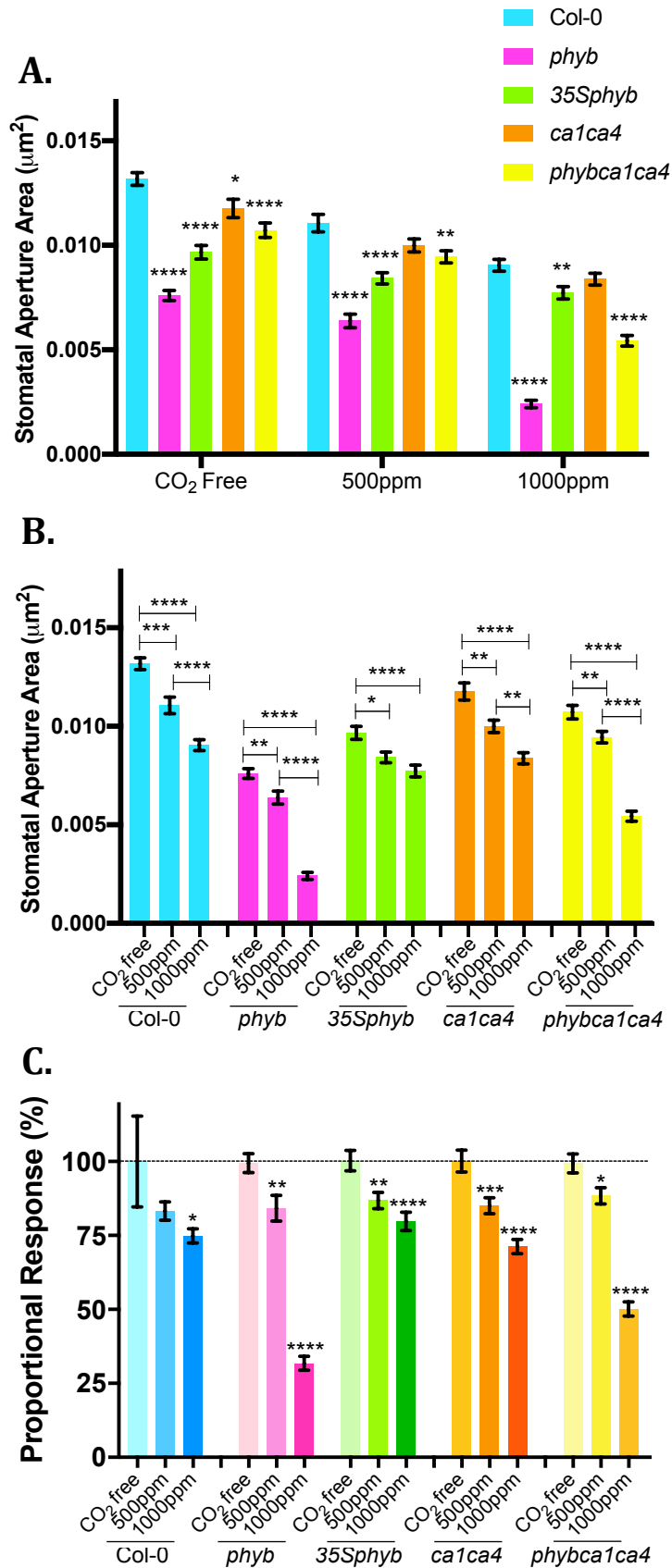


Fig.5.0.6 Shows stomatal aperture area (μm^2) of mature leaves for Col-0, *phyB*, *35sphyB*, *ca1ca4* and *phyBca1ca4*. Plants were grown at $130 \mu\text{mol m}^{-2} \text{s}^{-1}$ and 500 ppm. Epidermal peels of the plants were subjected to $[\text{CO}_2]$ free air, 500 ppm and 1000 ppm. A) shows stomatal aperture area plotted per treatment. B) shows stomatal aperture area plotted per genotype. C) shows the proportion of aperture response to $[\text{CO}_2]$ concentrations. Mean values are shown for each genotype ($n = 120$) with error bars indicating mean \pm SEM. Symbols indicate significant difference in aperture area compared with Col-0; one-way AVOVA with post-hoc Dunnett's test, ($p^* \leq 0.05$, $p^{**} \leq 0.01$, $p^{***} \leq 0.001$, $p^{****} \leq 0.0001$).

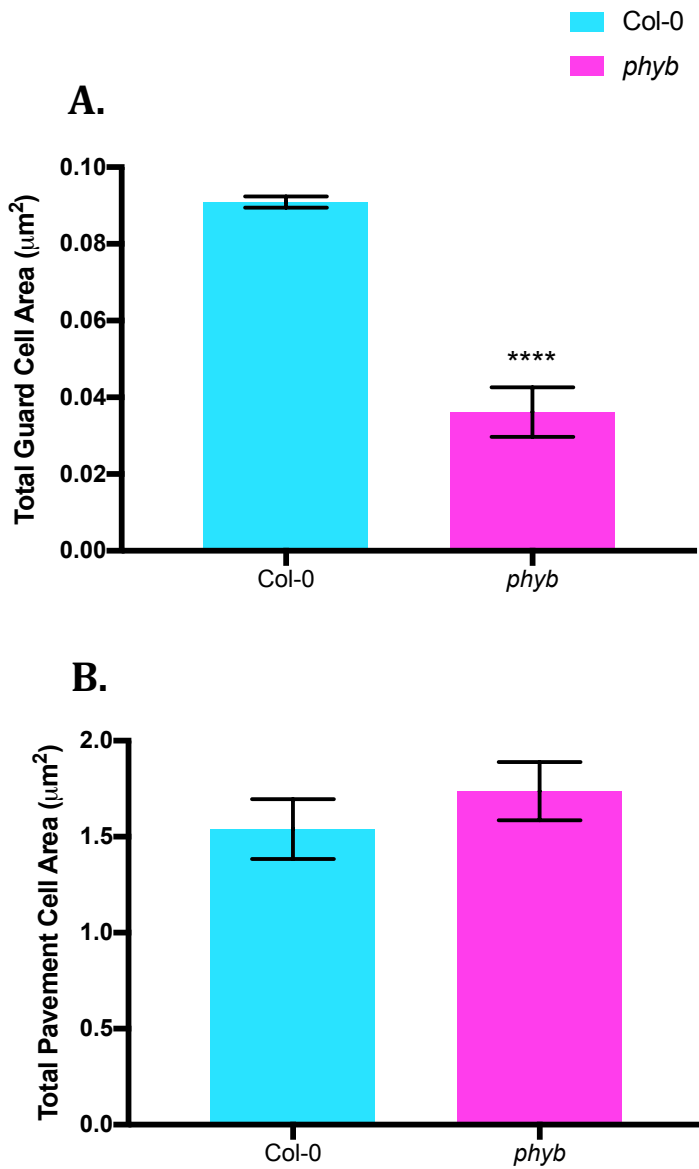


Fig.5.0.7 Shows total cell area (μm^2) of mature leaves for Col-0 and *phyB*. Plants were grown at $130 \mu\text{mol m}^{-2} \text{s}^{-1}$ and 500 ppm. Epidermal peels of the plants were subjected to $[\text{CO}_2]$ free air, 500 ppm and 1000 ppm. A) shows total guard cell area aperture area. B) shows total pavement cell area. Mean values are shown for each genotype ($n = 120$) with error bars indicating mean \pm SEM. Symbols indicate significant difference in aperture area compared with Col-0; student t-test analysis, ($p^* \leq 0.05$, $p^{**} \leq 0.01$, $p^{***} \leq 0.001$, $p^{****} \leq 0.0001$).

5.5 phyB mediates the level of ABA signaling and ABA biosynthesis genes

To investigate how phyB may be regulating the hypersensitive stomatal aperture response to elevated [CO₂] observed in Fig.5.0.6, qRT-PCR was used to analysis expression patterns of CO₂ signal response genes, ABA signaling and ABA biosynthesis genes found in guard cells. Leaf tissue from mature 35-day-old plants (grown at 130 μmol m⁻² s⁻¹ in 500 ppm [CO₂]) were transferred from 500 ppm to 1000 ppm [CO₂] for 6 hours. This aligns to the growth conditions and plant material used in the epidermal peel bioassays and in particular exams the response to elevated [CO₂], which appears to be regulated by phyB.

CA1 expression levels are higher in *phyB* compared to Col-0, across both conditions (Fig.5.0.8.A) with *phyB* showing a further up-regulation in *CA1* when subjected to elevated [CO₂] (1000 ppm). *CA4* gene expression is also higher in *phyB* at 500 ppm (Relative expression (RE) 1.28; SEM 0.098; P-value 0.06) compared to Col-0 (RE 1; SEM 0.102; P-value 0.1), although this is only significant when subjected to high [CO₂] (RE 1.4; SEM 0.019; P-value 0.0016) (Fig.5.0.8.B). Though our data is not entirely consistent with the literature regarding the role of *CA1* and *CA4* in regulating responses to [CO₂], this data indicates that at the gene expression level, phyB is required for WT responses to [CO₂]. The increased expression of *CA1* in particular, may correlate with the increased sensitivity to elevated [CO₂] (Fig.5.0.6).

Another mechanism by which phyB could be regulating this hypersensitivity is through abscisic acid (ABA.) Recent work has shown that CO₂ acts through ABA to mediate changes in stomatal aperture via ROS (Chater *et al.*, 2015). The expression of several ABA biosynthetic and signalling genes was therefore examined. *ABA1*, which is required for ABA biosynthesis, shows lower expression in *phyB* compared to Col-0 at 500 ppm but then appears unaffected by the elevation in

[CO₂] concentration from 500 ppm to 1000 ppm (Fig.5.0.8.C). NCED3, a key enzyme in ABA biosynthesis, shows higher expression levels in *phyB* compared to Col-0 at the same condition (500 ppm). In *phyB*, expression is significantly down-regulated after a shift to elevated [CO₂] but this is not observed in WT plants (Fig.5.0.8.D). The phosphatases ABI1 and HAB1 are negative regulators of ABA signalling and have been shown to inactivate OST1 via dephosphorylation to negatively regulate ABA-induced stomatal closure (Vlad *et al.*, 2009). Fig.5.0.8.E shows that *ABI1* is up-regulated in *phyB* at 500 ppm compared with Col-0 under the same conditions. However, expression levels of *ABI1* in *phyB* are down-regulated when subjected to high [CO₂], a response not seen in Col-0. In the case of *HAB1*, Col-0 does show up-regulation of *HAB1* when subjected to elevated [CO₂], whereas *phyB* shows consistently higher *HAB1* expression levels which don't appear to be affected by the increase in [CO₂] concentration (Fig.5.0.8.F). In contrast, there is no significant difference between Col-0 and *phyB* in expression of OST1 (Fig.5.0.8.G). Our results suggest that *phyB* could modulate the expression of CO₂-mediated stomatal aperture response genes as well as ABA-signaling and biosynthesis genes to regulate stomatal response to changes in [CO₂] concentration. The gene expression changes observed, particularly for *HAB1*, are not consistent with increased sensitivity to ABA but these genes can also be regulated at the post-transcriptional level. Actual levels of endogenous ABA or responsiveness to exogenous ABA remain untested in this study and could further enable understanding of the role of ABA in *phyB*-mediated light/CO₂ stomatal responses as could analysis of ABA receptor proteins.

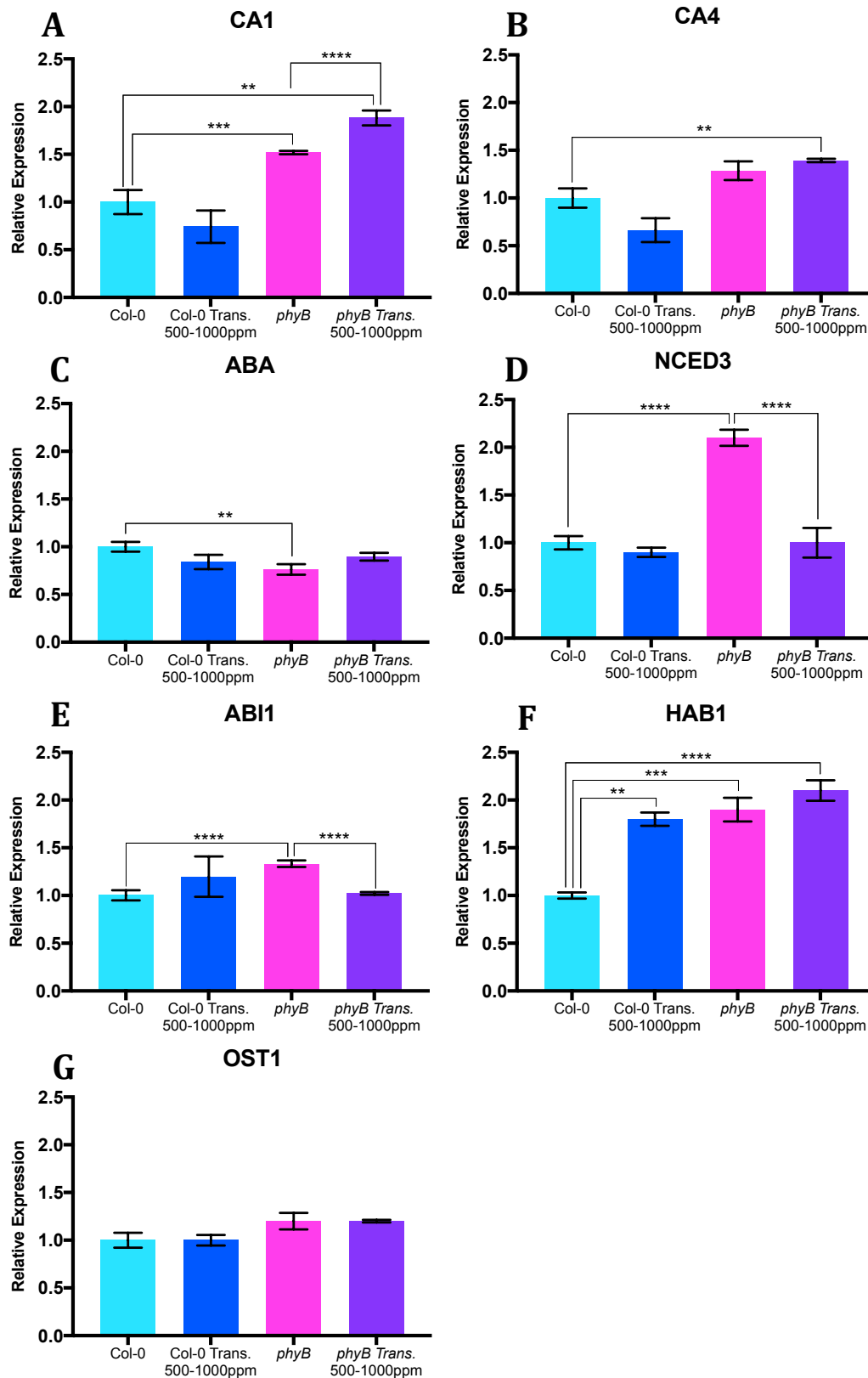


Fig.5.0.8 Shows gene expression analysis of mature leaves for Col-0 and *phyB*. Plants were grown at $130 \mu\text{mol m}^{-2} \text{s}^{-1}$ and 500 ppm. plants were grown for 35 days then transferred from 500 ppm to 1000 ppm. A) shows CA1 expression levels. B) shows CA4 expression levels. C) shows ABA1 expression levels. D) shows NCED3 expression levels. E) shows ABI1 expression levels. F) shows HAB1 expression levels. G) shows OST1 expression levels. Mean values are shown for each genotype (n = 3; with 3 technical repeats) with error bars indicating mean +/- SEM. Symbols indicate significant difference in aperture area compared with Col-0; t-test ($p^{**} \leq 0.01$, $p^{***} \leq 0.001$, $p^{****} \leq 0.0001$).

5.6 Carbon isotope discrimination

IRGA provides a transient insight in to how plants use water. A more long-term and integrative estimation of WUE is determined via carbon isotope discrimination (Δ). During carbon fixation RuBisCo discriminates against the heavier ^{13}C compared to ^{12}C (Farquhar *et al.*, 1989). If $[\text{CO}_2]$ levels within the leaf fall (C_i), RuBisCo will begin to utilise ^{13}C as the levels of ^{12}C are depleted. Therefore, plants with lower intracellular $[\text{CO}_2]$ (C_i) levels will incorporate more of the heavier ^{13}C compared to ^{12}C resulting in reduced carbon isotope discrimination. In contrast, plants with higher C_i have increased levels of the lighter ^{12}C compared to ^{13}C . In order to investigate if short-term and long-term plant WUE correlated and what role *phyB* may play, carbon isotope analysis was determined. Plants were grown until bolting stage, to indicate that the plants had completed their development phase and had progressed to flowering. Five leaves from three separate plants were combusted and analysed using mass spectrometry to determine carbon ratios. Fig.5.0.9 shows carbon isotope discrimination (Δ) data for *phyB* and Col-0 plants grown under $50 \mu\text{mol m}^{-2} \text{s}^{-1}$ (low light) or $250 \mu\text{mol m}^{-2} \text{s}^{-1}$ (high light) and 200 ppm (low $[\text{CO}_2]$), 500 ppm (medium $[\text{CO}_2]$) and 1000 ppm (high $[\text{CO}_2]$). In most instances *phyB* behaves like wild-type in long-term WUE with step-wise increases in Δ as CO_2 concentration increases irrespective of irradiance level (at 200 ppm and 500 ppm; Fig.5.0.9.B). The two conditions where *phyB* has improved long-term water use efficiency are plants grown in 500 ppm across both irradiance levels. Whilst the carbon isotope analysis did not analyse plants grown at $130 \mu\text{mol m}^{-2} \text{s}^{-1}$, there is still good correlation between the WUE_i data and this longer term WUE data (Fig.5.0.1 and Fig.5.0.8).

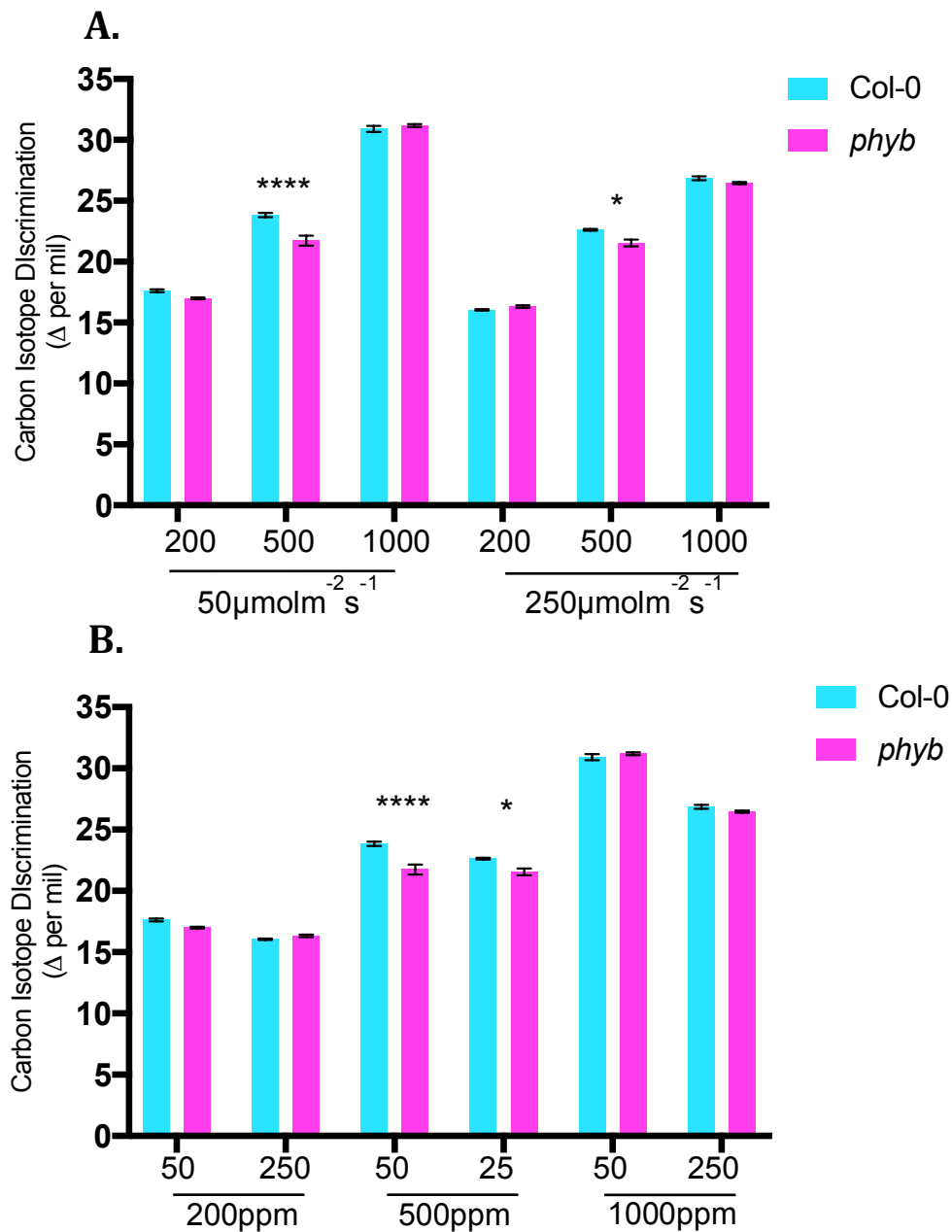


Fig.5.0.9 Carbon isotope analysis ($^{12}\text{C}:^{13}\text{C}$) of mature leaves for Col-0 and *phyB*. Plants were grown at irradiances of $50 \mu\text{mol m}^{-2} \text{s}^{-1}$ or $250 \mu\text{mol m}^{-2} \text{s}^{-1}$ and $[\text{CO}_2]$ concentrations of 200 ppm, 500 ppm or 1000 ppm. A) shows carbon ratios across $[\text{CO}_2]$ concentrations. B) shows carbon ratios across irradiances. Mean values are shown for each genotype ($n = 15$) with error bars indicating mean \pm SEM. Symbols indicate significant difference in carbon ratios compared with Col-0; two-way AVOVA with post-hoc Tukey test, ($p^* = \leq 0.05$, $p^{**} = \leq 0.01$, $p^{***} = \leq 0.001$, $p^{****} = \leq 0.0001$).

5.7 Discussion

In general, *phyB* improves WUE_i when subjected to $[CO_2]$ levels that exceed the $[CO_2]$ concentration in which it was grown (IRGA data). This can be clearly seen in 500 ppm grown plants across all irradiances which shows that *phyB* WUE_i begins to improve compared to wild-type when subjected to 500 ppm ambient $[CO_2]$ levels. This difference in WUE_i between *phyB* and Col-0 increases as $[CO_2]$ concentration increases, with the greatest difference at the highest $[CO_2]$ concentration (1500 ppm), with *phyB* consistently more WUE_i across all irradiances (500 ppm grown). This result is less pronounced in 1000 ppm grown plants which show a dampened WUE_i , compared to the 500 ppm grown plants. It is possible that by extending the IRGA $[CO_2]$ concentration parameters to exceed 1500 ppm (highest experimental $[CO_2]$ concentration used in this study) differences in WUE_i could be better visualised for 1000 ppm grown plants. The $[CO_2]$ range used during IRGA analysis ranged from 40 ppm to 1500 ppm, meaning that the 500 ppm grown plants are subjected to a $[CO_2]$ range 1000 ppm (growth 500 ppm - highest experimental concentration 1500 ppm) greater than the growth condition, whereas the 1000 ppm grown plants were subjected to a maximum of 500 ppm higher than their growth condition (growth 1000 ppm - highest experimental concentration 1500 ppm).

Despite literature linking changes in stomatal density to changes in plant water use performance, the data in this study does not seem to always support this. Work conducted on *EPF2* mutants showed that a reduction in SD resulted in a reduction in the maximum conductance capacity of a leaf, which increased water use efficiency (Franks *et al.*, 2015). *phyB* grown at $250 \mu\text{mol m}^{-2} \text{s}^{-1}$ in 500 ppm shows a reduction in SD and conductance rates and yet no significant impact on assimilation, despite reduced chlorophyll levels. Together this then correlates with improved WUE_i and fits with the literature. This isn't the case for $250 \mu\text{mol m}^{-2} \text{s}^{-1}$ and 1000 ppm grown *phyB* plants. Under these conditions there is no difference in

WUE_i. In this case, the SD of *phyB* leaves is similar to WT (chapter 3, fig. 3.1), yet there is a significant reduction in conductance rate, which may therefore be due to the reduced size of stomata in *phyB*. However, in this instance, the reduced conductance of the *phyB* mutant is offset by the reduction in assimilation. Therefore, the factors driving differences of *phyB* WUE_i differ per condition and further support a role for phyB in mediating developmental as well as physiological response to light and CO₂. There are limitations to improving WUE via reductions in SD or stomatal aperture as the uptake of [CO₂] may become limited by a reduction of total stomatal pore area resulting in a negative impact on assimilation rates, which we do see in *phyB*. Therefore, any improvements gained via a reduction in total pore area are finely balanced to the impact on assimilation. However, further comparisons of the assimilation data (A/C_i curves; Fig.5.0.2) reveal that *phyB* has a consistently reduced C_i, which does not appear to be strictly observed in the A/C_i vs C_a comparisons (Fig.5.0.4). This seems strange when we consider that *phyB* have smaller stomata with a reduced aperture area which should cause limitations to C_i levels.

The relationship between stomatal density and stomatal conductance, net assimilation rate and water use efficiency has been suggested to positively correlate in the perennial grass, *Leymus chinensis* (Xu and Zhou, 2008). This positive correlation is can also be observed within the data of this study, *phyB* has a reduced stomatal density, reduced stomatal conductance and increased water use efficiency generally. The relationship between stomatal density and leaf area has been proposed to negatively correlate, although further research is required before strict coupling can be determined. Therefore, it would be interesting to further analyse the relationship between stomatal density and leaf area of *phyB* to determine whether there is a link between stomatal density and leaf area.

The reduction in total chlorophyll apparent in *phyB* across all conditions suggests that *phyB* should have consistently reduced photosynthetic capacity compared to Col-0. This is not always the case when we consider the A/Ci curves show cases of reduced assimilation in *phyB* as well as instances of Col-0-like assimilation. Perhaps further analysis of photosynthetic efficiency may need to be explored in order to provide further insight in to the causation of differences in assimilation of *phyB* between conditions. Chlorophyll fluorescence measurements, to examine photosynthetic performance in plants, have become a widespread practice in physiological studies (Baker, 2008). Understanding chlorophyll concentration as well as assessment of photosynthetic performance in vivo could help to identify possible causes of changes in photosynthesis and plant performance (Baker, 2008).

It is important to note that, in terms of light/CO₂ signals, *phyB* mediates developmental and physiological response differently. Developmentally, *phyB* is insensitive to high [CO₂] but is hypersensitive in terms of aperture response (bioassay data; physiological response). Therefore, it appears that *phyB* mutants have compensated for their lack of developmental response by becoming more physiologically responsive which could be an explanation for why we don't a change in WUE at high [CO₂] (1000 ppm). A trade-off between developmental and physiological responses to [CO₂] has been proposed to explain the differential responses of different plant species (Haworth *et al.*, 2013). This data suggests that *phyB* might be a pivotal component in regulating this trade-off and it would be interesting to examine phytochrome signalling in plants that are either developmental or physiological responders.

In addition to stomatal movement, in terms of aperture area, is the speed at which this movement occurs in response to environmental stimuli (Lawson, 2014). Stomatal movement is not always synchronised to other plant responses, such as photosynthesis, as these movements can be an order of magnitude slower than the

more rapid photosynthetic responses to the same environmental stimuli (Pearcy, 1990; Lawson *et al.*, 2010; Lawson and Blatt, 2014). Further analysis to determine the role of *phyB* in terms of stomatal responsiveness (speed and aperture response) could provide a means of reducing water lost via transpiration without compromising on carbon gain.

This suggests that *phyB* may be responsible for mediating ABA biosynthesis in a CO₂-dependent manner.

Our expression data focused on examining known CO₂ or ABA signalling components to determine whether their expression in mature leaves could explain the hypersensitive of *phyB* guard cells to high [CO₂]. Certainly, we could identify differences in the expression profiles of the genes tested between Col-0 and *phyB* and how these genes respond to CO₂ in these genotypes. Given that the data in this thesis is inconclusive with regards the roles of *CA1* and *CA4* in regulating CO₂ responses, it is therefore difficult to comment on the importance of the differences observed, particularly with regards *CA1* expression. Perhaps if this is considered an output of CO₂ signalling then it can at least be concluded that this shows that *phyB* mutants do show differential responses to [CO₂] at the gene expression level, rather than imply any role in *CA1* or *CA4* in determining sensitivity.

CO₂ has been shown to utilise components of the ABA signalling pathway to mediate changes in stomatal aperture (Chater *et al.*, 2015). *NCED3* expression suggests that *phyB* mutants may have the potential for increased ABA levels, though this is not evident at elevated [CO₂], which therefore does not fit with *phyB* hypersensitivity to CO₂ acting through ABA. Analysis of the ABA signalling components contradicts previous research which shows significantly reduced *HAB1* expression in *phyB-5* (*Ler* background) compared to wild-type (González *et al.*, 2012). Despite *HAB1* functioning as a negative regulator of ABA-signaling, its overexpression can be mitigated by increasing in parallel the expression of the ABA receptor *PYL5* (Santiago *et al.*, 2009). It would therefore be necessary to analyse

this interaction in greater depth by also examining ABA receptor expression as well as measuring ABA levels in leaves following a change in [CO₂]. Also, examining the sensitivity of *phyB* mutants to exogenous ABA may provide insights into the mechanism through which phyB confers altered guard cell sensitivity to ABA.

5.8 Key findings:

- *phyB* improves water use efficiency by regulating stomatal number, size and responsiveness.
- Stomatal and non-stomatal limitations are not strictly coupled with assimilation and conductance rates.
- *phyb* has reduced chlorophyll concentrations.
- *phyB* is hypersensitive to elevated [CO₂].
- *phyB* controls stomatal size.
- *phyB* mediates the level of ABA signaling and ABA biosynthesis genes.

6.0

Discussion

6.0.1 Introduction

With climate change exacerbating the current issues surrounding the increasing population, food security and rapid depletion of the global freshwater table, increasing the efficiency of crops (in terms of water use and yield) has become of major importance within the global sphere. Despite these issues being associated with 'third world' countries, it is now becoming apparent that these combined issues are increasing in severity and affecting traditionally more affluent and developed countries.

Throughout this thesis I have described a mechanism for integrating light and CO₂ signals to effect plant water use efficiency. Although, further analysis needs to be conducted to understand the role within yield levels, there is scope for future application in crop species to generate more efficient lines for cultivation.

6.0.2 Investigating the effects of light and CO₂ signal integration on stomatal development.

Genetic analysis revealed that the photoreceptors (phyB, CRY1 and CRY2) regulate stomatal development in response to changes in [CO₂] conditions, although this is in a condition-specific manner and did not present an obvious mechanism. The results were further complicated by the responsiveness of the photoreceptor mutants to changes in irradiance, an increase in irradiance resulted in an increase in the basal level of stomatal development. Here we theorised that either there is substantial redundancy between the photoreceptors or that they function additively to regulate the basal number of stomata. In either case, analysis of higher order mutants (to include more of the phys and crys) could help clarify this. The over-arching response across all tested genotypes indicated that phyB likely regulates changes in

stomatal development in response to [CO₂] levels post-transcriptionally (Lee *et al.*, 2017). Whilst photoreceptors are able to mediate responses through transcriptional mechanisms, with HY5 a prominent transcription factor in these pathways, such a HY5 mechanism does not appear to be the case under our growth conditions. Based on the data within this study, it appears likely that the major mechanism through which phyB (and cryptochromes) regulate stomatal development is via inhibition of COP1 and thus promoting SPCH, ICE1 and SCRM2/ICE2 activity to positively regulate stomatal development.

6.0.3 Photoreceptor regulation of stomatal development in response to [CO₂].

Gene expression analysis has revealed that CRY1 CRY2 is required to mediate expression of CO₂-signaling genes to regulate stomatal development in response to sub-ambient [CO₂] (200ppm [CO₂]). Although there appeared to be no direct role of cry1cry2 in regulating *SPCH*, *MUTE* and *FAMA* expression, there does appear to be CRY1 CRY2 –mediated regulation of *STOM*, *EPF2* and *CRSP* to potentially maintain correct expression levels at sub-ambient [CO₂]. This could be a mechanism for controlling the basal number of stomata at sub-ambient [CO₂] concentrations.

In terms of elevated [CO₂] (1000ppm [CO₂]), phyB appears to regulate *EPF2* expression that could potentially reflect a balance mechanism to promote degradation of SPCH and inhibit progression through the stomatal development pathway. SPCH is essential for initiation into the lineage but there is a fine balance as stabilising SPCH activity results in successive cell divisions and prohibits progression through the lineage, therefore degradation is also a necessary step.

Previous research has shown that phyB inhibits COP1 activity which targets ICE1 for degradation (as well as SPCH potentially; unpublished data). In addition to this, SPCH has also been shown to directly regulate the expression of *EPF2*, therefore *EPF2* expression patterns can be used as an indicator of SPCH activity. My data showed no transcriptional control of SPCH under these growth conditions and therefore further supported the hypothesis that phyB operates post-transcriptionally to regulate changes in stomatal development and physiological responses.

6.0.4 Physiological effects of phyB on plant water use efficiency.

In this thesis the relationship between stomatal density and water use efficiency was tested using intrinsic and carbon isotope techniques. In terms of water use efficiency phyB has been shown to regulate this in response to [CO₂] concentrations, with water use efficiency increasing as [CO₂] concentration increases. The mechanism by which phyB regulates this response is through the control of stomatal and non-stomatal mechanisms. I have shown that phyB regulates stomatal number, size and aperture in response to changes in light and CO₂ signals. Developmentally, *phyB* mutants appears to be insensitive to elevated [CO₂], however this is compensated by hypersensitivity in terms of stomatal aperture response.

The number, size and responsiveness of stomata to changes in environmental stimuli are crucial for effective regulation of gas exchange and thus plant water use efficiency. For example, the longer stomata take to close and reach a new g_s value appropriate for a particular light level and assimilation rate, the greater the surplus in transpiration (the lag in response leads to unnecessary water

loss) and subsequent reduction in WUE. The data in this study suggests that *phyB* affects the speed of stomatal response, the reduction in conductance levels compared to wild-type coupled with improved water use efficiency may, in part, be a result of improved stomatal response times.

General reduction in chlorophyll levels suggests a reduced photosynthetic capacity, although this wasn't always apparent from the assimilation levels, which appeared to be affected in a condition-specific manner. Further analysis of the functionality of the photosystems, in regards to *phyB*, may provide information to help explain the differences in photosynthetic ability between conditions.

There were inconclusive results of *phyB* interacting with ABA signalling components that could perhaps help explain the hypersensitivity of *phyB* to elevated [CO₂]. This was based on a very limited number of genes and so this could be expanded to include other components of ABA and CO₂ signalling. A preliminary experiment in which thermal imaging was used to examine *phyB* sensitivity to exogenous ABA levels was performed, however, the results were inconclusive and therefore were not included within this thesis. Col-0 and *phyB* were treated with 1µmol and 5µmol concentrations of ABA. However, previous drought tolerance experiments of *phyB-5* (*Ler* background) have shown that as much as 100µmol ABA is necessary to induce stomatal closure despite 1µmol being sufficient for stomatal closure in wild-type (González *et al.*, 2012). This may explain the results from my experiment, which will need to be repeated using a range of concentrations.

Elevated atmospheric [CO₂] concentrations may provide plants with increased water use efficiency due to reduced stomatal conductance (and reduced transpiration), however, a consequence of this reduced stomatal aperture response is higher leaf temperature which has been predicted to contribute to heat stress in plants resulting in possible reductions in crop yield. There is also the further

complication that a number of recent reports have indicated that increased temperature alters photoreceptor reversion rates (Legris *et al.*, 2016; Fujii *et al.*, 2017). It is therefore possible that some of the phytochrome responses reported here must be considered in the context of CO₂ mediated increases in leaf temperature.

6.0.5 Conclusion

From my previous discussions and conclusions it is clear that photoreceptors play a complex role within the regulation of stomatal responses to changes in light and [CO₂]. I have demonstrated that phyB is key to regulating stomatal number, size and aperture in response to changes in [CO₂] concentration in order to mediate plant water use efficiency. There is also evidence to implicate cry1cry2 in the mediation of stomatal development at sub-ambient [CO₂] concentration. Although further analysis is required to clarify the extent to which phyB mediates development and physiological responses, particularly potential phyB-ABA interactions to regulate aperture responses. Therefore, it would be of interest to analyse plants that are either developmental or physiological responders to stimuli. It should also be highlighted that there is potential to move this research in to crop models in the future as phyB is well conserved across plant species such as wheat.

This study has also highlighted the need to produce a guide to standardise research techniques within the plant science field when analysing the effects of light and CO₂. The use of terms such as, 'optimal' or 'medium' light has been used to describe irradiances ranging from 130 to 175 $\mu\text{mol m}^{-2} \text{s}^{-1}$. Inconsistency in other conditions also includes differences in photoperiod, temperature ranges and [CO₂] concentrations as well as mutant backgrounds. Such differences in terminology and

concentrations have made reproducing published results problematic and therefore comparisons from this study to published data have also been subsequently difficult.

6.0.6 Application

In order to address the current issues surrounding food security and the depletion of the global freshwater table, advances in understanding the regulation of plant water use efficiency without the cost of reduced biomass has become increasingly important. There is now a good understanding of the effects of environmental stimuli (as an isolated signal) on the regulation of core plant development pathways, such as stomatal development. Research should now look to unravel the integration of such signals within plants to better representative the dynamic environments in which these crops are cultivated, both in terms of number of stimuli but also fluctuating levels. Understanding such responses could help scientists engineer crop lines to better suit the surrounding environment (cultivation site) in which they are grown. Plants with improved water use efficiency would be useful for more arid climates where inefficient and unsustainable irrigation systems are currently used to enable crop production. If we can understand environmental signal integration then this could enable the generation of such crop lines as described above therefore helping to combat the current food security and global freshwater crisis.

6.0.7 Future work

In addition to the proposed experiments described within the previous sections, further work needs to be carried out to establish the role of plant hormones in phyB-regulated stomatal development and physiological responses to [CO₂].

Further analysis of hormone mutants defective in brassinosteroid, auxin and ABA signaling would be useful to determine the effects on stomatal development, light signalling and CO₂ signalling genes. Stomatal impression work and gene expression analysis of these lines would be used to further characterise the genetic interactions between light and CO₂ signalling, potential adding to my model. Gene expression analysis would also be used to analyse targets of SPCH activity, such as *BASL*, to clarify the question of possible stable SPCH activity in *phyB* at elevated [CO₂] (described in chapter 3).

Utilising Pulse Amplitude Modulation (PAM) imaging chlorophyll fluorometer to examine photosynthetic performance in the *phyB* mutant could help provide detailed and extensive information regarding the efficiency of PSII within the electron transport chain. Light energy absorbed by chlorophyll can drive photosynthesis (photochemistry), become re-emitted as heat or become re-emitted as light (fluorescence). PAM imaging could provide important and detailed information regarding the quantum efficiency of the photochemistry and heat dissipation of each genotype (Baker, 2008; Murchie and Lawson, 2013). Compared to IRGA, Pam imaging offers a wider range of analysis which includes data collection for; PSII efficiency, electron transport efficiency, plastoquinone pool, amount of energy emitted as fluorescence, quenching and non-photochemical quenching (Baker, 2008; Murchie and Lawson, 2013). This comprehensive data set, coupled with the chlorophyll concentration data within this study, could help clarify the extent of which chlorophyll effects assimilation and subsequently WUE.

The hypersensitive response of *phyB* guard cells to elevated [CO₂] could be investigated by examining interactions with known components of the CO₂ and ABA stomatal closure pathways. This thesis did attempt to address this by utilising *ca1ca4* mutants but alternatives to consider include key mutants such as *ost1*, *ht1* and those defective in ROS generation such as *rbohDF* mutants. As indicated earlier, a more extensive gene expression analysis could be performed, either by

qRT-PCR or RNA-seq to determine whether phyB is regulating relevant pathways such as ABA, ROS or Ca²⁺ signalling.

Thorough characterisation the role of phyB in mediating stomatal developmental and physiological response to light and CO₂ signals (with the potential inclusion of plant hormone signalling components) could provide a viable mechanism, transferrable to crop lines, to control plant water use efficiency without negatively impacting yield. This could be a potential tool in combating current food security and freshwater issues to feed the growing population, provide people with vital freshwater and improve sustainability.

7.0 References

- Ahmad, M. and Cashmore, A.R. (1993) HY4 gene of *A. thaliana* encodes a protein with characteristics of a blue-light photoreceptor. *Nature*, **366:162–166**.
- Alexandratos, N. and Bruinsma, J. (2012) World Agriculture Towards 2030/2050: the 2012 revision. ESA Working Paper No.12-03 153pp. Rome, FAO.
- Andriankaja, M., Dhondt, S., De Bodt, S., Vanhaeren, H., Coppens, F., De Milde, L., Mühlenbock, P., Skiryecz, A., Gonzalez, N., Beemster, G.T. and Inzé, D. (2012) Exit from proliferation during leaf development in *Arabidopsis thaliana*: a not-so-gradual process. *Dev Cell*, **22(1):64-78**.
- Assmann, S.M. and Shimazaki, K. (1999) The multisensory guard cell: stomatal responses to blue light and abscisic acid. *Plant Physiol*, **119:809-816**.
- Baker, N. (2008) Chlorophyll Fluorescence: A Probe of Photosynthesis In Vivo. *Annu. Rev. Plant Biol.* **59:89-113**.
- Balcerowicz, M., Hoecker, U. (2014) Auxin--a novel regulator of stomata differentiation. *Trends Plant Sci.* **19(12):747-9**. Balcerowicz, M., Ranjan, A., Rupprecht, L., Fiene, G., Hoecker, U. (2014) Auxin represses stomatal development in dark-grown seedlings via Aux/IAA proteins. *Development*. **141(16):3165-76**.
- Ballaré, C.L., Scopel, A.L., Sánchez, R.A. (1990) Far-red radiation reflected from adjacent leaves: an early signal of competition in plant canopies. *Science*. **1247(4940):329-32**.
- Baroli, I., Price, G.D., Badger, M.R. and von Caemmerer, S. (2008) The contribution of photosynthesis to the red light response of stomatal conductance. *Plant Physiol*, **146:737-747**.
- Berger, D. and Altmann, T. (2000) A subtilisin-like serine protease involved in the regulation of stomatal density and distribution in *Arabidopsis thaliana*. *Genes & Development*, **14:1119-1131**.
- Bergmann, D.C., Lukowitz, W. and Somerville C.R., (2004) Stomatal development and pattern controlled by a MAPKK Kinase. *Science*, **304:1494-1497**.
- Bhave, N.S., Velez, K.M., Nadeau, J.A., Lucas, J.R., Bhave, S.L. and Sack, F.D. (2009) TOO MANY MOUTHS promotes cell fate progression in stomatal development of *Arabidopsis* stems. *Planta*, **229:357-367**.
- Bierhuizen, J.F. and Slatyer, R.O. (1965) Effect of atmospheric concentration of water vapour and CO₂ in determining transpiration-photosynthesis relationships of cotton leaves. *Agri Met.* **2(4):259-270**.
- Boccalandro, H.E., Rugnone, M.L., Moreno, J.E., Ploschuk, E.L., Serna, L., Yanovsky, M.J., Casal, J.J. (2009) Phytochrome B enhances photosynthesis at the expense of water-use efficiency in *Arabidopsis*. *Plant Physiol*. **150(2):1083-92**.
- Boccalandro, H.E., Giordano, G.V., Ploschuk, E.L., Piccoli, P.N., Bottini, R., Casal, J.J. (2012) Phototropins But Not Cryptochromes Mediate the Blue Light-Specific

Promotion of Stomatal Conductance, While Both Enhance Photosynthesis and Transpiration under Full Sunlight. *Plant Physiol.* **158(3): 1475–1484.**

Borthwick, H.A., Hendricks, S.B., Parker, M.W., Toole, E.H., Toole, V.K. (1952) A Reversible Photoreaction Controlling Seed Germination. *Proc Natl Acad Sci U S A.* **38(8):662-6.**

Briggs, W.R., Christie, J.M. (2002) Phototropins 1 and 2: versatile plant blue-light receptors. *Trends Plant Sci.* **7(5):204-10.**

Burney, J.A., Davis, S.J. and Lobell, D.B. (2010) Greenhouse gas mitigation by agricultural intensification. *Proc Natl Acad Sci*, **107:12052–12057.**

Carter, R., Woolfenden, H., Baillie, A., Amsbury, S., Carroll, S., Healicon, E., Sovatzoglou, S., Braybrook, S., Gray, J.E., Hobbs, J., Morris, R.J., Fleming, A.J. (2017) Stomatal Opening Involves Polar, Not Radial, Stiffening Of Guard Cells. *Curr Biol.* **27(19):2974-2983.**

Casal, J.J. and Mazzella, M.A. (1998) Conditional synergism between cryptochrome 1 and phytochrome B is shown by the analysis of phyA, phyB, and hy4 simple, double, and triple mutants in Arabidopsis. *Plant Physiol.* **118(1):19-25.**

Casal, J.J. (2000) Phytochromes, cryptochromes, phototropin: photoreceptor interactions in plants. *Photochem Photobiol*, **71:1–11.**

Cashmore, A.R., Jarillo, J.A., Wu, Y.J., Liu, D. (1999) Cryptochromes: blue light receptors for plants and animals. *Science.* **284(5415):760-5.**

Casson, S.A. and Gray, J. E., (2008) Influence of environmental factors on stomatal development. *New Phytologist*, **178:9–23.**

Casson, S.A., Franklin, K.A., Gray, J.E., Grierson, C.S., Whitlam, G.C. and Hetherington, A.M. (2009) Phytochrome B and PIF4 regulate stomatal development in response to light quantity. *Curr Biol*, **19(3):229-34.**

Casson, S.A. and Hetherington, A.M. (2010) Environmental regulation of stomatal development. *Current Opinion in Plant Biology*, **13(1):90 –95.**

Casson, S.A. and Hetherington, A.M. (2014) Phytochrome B Is required for light-mediated systemic control of stomatal development. *Curr Biol*, **24(11):1216-21.**

Chang, C., Bowman, J.L., Meyerowitz, E.M. (2016) Field guide to plant model systems. *Cell.* **167(2): 325–339.**

Chater, C., Gray, J.E. and Beerling D. (2013) Early evolutionary acquisition of stomatal control and development gene signalling networks. *Current opinion in plant biology*, **16:638-646.**

Chater, C., Peng, K., Movahedi, M., Dunn, J.A., Walker, H.J., Liang, Y.K., McLachlan, D.H., Casson, S., Isner, J.C., Wilson, I., Neill, S.J., Hedrich, R., Gray, J.E. and Hetherington, A.M. (2015) Elevated CO₂-Induced Responses in Stomata Require ABA and ABA Signaling. *Curr Biol*, **25(20):2709-2716.**

Chen, H., Zhang, J., Neff, M.M., Hong, S.W., Zhang, H., Deng, X.W., Xiong, L. (2008) Integration of light and abscisic acid signaling during seed germination and early seedling development. *Proc Natl Acad Sci U S A.* **105(11):4495-500.**

- Chen, C., Xiao, Y., Li, X. and Ni, M. (2012) Light-Regulated Stomatal Aperture in *Arabidopsis*. *Molecular Plant*, **5**:566-572.
- Christie, J.M., Reymond, P., Powell, G.K., Bernasconi, P., Raibekas, A.A., Liscum, E. et al. (1998) *Arabidopsis* NPH1: a flavoprotein with the properties of a photoreceptor for phototropism. *Science*. **282**:1698-1701.
- Christie, J.M., Salomon, M., Nozue, K., Wada, M. and Briggs, W.R. (1999) LOV (light, oxygen, or voltage) domains of the blue-light photoreceptor phototropin (nph1): binding sites for the chromophore flavin mono- nucleotide. *Proc. Natl Acad. Sci. USA*. **96**:8779-8783.
- Christie, J.M. (2007) Phototropin blue-light receptors. *Annu Rev Plant Biol*. **58**:21-45.
- Christie, J.M., Blackwood, L., Petersen, J. and Sullivan, S. (2015) Plant flavoprotein photoreceptors. *Plant Cell Physio*, **56**(3):401-13.
- Christie, J.M., Reymond, P., Powell, G.K., Bernasconi, P., Raibekas, A.A., Liscum, E. and Briggs, W.R. (1998) *Arabidopsis* NPH1: a flavoprotein with the properties of a photoreceptor for phototropism. *Science*, **282**(5394):1698-701.
- Clack, T., Mathews, S., Sharrock, R.A. (1994) The phytochrome apoprotein family in *Arabidopsis* is encoded by five genes: the sequences and expression of PHYD and PHYE. *Plant Mol Biol*. **25**(3):413-27.
- Coupe, S.A., Palmer, B.G, Lake, J.A., Overy, S.A., Oxborough, K., Woodward, F.I, Gray, J.E., Quick, W.P. (2006) Systemic signalling of environmental cues in *Arabidopsis* leaves. *J of Exp Bot*. **57**:329-341.
- Damkjaer, S. and Taylor, R. (2017) The measurement of water scarcity: Defining a meaningful indicator. *Ambio*. **46**(4):513–531.
- Delgado, D., Ballesteros, I., Torres-Contreras, J., Mena, M., Fenoll, C. (2012) Dynamic analysis of epidermal cell divisions identifies specific roles for COP10 in *Arabidopsis* stomatal lineage development. *Planta*. **236**(2):447-61.
- Deng, X.W., Caspar, T. and Quail, P.H. (1991) cop1: a regulatory locus involved in light-controlled development and gene expression in *Arabidopsis*. *Genes Dev*, **5**(7):1172-82.
- Ding, Z., Millar, A.J., Davis, A.M. and Davis, S.J. (2007) TIME FOR COFFEE encodes a nuclear regulator in the *Arabidopsis thaliana* circadian clock. *Plant Cell*, **19**(5):1522-36.
- Dong, J., MacAlister, C.A., Bergmann, D.C. (2009) BASL Controls Asymmetric Cell Division in *Arabidopsis*. *Cell*. **137**(7):1320-30.
- Edwards, K., Johnstone C. and Thompson, C. (1991) A simple and rapid method for the preparation of plant genomic DNA for PCR analysis. *Nucleic Acids Research*, **19**:1349-1349.
- Endo, M., Tanigawa, Y., Murakami, T., Araki, T. and Nagatani, A. (2013) PHYTOCHROME-DEPENDENT LATE-FLOWERING accelerates flowering through physical interactions with phytochrome B and CONSTANS. *PNAS*, **110**(44):18017-22.

Engineer, C.B., Ghassemian, M., Anderson, J.C., Peck, S.C., Hu, H. and Schroeder, J.I. (2014) Carbonic anhydrases, *EPF2* and a novel protease mediate CO₂ control of stomatal development. *Nature*, **513:246-250**.

Engineer, C.B., Ghassemian, M., Anderson, J.C., Peck, S.C., Hu, H. and Schroeder, J.I. (2014) Carbonic anhydrases, *EPF2* and a novel protease mediate CO₂ control of stomatal development. *Nature*, **11:513-517**.

Engineer, C.B., Hashimoto-Sugimoto, M., Negi, J., Israelsson-Nordström, M., Azoulay-Shemer, T., Rappel, W.J., Iba, K. and Schroeder, J.I. (2016) CO₂ Sensing and CO₂ Regulation of Stomatal Conductance: Advances and Open Questions. *Trends Plant Sci*, **21(1):16-30**.

Farquhar, G.D., Ehleringer, J.R. and Hubick, K.T. (1989) CARBON ISOTOPE DISCRIMINATION AND PHOTOSYNTHESIS. *Ann. Rev. Plant Physiol. Mol. Biol.* **40:503-37**.

Farquhar, G.D. and Richards, R.A. (1984) Isotopic composition of plant carbon correlates with water-use efficiency of wheat genotypes. *Functional Plant Biology*, **11:539-552**.

Farquhar, G.D. and Sharkey, T.D. (1986) Stomatal conductance and photosynthesis. *Annual Review of Plant Physiology*. **33:317-345**.

Fischer, R.A. and Turner, N.C. (1978) Plant Review of Plant Physiology. *Ann. Rev. Plant. Physiol.* **29:277-317**.

Franklin, K.A., Larner, V.S. and Whitelam, G.C. (2005) The signal transducing photoreceptors of plants. *Int J Dev Biol*, **49(5-6):653-64**.

Franklin, K.A., Quail, P.H. (2010) Phytochrome functions in Arabidopsis development. *J Exp Bot.* **61(1):11-24**.

Franklin, K.A., Lee, S.H., Patel, D., Kumar, S.V., Spartz, A.K., Gu, C., Ye, S., Yu, P., Breen, G., Cohen, J.D., Wigge, P.A., Gray, W.M. (2011) Phytochrome-interacting factor 4 (PIF4) regulates auxin biosynthesis at high temperature. *Proc Natl Acad Sci U S A.* **108(50):20231-5**.

Franklin, K.A. and Quail, P.H. (2016) Phytochrome functions in Arabidopsis development. *J Exp Bot*, **61(1):11-24**.

Franks, P.J., Doheny-Adams, T., Britton-Harper, Z.J., Gray, J.E. (2015) Increasing water-use efficiency directly through genetic manipulation of stomatal density. *New Phytol.* **207(1):188-95**.

Fujii, Y., Tanaka, H., Konno, N., Ogasawara, Y., Hamashima, N., Tamura, S., Hasegawa, S., Hayasaki, Y., Okajima, K., Kodama, Y. (2017) Phototropin perceives temperature based on the lifetime of its photoactivated state. *Proc Natl Acad Sci U S A.* **114(34):9206-9211**.

Furuya, M. and Song, P.S. (1994) Assembly and properties of holophytochrome. *Photomorphogenesis in plants*. **105-140**.

Gagoa, J., Douthea, C., Florez-Sarasab, I., Escalonaa, J. M., Galmesa, J., Fernieb, A.R., Flexasa, J. and Medranaa, H. (2014) Opportunities for improving leaf water use efficiency under climate change conditions. *Plant Science*, **226:108-119**.

Gerhart, L.M., Ward, J.K. (2010) Plant responses to low [CO₂] of the past. *New Phytol.* **188(3):674-95.**

Gleeson, T. and Wada, Y. (2013) Assessing regional groundwater stress for nations using multiple data sources with the groundwater footprint. *Environ. Res. Lett.* **8.**

Glover, B.J. (2000) Differentiation in plant epidermal cells. *Journal of Experimental Botany*, **51:497-505.**

González, C.V., Ibarra, S.E., Piccoli, P.N., Botto, J.F., Boccalandro, H.E. (2012) Phytochrome B increases drought tolerance by enhancing ABA sensitivity in *Arabidopsis thaliana*. *Plant, Cell and Environment*. **35:1958-1968.**

Gray, J.E., Holroyd, G.H., van der Lee, F.M., Bahrami, A.R., Sijmons, P.C., Woodward, F.I., Schuch, W., Hetherington, A.M. (2000) The HIC signalling pathway links CO₂ perception to stomatal development. *Nature*. **408(6813):713-6.**

Gray, J.E. and Hetherington, A.M. (2004) Plant Development: YODA the Dispatch Stomatal Switch. *Current Biology*, **14:488-490.**

Groll, U.V., Berger, D. and Altmann, T. (2002) The subtilisin-like serine protease SDD1 mediates cell-to-cell signalling during *Arabidopsis* stomatal development. *Genes & Development*, **14:1527-1539.**

Gudesblat, G.E., Schneider-Pizoń, J., Betti, C., Mayerhofer, J., Vanhoutte, I., van Dongen, W., Boeren, S., Zhiponova, M., De Vries, S., Jonak, C. and Russinova, J.E. (2012) SPEECHLESS integrates brassinosteroid and stomata signalling pathways. *Nat Cell Biol*, **14(5):548-54.**

Hanstein, S., de Beer, D. Felle, H.H. (2001) Miniaturised carbon dioxide sensor designed for measurements within plant leaves. *Sensors and Actuators B Elsevier*. **81:107-114.**

Hara, K., Kajita, R., Torii, K.U., Bergmann, D.C. and Kakimoto, T. (2007) The secretory peptide gene EPF1 enforces the stomatal one-cell-spacing rule. *Genes & Development*, **21:1720-1725.**

Hara, K., Yokoo, T., Kajita, R., Onishi, T., Yahata, S., Peterson, K.M., Torii, K.U. and Kakimoto T. (2009) Epidermal cell density is auto-regulated via secretory peptide, EPIDERMAL PATTERNING FACTOR2 in *Arabidopsis* leaves. *Plant Cell Physiology*, **50:1019-1031.**

Hashimoto, M., Negi, J., Young, J., Israelsson, M., Schroeder, J.I., Iba, K. (2006) *Arabidopsis* HT1 kinase controls stomatal movements in response to CO₂. *Nat Cell Biol*. **8(4):391-7.**

Haworth, M., Elliott-Kingston, C., McElwain, J.C. (2013) Co-ordination of physiological and morphological responses of stomata to elevated [CO₂] in vascular plants. *Oecologia*. **171(1):71-82.**

Hetherington, A.M. and Woodward, F.I. (2003) The role of stomata in sensing and driving environmental change. *Nature*, **424(6951):901-8.**

Hetherington, A.M. and Brownlee, C. (2004) The generation of Ca⁽²⁺⁾ signals in plants. *Annual Review Plant Biology*, **55:401-427.**

Holbrook, N.M. Shashidhar, V.R., James, R.A. and Munns, R. (2002) Stomatal control in tomato with ABA-deficient roots: response to grafted plants to soil drying. *Journal of Experimental Botany*, **46**:525-530.

Holm, M., Ma, L.G., Qu, L.J., Deng, X.W. (2002) Two interacting bZIP proteins are direct targets of COP1-mediated control of light-dependent gene expression in *Arabidopsis*. *Genes Dev.* **16**:1247-1259.

Hronková, M., Wiesnerová, D., Šimková, M., Skůpa, P., Dewitte, W., Vráblová, M., Zažímalová, E. and Šantrůček, J. (2015) Light-induced STOMAGEN-mediated stomatal development in *Arabidopsis* leaves. *Journal of Experimental Botany*, **66**(15):4621-30.

Hronková, M., Wiesnerová, D., Šimková, M., Skůpa, P., Dewitte, W., Vráblová, M., Zažímalová, E. and Šantrůček, J. (2015) Light-induced **STOMAGEN**-mediated stomatal development in *Arabidopsis* leaves. *Journal of Experimental Botany*. **66**(15):4621-30.

Hu, H., Boisson-Dernier, A., Israelsson-Nordström, M., Böhmer, M., Xue, S., Ries, A., Godoski, J., Kuhn, J.M. and Schroeder, J.I. (2010) Carbonic anhydrases are upstream regulators of CO₂-controlled stomatal movements in guard cells. *Nat Cell Biol*, **12**(1):87-93.

Hunt, L. and Gray, J.E. (2009) The signalling peptide EPF2 controls asymmetric cell divisions during stomatal development. *Current Biology*, **19**:864-869.

Hunt, L., Bailey, K.J., Gray, J.E. (2010) The signalling peptide EPFL9 is a positive regulator of stomatal development. *New Phytol*, **186**(3):609-614.

Inoue, S.I., Kinoshita, T., Matsumoto, M., Nakayama, K.I., Doi, M., Shimazaki, K. (2008) Blue light-induced autophosphorylation of phototropin is a primary step for signalling. *Proc Natl Acad Sci U S A*. **105**(14):5626-5631.

Inoue, S., Takemiya, A., Shimazaki, K. (2010) Phototropin signaling and stomatal opening as a model case. *Curr Opin Plant Biol*. **13**(5):587-93.

IPCC, 2014 Climate change 2014: Synthesis Report. Contribution of Working Groups I, II and III to the Fifth Assessment Report of the Intergovernmental Panel on Climate Change (Core Writing Team; Pachauri, R.K., Meyer, L.A.; (eds); Edenhofer, O., Pichs-Madruga, R., Sokona, Y., Minx, J.C., Farahani, E., Kadner, S., Seyboth, Adler, A., Baum, I., Brunner, S., Eickemeier, P., Kriemann, B., Savolainen, J., Schlomer, S., von Stechow, C., Zwickel, T.) IPCC, Geneva, Switzerland, 151pp.

Israelsson, M., Siegel, R.S., Young, J., Hashimoto, M., Iba, K., Schroeder, J.I. (2006) Guard cell ABA and CO₂ signaling network updates and Ca²⁺ sensor priming hypothesis. *Curr Opin Plant Biol*. **9**(6):654-63.

Kanaoka, M.M., Pillitteri, L.J., Fujii, H., Yoshida, Y., Bogenschutz, N.L., Takabayashi, J., Zhu, J.K., Torii, K.U. (2008) SCREAM/ICE1 and SCREAM2 specify three cell-state transitional steps leading to *Arabidopsis* stomatal differentiation. *Plant Cell*. **20**(7):1775-85.

Kang, C.Y., Lian, H.L., Wang, F.F., Huang, J.R. and Yang, H.Q. (2009) Cryptochromes, phytochromes, and COP1 regulate light-controlled stomatal development in *Arabidopsis*. *Plant Cell*, **21**(9):2624-41.

- Kendall, H.W. and Pimentel, D. (1994). Constraints on the expansion of the global food supply. *Ambio*, **23**: 198-205.
- Kim, Y.M., Woo, J.C., Song, P.S., Soh, M.S. (2002) HFR1, a phytochrome A-signalling component, acts in a separate pathway from HY5, downstream of COP1 in *Arabidopsis thaliana*. *The Plant Journal*. **30**:711-719.
- Kim, T.H., Böhmer, M., Hu, H., Nishimura, N., Schroeder, J.I. (2010) Guard Cell Signal Transduction Network: Advances in Understanding Abscisic Acid, CO₂, and Ca²⁺ Signaling. *Anna Rev Plant Biol*. **6(1)**:561-591.
- Kim, T.W., Michniewicz, M., Bergmann, D.C. and Wang, Z.Y. (2012) Brassinosteroid regulates stomatal development by GSK3-mediated inhibition of a MAPK pathway. *Nature*, **482(7385)**:419-22.
- Kinoshita, T., Doi, M., Suetsugu, N., Kagawa, T., Wada, M., and Shimazaki, K. (2001). phot1 and phot2 mediate blue light regulation of stomatal opening. *Nature*. **414**:656-660.
- Kinoshita, T. and Hayashi, Y. (2011) New insights into the regulation of stomatal opening by blue light and plasma membrane H⁽⁺⁾-ATPase. *Int Rev Cell Mol Biol*. **289**:89-115.
- Kircher, S., Kozma-Bognar, L., Kim, L., Adam, E., Harter, K., Schafer, E. and Nagy F. (1999) Light quality-dependent nuclear import of the plant photoreceptors phytochrome A and B. *Plant Cell*, **11(8)**:1445–1456.
- Kondo, T., Kajita, R., Miyazaki, A., Hokoyama, M., Nakamura-Miura, T., Mizuno, S., Masuda, Y., Irie, K., Tanaka, Y., Takada, S., Kakimoto, T. and Sakagami, Y. (2010) Stomatal density is controlled by a mesophyll-derived signaling molecule. *Plant Cell Physiol*, **51(1)**:1-8.
- Łabuz, J., Sztatelman, O., Banaś, A.K., Gabryś, H. (2012) The expression of phototropins in *Arabidopsis* leaves: developmental and light regulation. *J Exp Bot*. **63(4)**:1763-71.
- Lake, J.A., Quick, W.P., Beerling, D.J. and Woodward, F.I. (2001) Plant development: Signals from mature to new leaves. *Nature*, **411**:154.
- Lampard, G.R., MacAlister, C.A. and Bergmann, D.C. (2008) *Arabidopsis* stomatal initiation is controlled by MAPK-mediated regulation of the bHLH SPEECHLESS. *Science*, **322**:1113-1116.
- Lau, O.S. and Deng, X.W. (2012) The photomorphogenic repressors COP1 and DET1: 20 years later. *Trends Plant Sci*, **17(10)**:584-93.
- Lau, O.S., Davies, K.A., Chang, J., Adrian, J., Rowe, M.H., Ballenger, C.E., Bergmann, D.C. (2014) Direct roles of SPEECHLESS in the specification of stomatal self-renewing cells. *Science*. **26;345(6204)**:1605-9.
- Lawson, T., Blatt, M.R. (2014) Stomatal Size, Speed, and Responsiveness Impact on Photosynthesis and Water Use Efficiency. *Plant Physiology*. **164**:1556-1570.
- Le, J., Zou, J., Yang, K. and Wang M. (2014) Signalling to stomatal initiation and cell division. *Frontiers in Plant Science*, **5 (297)**:1-6.

- Lee, J., He, K., Stolc, V., Lee, H., Figueroa, P., Gao, Y., Tongprasit, W., Zhao, H., **Lee, I.** and Deng, X.W. (2007) Analysis of transcription factor HY5 genomic binding sites revealed its hierarchical role in light regulation of development. *Plant Cell*, **19(3):731-49.**
- Lee, J.S., Kuroha, T., Hnilova, M., Khatayevich, D., Kanaoka, M.M, McAbee, J.M., Sarikaya, M., Tamerler, C. and Torii, K.U. (2012) Direct interaction of ligand-receptor pairs specifying stomatal patterning. *Genes & Development*, **26:126-136.**
- Lee, J.S., Hnilova, M., Maes, M., Lin, Y.C., Putarjunan, A., Han, S.K., Avila, J., Torii, K.U. (2015) Competitive binding of antagonistic peptides fine-tunes stomatal patterning. *Nature*. **522(7557):439-43.**
- Lee, J.H., Jung, J.H. and Park, C.M. (2017) Light Inhibits COP1-Mediated Degradation of ICE Transcription Factors to Induce Stomatal Development in Arabidopsis. *Plant Cell*, **29(11):2817-2830.**
- Legris, M., Klose, C., Burgie, E.S., Rojas, C.C., Neme, M., Hiltbrunner, A., Wigge, P.A., Schäfer, E., Vierstra, R.D., Casal, J.J. (2016) Phytochrome B integrates light and temperature signals in Arabidopsis. *Science*. **354(6314):897-900.**
- Leivar, P. and Monte, E. (2014) PIFs: systems integrators in plant development. *Plant Cell*, **26(1):56-78.**
- Li, J. and Nam, K.H. (2002) Regulation of brassinosteroid signalling by a GSK3/SHAGGY-like kinase. *Science*, **295:1299-1301.**
- Li, J., Li, G., Wang, H., Deng, X.W (2011). Phytochrome Signaling Mechanisms. *American Society of Plant Biologists*, **9.**
- Li, F.W., Melkonian, M., Rothfels, C.J., Villarreal, J.C., Stevenson, D.W., Graham, S.W., Wong, G.K., Pryer, K.M. and Mathews, S. (2015) Phytochrome diversity in green plants and the origin of canonical plant phytochromes. *Nat Commun*, **6:7852.**
- Lipton, M., Longhurst, R. (1990) New seeds and poor people. *Agricultural Systems*. **33(4):378-380.**
- Lin, C. and Shalitin, D. (2003) Cryptochrome structure and signal transduction. *Annu Rev Plant Biol*. **54:469-96.**
- Liu, H., Yu, X., Li, K., Klejnot, J., Yang, H., Lisiero, D. and Lin, C. (2008) Photoexcited CRY2 interacts with CIB1 to regulate transcription and floral initiation in Arabidopsis. *Science*, **322(5907):1535-9.**
- Liu, T., Ohashi-Ito, K., and Bergmann, D.C. (2009). Orthologs of *Arabidopsis thaliana* stomatal bHLH genes and regulation of stomatal development in grasses. *Development*. *Science*. **136: 2265–2276.**
- Liu, H., Liu, B., Zhao, C., Pepper, M., Lin, C. (2011) The action mechanisms of plant cryptochromes. *Trends Plant Sci*. **16(12):684-91.**
- Lohse, G., Hedrich, R. (1995) **Anions modify the response of guard-cell anion channels to auxin**, *Planta*. **197(3):546-552.**

Lorrain, S., Allen, T., Duek, P.D., Whitelam, G.C., Fankhauser, C. (2008) Phytochrome-mediated inhibition of shade avoidance involves degradation of growth-promoting bHLH transcription factors. *Plant J.* **53(2):312-23.**

MacAlister, C.A., Ohashi-Ito, K. and Bergmann, D.C. (2007) Transcription factor control of asymmetric cell divisions that establish the stomatal lineage. *Nature*, **445(7127):537-40.**

Mao, J., Zhang, Y.C., Sang, Y., Li, Q.H. and Yang, H.Q. (2005) A role for *Arabidopsis* cryptochromes and COP1 in the regulation of stomatal opening. *PNAS*, **102:12270-12275.**

Mao, J., Zhang, Y.C., Sang, Y., Li, Q.H. and Yang, H.Q. (2005) From the cover: A role for *Arabidopsis* cryptochromes and COP1 in the regulation of stomatal opening. *Proc. Natl Acad. Sci*, **102:12270-12275.**

Marris, E., (2008) Water: more crop per drop. *Nature* **20;452 (7185): 273-7.**

Masle, J., Gilmore, S.R. and Farquhar, G.D. (2005) The *ERECTA* gene regulates plant transcription efficiency in *Arabidopsis*. *Nature*, **436:866-870.**

Matrosova, A., Bogireddi, H., Mateo-Peñas, A., Hashimoto-Sugimoto, M., Iba, K., Schroeder, J.I., Israelsson-Nordström, M. (2015) The HT1 protein kinase is essential for red light-induced stomatal opening and genetically interacts with OST1 in red light and CO₂-induced stomatal movement responses. *New Phytol.* **208(4):1126-37.**

Mawphlang, O. and Kharshiing, E.V. (2017) Photoreceptor Mediated Plant Growth Responses: Implications for Photoreceptor Engineering toward Improved Performance in Crops. *Front Plant Sci.* **8:1181.**

McAusland, L., Violet-Chabrand, S., Davey, P., Baker, N., Brendel, O., Laswon, T. (2016) Effects of kinetics of light-induced stomatal responses on photosynthesis and water-use efficiency. *New Phytologist.* **211:1209-1220.**

Medrano, H., Tomás, M., Martorell, S., Escalona, J., Pou, A., Fuentes, S., Flexas, J., Bota, J. (2015) Improving water use efficiency of vineyards in semi-arid regions. *A review. Agron. Sustain. Dev.* **35:499–517.**

Misyura, M., Colasanti, J. and Rothstein, S.J. (2013) Physiological and genetic analysis of *Arabidopsis thaliana* anthocyanin biosynthesis mutants under chronic adverse environmental conditions. *Journal of Experimental Botany*, **64 (1):229-40.**

Mockler, T.C., Guo, H., Yang, H., Duong, H., Lin, C. (1999) Antagonistic actions of *Arabidopsis* cryptochromes and phytochrome B in the regulation of floral induction. *Development.* **126(10):2073-82.**

Monte. E., Al-Sady, B., Leivar. P., Quail, P.H. (2007) Out of the dark: how the PIFs are unmasking a dual temporal mechanism of phytochrome signalling. *Journal of Experimental Botany.* **58:3125–3133.**

Morison, J.I.L., Baker, N.R., Mullineaux, P.M. and Davies W.J., (2008) Improving water use in crop production. *Phil. Trans. R. Soc.* **363:639–658.**

Morrison, J., Kwok, R., Peralta-Ferriz, Alkire, M., Rigor, I., Anderson, R., Steele, M. (2012) Changing Arctic Ocean freshwater pathways. *Nature.* **481:66-70.**

Murchie, E.H., Lawson, T. (2013) Chlorophyll fluorescence analysis: a guide to good practice and understanding some new applications. *Journal of Experimental Botany*. **64(13):3983-3998**.

Nadeau, J.A. and Sack, F.D. (2002) Control of stomatal distribution on the *Arabidopsis* leaf surface. *Science*, **296:1697-1700**.

Neff, M.N. and Chory, J. (1998) Genetic Interactions between Phytochrome A, Phytochrome B, and Cryptochrome 1 during *Arabidopsis* Development. *Plant Physiol.* **118(1):27-35**.

Ni, W., Xu, S.L., Tepperman, J.M., Stanley, D.J., Maltby, D.A., Gross, J.D., Burlingame, A.L., Wang, Z.Y. and Quail, P.H. (2014) A mutually assured destruction mechanism attenuates light signaling in *Arabidopsis*. *Science*, **344(6188):1160-1164**.

Ohashi-Ito, K. and Bergmann, D.C. (2006) *Arabidopsis* FAMA controls the final proliferation/differentiation switch during stomatal development. *Plant Cell*, **18(10):2493-505**.

Pearcy, R.W. (1990) Sunflecks and photosynthesis in plant canopies. *Annual Review of Plant Physiology and Plant Molecular Biology*. **41:421-453**.

Pedmale, U.V., Huang, S.C., Zander, M., Cole, B.J., Hetzel, J., Ljung, K., Reis, P.A.B., Sridevi, P., Nito, K., Nery, J.R., Ecker, J.R., Chory, J. (2016) Cryptochromes Interact Directly with PIFs to Control Plant Growth in Limiting Blue Light. *Cell*. **164(1-2):233-245**.

Pillitteri, L.J. and Torii, K.U. (2012) Mechanisms of Stomatal Development. *Annual Review Plant Biology*, **63:591-614**.

Pillitteri, L.J. and Dong J. (2013) Stomatal Development in *Arabidopsis*. *The American Society of Plant Biologists*, **11:1-26**.

Pillitteri, L.J., Sloan, D.B., Bogenschutz, N.L. and Torii, K.U. (2007) Termination of asymmetric cell division and differentiation of stomata. *Nature*, **445:501-505**.

Pimentel, D., Harman, R., Pacenza, M., Pecarsky, J. and Pimentel. M., (1994) Natural resources and an optimum human population. *Population and Environment*. **15 : 347-369**.

Porra, R.J., Thompson, W.A., Kriedemann, P.E. (1989) Determination of accurate extinction coefficients and simultaneous equations for assaying chlorophylls *a* and *b* extracted with four different solvents: verification of the concentration of chlorophyll standards by atomic absorption spectroscopy. *Bioenergetics*. **975(3):384-394**.

Prabhakar, M. (2002) Structure, Delimitation, Nomenclature and Classification of Stomata. *Acta Botanica Sinica*, **46(2):242-252**.

Quint, M., Delker, C., Franklin, K.A., Wigge, P.A., Halliday, K.J. and van Zanten, M. (2016) Molecular and genetic control of plant thermomorphogenesis. *Nat Plants*, **2:15190**.

Raven, J. (2002) Selection pressures on stomatal evolution. *New Phytologist, Tansley Review*, **131:371-386**.

Reddy, S.K. and Finlayson, S.A. (2014) Phytochrome B promotes branching in Arabidopsis by suppressing auxin signalling. *Plant Physiol*, **164(3):1542-50**.

Reed, J., Nagpal, P., Poole, D.S., Furuya, M., Chory, J. (1993) Mutations in the Gene for the Red/Far-Red Light Receptor Phytochrome B Alter Cell Elongation and Physiological Responses throughout Arabidopsis Development. *The Plant Cell*. **5:147-157**.

Richardson, L. and Torri, K.U. (2013) Take a deep breath: peptide signalling in stomatal patterning and differentiation. *Journal of Experimental Botany*, **64:5243-5251**.

Sairanen, I., Novák, O., Pěňčík, A., Ikeda, Y., Jones, B., Sandberg, G., Ljung, K. (2012) Soluble carbohydrates regulate auxin biosynthesis via PIF proteins in Arabidopsis. *Plant Cell*. **24(12):4907-16**.

Sancar, A. (1994) Structure and function of DNA photolyase. *Biochemistry*. **33:2-9**.

Sang, Y., Li, Q.H., Rubio, V., Zhang, Y.C., Mao, J., Deng, X.W., and Yang, H.Q. (2005) N-terminal domain-mediated homodimerization is required for photoreceptor activity of Arabidopsis CRYPTOCHROME 1. *Plant Cell*. **17: 1569–1584**.

Santiago, J., Rodrigues, A., Saez, A., Rubio, S., Antoni, R., Dupeux, F., Park, S.-Y., Márquez, J.A., Cutler, S.R., Rodriguez, P.L. (2009) Modulation of drought resistance by the abscisic acid receptor PYL5 through inhibition of clade A PP2Cs. *The Plant Journal*. **60:575–588**.

Schmittgen, T.D., Lee, E.J. and Jiang, J. (2008) High-throughput real-time PCR. *Methods Mol Biol*, **429:89-98**.

Seo, H.S., Yang, J.Y., Ishikawa, M., Bolle, C., Ballesteros, M.L., Chua, N.H. (2003) LAF1 ubiquitination by COP1 controls photomorphogenesis and is stimulated by SPA1. *Nature*. **423:995–999**.

Sharma, S., Kharshiing, E., Srinivas, A., Zikihara, K., Tokutomi, S., Nagatani, A., Fukayama, H., Bodanapu, R., Behera, R.K., Sreelakshmi, Y., Sharma, R. (2014) A Dominant Mutation in the Light-Oxygen and Voltage2 Domain Vicinity Impairs Phototropin1 Signaling in Tomato. *Plant Physiol*. **164(4):2030-2044**.

Sharrock, R.A. and Clack, T. (2002) Patterns of expression and normalized levels of the five Arabidopsis phytochromes. *Plant Physiol*. **130(1):442-56**.

Shimazaki, K., Doi, M., Assmann, S.M., Kinoshita, T. (2007) Light regulation of stomatal movement. *Annu Rev Plant Biol*. **58:219-47**.

Shinomura, T., Nagatani, A., Hanzawa, H., Kubota, M., Watanabe, M., Furuya, M. (1996) Action spectra for phytochrome A- and B-specific photoinduction of seed germination in Arabidopsis thaliana. *Proc Natl Acad Sci U S A*. **93(15):8129-33**.

Shpak, E.D., McAbee, J.M., Pillitteri, L.J. and Torii, K.U. (2005) Stomatal patterning and differentiation by synergistic interactions of receptor kinases. *Science*, **309:290-293**.

- Stout, R. G. (1988) Fusicoccin activity and binding in *Arabidopsis thaliana*. *Plant Physiol.* **88**:999-1001.
- Sugano, S.S., Shimada, T., Iami, Y., Okawa, K., Tamai, A., Mori, M. and Hara-Nishimura I. (2010) Stomagen positively regulates stomatal density in *Arabidopsis*. *Nature*, **463**:241-144.
- Sun, J., Qi, L., Li, Y., Zhai, Q. and Li, C. (2013) PIF4 and PIF5 transcription factors link blue light and auxin to regulate the phototropic response in *Arabidopsis*. *Plant Cell*, **25**(6):2102-14.
- Suzuki, G., Yanagawa, Y., Kwok, S.F., Matsui, M., Deng, X.W. (2002) *Arabidopsis* COP10 is a ubiquitin-conjugating enzyme variant that acts together with COP1 and the COP9 signalosome in repressing photomorphogenesis. *Genes Dev.* **16**(5):554-9.
- Tanaka, Y., Nose, T., Jikumaru, Y., Kamiya, Y. (2013) ABA inhibits entry into stomatal-lineage development in *Arabidopsis* leaves. *Plant J.* **74**(3):448-57.
- Takemiya, A., Inoue, S., Doi, M., Kinoshita, T., Shimazaki, K. (2005) Phototropins promote plant growth in response to blue light in low light environments. *Plant Cell.* **17**(4):1120-7.
- Takemiya, A., Sugiyama, N., Fujimoto, H., Tsutsumi, T., Yamauchi, S., Hiyama, A., Tada, Y., Christie, J.M. and Shimazaki, K. (2013) Phosphorylation of BLUS1 kinase by phototropins is a primary step in stomatal opening. *Nat Commun*, **4**:2094.
- Talbott, L.D., Shmayevich, I.J., Chung, Y., Hammad, J.W., and Zeiger, E. (2003) Blue light and phytochrome-mediated stomatal opening in the npq1 and phot1 phot2 mutants of *Arabidopsis*. *Plant Physiol*, **133**:1522–1529.
- Terry, M.J. (1997) Phytochrome chromophore-deficient mutants. *Plant, Cell and Environemnt.* **20**(6)740–745.
- Teng, N., Wang, J., Chen, T., Wu, X., Wang, Y., Lin, J. (2006) Elevated CO₂ induces physiological, biochemical and structural changes in leaves of *Arabidopsis thaliana*. *New Phytol.* **172**(1):92-103.
- Tian, W., Hou, C., Ren, Z., Pan, Y., Jia, J., Zhang, H., Bai, F., Zhang, P., Zhu, H., He, Y., Luo, S., Li, L., Luan, S. (2015) A molecular pathway for CO₂ response in *Arabidopsis* guard cells. *Nat Comms.* **6**(6057):1-10.
- Ticha, I. (1982) Photosynthetic characteristics during ontogenesis of leaves. 7. Stomatal density and sizes. *Photosynthetica*, **16**:375-471.
- Torii, K.U. (2015) Stomatal differentiation: the beginning and the end. *Curr Opin Plant Biol*, **28**:16-22.
- Torii, K.U., Mitsukawa, N., Oosumi, T., Matsuura, Y., Yokoyama, R., Whittier, R.F. and Komeda, Y. (1996) The *Arabidopsis* ERECTA gene encodes a putative receptor kinase with extracellular leucine-rich repeats. *Plant cell*, **8**:735-746.
- Vahisalu, T., Kollist, H., Wang, Y.F., Nishimura, N., Chan, W.Y., Valerio, G., Lamminmäki, A., Brosché, M., Moldau, H., Desikan, R., Schroeder, J.I., Kangasjärvi, J. (2008) SLAC1 is required for plant guard cell S-type anion channel function in stomatal signalling. *Nature*. **452**(7186):487-91.

- Vatén, A. and Bergmann, D.C. (2012) Mechanisms of stomatal development: an evolutionary view. *EvoDevo*, **3**:11.
- Vörösmarty, C.J., Green, P., Salisbury, J. and Lammers, R.B. (2000) Global Water Resources: Vulnerability from Climate Change and Population Growth. *Science*. **289**(5477):284-288.
- Viczián, A., Klose, C., Ádám, É. and Nagy, F. (2017) New insights of red light-induced development. *Plant Cell Environ*, **40**(11):2457-2468.
- Vlad, F., Rubio, S., Rodrigues, A., Sirichandra, C., Belin, C., (2009) Protein phosphatases 2C regulate the activation of the Snf1-related kinase OST1 by abscisic acid in *Arabidopsis*. *Plant Cell*. **21**(10):3170-84.
- Wang, H., Ma, L.G., Li, J.M., Zhao, H.Y., Deng, X.W. (2001) Direct interaction of *Arabidopsis* cryptochromes with COP1 in light control development. *Science*. **294**(5540):154-8.
- Wang, H., Ngwenyama, N., Liu, Y., Walker, J.C. and Zhang, S., (2007) Stomatal development and patterning are regulated by environmentally responsive mitogen-activated protein kinases in *Arabidopsis*. *The Plant Cell*, **19**:63-73.
- Wang, F.F., Lian, H.L., Kang, C.Y. and Yang, H.Q. (2010) Phytochrome B is involved in mediating red light-induced stomatal opening in *Arabidopsis thaliana*. *Mol Plant*, **3**(1):246-59.
- Wang, L., Li, Z., Qian, W., Guo, W., Gao, X., Huang, L., Wang, H., Zhu, H., Wu, J.W., Wang, D. and Liu, D. (2011) The *Arabidopsis* purple acid phosphatase AtPAP10 is predominantly associated with the root surface and plays an important role in plant tolerance to phosphate limitation. *Plant Physiol*, **157**(3):1283-99.
- Wang, W., Shao, Q., Peng, S., Xing, W., Yang, T., Luo, Y., Yong, B., Xu, J. (2012) Reference evapotranspiration change and the causes across the Yellow River Basin during 1957-2008 and their spatial and seasonal differences. *Water Resources Research*. **48**(5):1-27.
- Webb, A.R. and Hetherington, A.M. (1997) Convergence of the Abscisic Acid, CO₂, and Extracellular Calcium Signal Transduction Pathways in Stomatal Guard Cells. *Plant Physiol*. **114**:1557-1560.
- Weigel, D. (2012) Natural Variation in *Arabidopsis*: From Molecular Genetics to Ecological Genomics. *Plant Physiology*, **158**:12-22.
- Weller, J.L., Beauchamp, N., Huub, L., Kerckhoffs, J., Damien, J., Platten, Reid, J.B. (2001) Interaction of phytochromes A and B in the control of de-etiolation and flowering in pea. *The plant journal Volume*. **26**(3):283-294.
- Weyers, J.D.B. and Johansen, L.G. (1985) Accurate estimation of stomatal aperture from silicone rubber impressions. *New Phytol*. **101**: 109-115.
- Woodward, F.I. (1987) Stomatal numbers are sensitive to increases in CO₂ from pre-industrial levels. *Nature*. **327**:617-618.
- Woodward, F.I. and Kelly, C.K. (1995) The influence of CO₂ concentration on stomatal density. *New Phyt*. **131**(3):311-327.
- Xu, X., Paik, I., Zhu, L. and Huq, E. (2015) Illuminating Progress in Phytochrome-Mediated Light Signaling Pathways. *Trends Plant Sci*, **20**(10):641-50.

- Xu, F., He, S., Zhang, J., Mao, Z., Wang, W., Li, T., Hua, J., Du, S., Xu, P., Li, L., Lian, H., Yang, H.Q. (2017) Photoactivated CRY1 and phyB Interact Directly with **AUX/IAA** Proteins to Inhibit Auxin Signaling in Arabidopsis. *Mol Plant*. **2052(17):30373-8.**
- Xu, Z., Zhou, G. (2008) Responses of leaf stomatal density to water status and its relationship with photosynthesis in a grass. *Journal of Experimental Biology*, **59(12) 3317-3325.**
- Xue, S., Hu, H., Ries, A., Merilo, E., Kollist, H., Schroeder, J.I. (2011) Central functions of bicarbonate in S-type anion channel activation and OST1 protein kinase in CO₂ signal transduction in guard cell. *EMBO J*. **30(8):1645-58.**
- Yamaguchi, R., Nakamura, M., Mochizuki, N., Kay, S.A. and Nagatani, A. (1999) Light-dependent translocation of a phytochrome B-GFP fusion protein to the nucleus in transgenic Arabidopsis. *Journal of Cell Biology*, **145(3):437-45.**
- Yang, M. and Sack, F.D. (1995) The *too many mouths* and *four lips* mutants affect stomatal production in Arabidopsis. *Plant Cell*, **7:2227-2239.**
- Yang, H.Q., Wu, Y.J., Tang, R.H., Liu, D., Liu, Y., Cashmore, A.R. (2000) The C termini of Arabidopsis cryptochromes mediate a constitutive light response. *Cell*. **103(5):815-27.**
- Yang, H.Q., Tang, R.H., Cashmore, A.R. (2001) The Signaling Mechanism of Arabidopsis CRY1 Involves Direct Interaction with COP1. *Plant Cell*. **13(12):2573-2588.**
- Young, J.J., Mehta, S., Israelsson, M., Godoski, J., Grill, E., Schroeder, J.I. (2006) CO₂ signaling in guard cells: Calcium sensitivity response modulation, a Ca²⁺-independent phase, and CO₂ insensitivity of the *gca2* mutant. *PNAS*. **103(19):7506-7511.**
- Zhang, J.Y., He, S.B., Li, L. and Yang, H.Q. (2014) Auxin inhibits stomatal development through MONOPTEROS repression of a mobile peptide gene *STOMAGEN* in mesophyll. *PNAS*, **111:3015-3023.**
- Zhang, Y., Wang, P., Shao, W., Zhu, J.K., Dong, J. (2015) The BASL Polarity Protein Controls a MAPK Signaling Feedback Loop in Asymmetric Cell Division. *Dev Cell*. **33(2):136-149.**
- Zoulias, N., Harrison, E.L., Casson, S.A., Gray, J.E. (2018) Molecular control of stomatal development. *Biochem J*. **475(2):441-454.**
- Zuo, Z., Liu, H., Liu, B., Liu, X., Lin, C. (2011) Blue light-dependent interaction of CRY2 with SPA1 regulates COP1 activity and floral initiation in Arabidopsis. *Curr Biol*. **21(10):841-7.**
- Zuo, Z.C., Meng, Y.Y., Yu, X.H., Zhang, Z.L., Feng, D.S., Sun, S.F., Liu, B. and Lin, C.T. (2012) A study of the blue-light-dependent phosphorylation, degradation, and photobody formation of Arabidopsis CRY2. *Mol Plant*, **5(3):726-33.**

8.0 Appendix

Appendix 8.1. $50\mu\text{mol m}^{-2} \text{s}^{-1}$ at 200ppm grown plants



Appendix 8.2. $50\mu\text{mol m}^{-2} \text{s}^{-1}$ at 500ppm grown plants



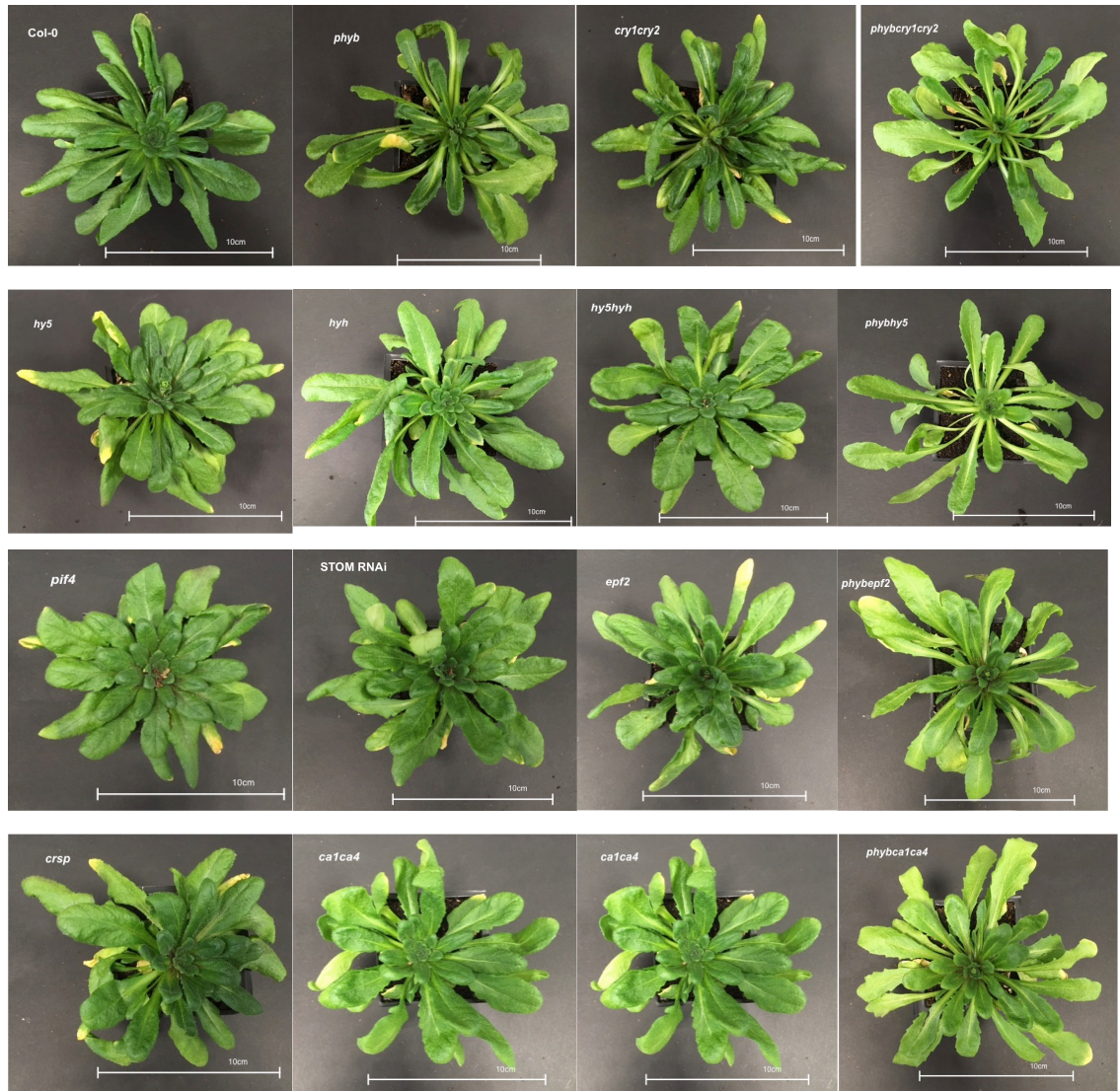
Appendix 8.3. $50\mu\text{mol m}^{-2} \text{s}^{-1}$ at 1000ppm grown plants



Appendix 8.4. $250\mu\text{mol m}^{-2} \text{s}^{-1}$ at 200ppm grown plants



Appendix 8.5. $250\mu\text{mol m}^{-2} \text{s}^{-1}$ at 500ppm grown plants



Appendix 8.6. $250\mu\text{mol m}^{-2} \text{s}^{-1}$ at 1000ppm grown plants

